UiT
THE ARCTIC
UNIVERSITY
OF NORWAY

Faculty of Science and Technology
Department of Geosciences

Characterisation of palaeosols in the Lower Cretaceous Helvetiafjellet Formation, Svalbard

—Palaeo-climatic implications

Ingrid Tennvassås

GEO-3900 Master Thesis in Geology, May 2018

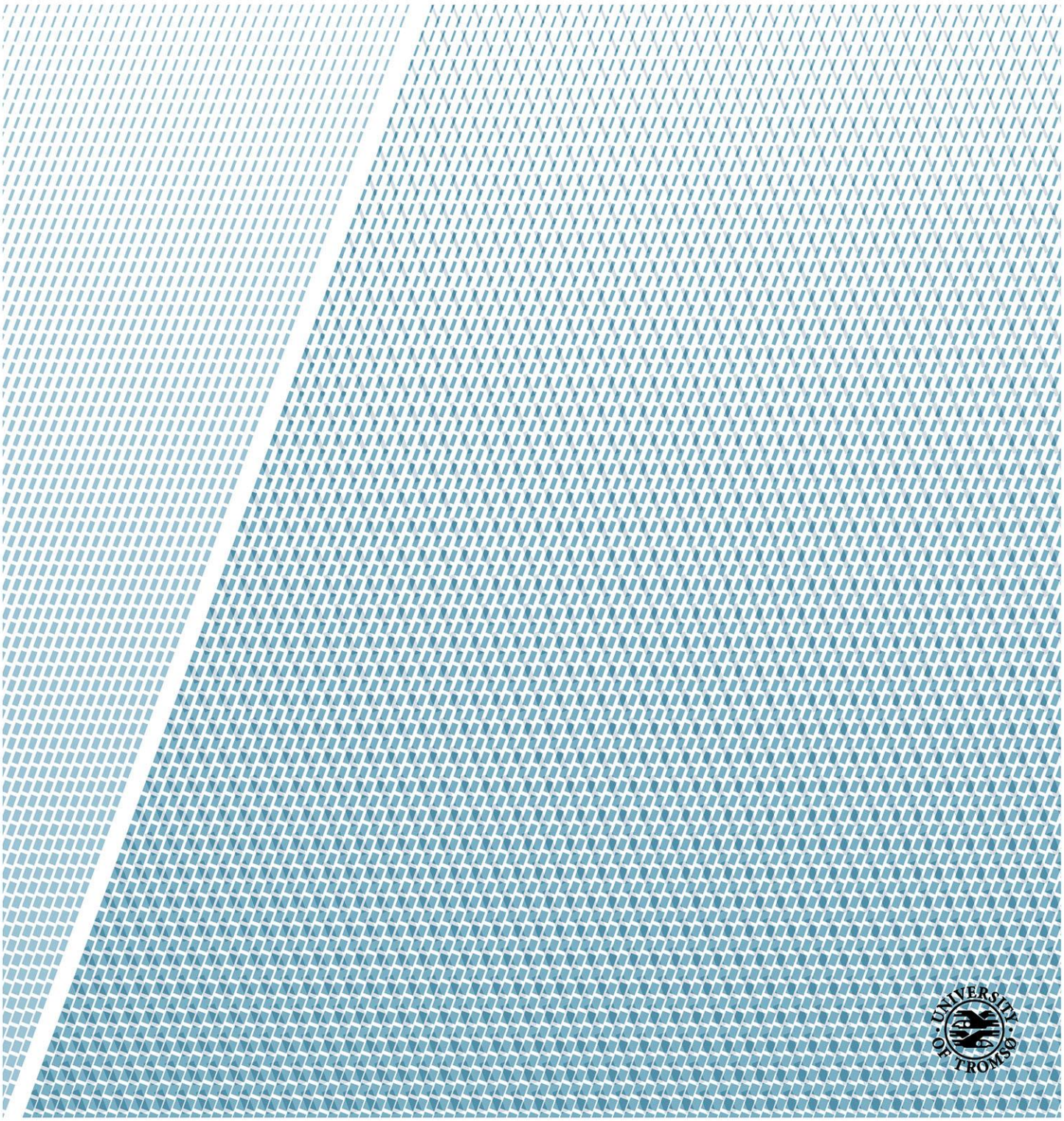


ARCEx
Research Centre for
Arctic Petroleum Exploration


UNIS

Abstract

Although the Cretaceous period is known to have been dominated by greenhouse conditions, the Early Cretaceous climatic conditions in Svalbard have been under some debate. Both indicators of warm climate such as coal seams, Ornithopod tracks and warm-water dinoflagellates, and indicators of cold climate such as arctic belemnites, glendonites and ice rafted debris have been reported. This study characterises two palaeosols (Palaeosol 1 and 2) developed within the Lower Cretaceous Glitrefjellet Member of the Helvetiafjellet Formation, and investigates their validity as palaeo-climatic proxies. This analysis is based on observed features through the logging of two cores (DH-1 and DH-1A), petrographic analysis of thin sections and XRD-analysis. The petrographic analysis revealed a high percentage of quartz within both palaeosols. The combination of high quartz content and the observation of kaolinite through XRD-analysis suggests highly leached conditions. The formation of kaolinite is favoured by subhumid to perhumid climates. Both palaeosols were interpreted to be composed of two main horizons. An upper horizon A, recognized by the accumulation of organic content and a mineral fraction, and a lower horizon C, which was recognized by a pale colour, high quartz content and relict primary structures, indicating modest alteration due to soil forming processes. As a result, the two palaeosols were characterised as enitsols. Such palaeosols are regarded as immature and are thus not indicative of specific climatic conditions. The immaturity of the palaeosols was interpreted to be a consequence of several factors, where (1) high quartz content, (2) palaeosol development within crevasse splay and floodplain deposits and (3) unfavourable clastic sedimentary environment where time for plant growth and accumulation was limited were regarded as the main contributing factors.

During thin section analysis, iron ooids were observed within the transgressive lag that marks the top of the Helvetiafjellet Formation. Their formation was interpreted to be a result of sediment starvation on a shallow-marine shelf that formed due to transgression and flooding of the proximal coastal plain of the Helvetiafjellet Formation. Such deposits are indicative of warm climates. Therefore, although palaeosols 1 and 2 could not be classified with regards to specific climatic conditions, other observations such as high degree of leaching, kaolinite content and iron ooids supports warm and humid climatic conditions.

Acknowledgements

This research is funded by ARCEx partners and the Research Council of Norway (grant number 228107).

I would like to thank my supervisor Assoc. Prof. Sten-Andreas Grundvåg (UiT) for giving me the opportunity to experience Svalbard, and for his continued guidance throughout my thesis. His feedback has been invaluable during this project. Many thanks are also given to my co-supervisor Prof. Snorre Olaussen (UNIS), whose door was always open during the preliminary logging work of my thesis.

I also wish to thank technical staff Trine Dahl and Karina Monsen with the Department of Geosciences at the University of Tromsø for producing my many thin sections.
Irina Maria Dumitru with EARTHLAB at the University of Bergen is thanked for performing the XRD-analysis and for guiding me through the interpretation of the results.

A special thanks is extended to Thea Engen who has given me guidance, reassurance and so many laughs throughout our years of studentship. You are the very definition of a friend.

And last, but certainly not least, endless thanks to my family and my partner Arin Ludvigsen for their continued support throughout my studies.

Ingrid Tennvassås Tromsø, May 2018

Table of Contents

Preface

In relation to a CO_2 storage project (Braathen et al., 2012), seven fully cored wells were drilled in the Adventpynten and Adventdalen area (DH-1, DH-1A, DH-3, DH-4, DH-5R, DH-6 and DH-7; Fig. 7). The primary targets were the Triassic to Middle Jurassic successions, but the Lower Cretaceous succession was also penetrated. The wells DH-5R, DH-6 and DH-7 were the initially targeted wells for this thesis because they are known to contain well-developed palaeosols. These cores were stored in Endalen outside Longyearbyen. However, unfortunately parts of the road to the core storage facility collapsed prior to the data collection, effectively hindering access to these cores. Therefore the cores DH-1 and DH-1A, stored in container at UNIS, were examined and logged instead. The examination of these cores offers a unique opportunity in describing features within the Helvetiafjellet Formation at a level of detail not achievable in conventional outcrop studies.

Two students (Thea Engen and Ingrid Tennvassås) have been working together on the logging aspect of this project. Although the logging was performed together, the two students have different aims for their thesis. In Thesis 1 (Thea Engen), cores DH-1 and DH-1A are used as a basis for a detailed facies analysis and sedimentological characterisation of the Helvetiafjellet Formation and the Glitrefjellet Member in particular. In Thesis 2 (Ingrid Tennvassås), the described cores are used as a basis for a petrographic characterisation of palaeosols in the Glitrefjellet Member of the Helvetiafjellet Formation. The intention is to evaluate the potential of the two palaeosols as palaeo-climatic proxies.

Due to the similarities of the projects, the chapters 2 and 3 were largely written as a collaboration between the two students. From chapter 4 and onward, this thesis will focus on the project objectives of Thesis 2.

1 Introduction

1.1 Background and motivation

During the Cretaceous period, the Earth was dominated by greenhouse conditions, thus making it one of the warmest periods in the geological history (Nemec, 1992; Harland & Kelly, 1997). Large scale magmatism has previously been linked to changes in global climatic conditions (Senger et al., 2014). In Svalbard, the emplacement of the HALIP (High Arctic Large Igneous Province) constitutes such large scale magmatism (Maher, 2001; Corfu et al., 2013). Igneous intrusions occurring within both the Helvetiafjellet and the Rurikfjellet formations were dated at approximately 124.5 Ma, through U-Pb isotope records by Corfu et al., (2013). Thus, the emplacement of the intrusions correlates relatively well with the known global anoxic event OAE1a, which is dated at 121 Ma (Corfu et al., 2013; Senger et al., 2014; Midtkandal et al., 2016). This provides a potential link between the emplacement of the HALIP and global anoxic conditions during the Cretaceous period.

The Svalbard archipelago, which was located at 63 to 66^{O}N during the Cretaceous period, had a relatively warm climate, with mean temperatures of 7–10^{O}C (Hurum et al., 2016; Hurum et al., 2016 A; Grundvåg & Olaussen, 2017). The observation of coal seams and seatearths, in combination with Ornithopod tracks within the Helvetiafjellet Formation suggests a relatively humid climate with a rich plant life. This supported an "Arctic" dinosaur population in the Early Cretaceous period (Steel & Worsley, 1984; Nemec, 1992; Harland et al., 2007; Hurum et al., 2016). Dinoflagellates have also previously been observed throughout the Lower Cretaceous succession (Århus, 1992; Grøsfjeld, 1992). Dinoflagellates are one-celled aquatic organisms that that typically occur in any oceanic conditions, except within cold seas (Harland, 1994). The abovementioned findings within the Lower Cretaceous succession all point towards an at least seasonably warm and humid climate. In this thesis, the observation of iron ooids has also been documented within the Helvetiafjellet Formation for the first time. Such deposits are interpreted as another indicator of warm climate (Mutrux et al., 2008). Their formation is discussed further in chapter *5.5*.

Arctic belemnites, which is an extinct order of cephalopods, have also been observed within the Lower Cretaceous succession (Harland & Kelly, 1997; Price & Nunn, 2010). Their occurrence within the succession has been related to the influence of cold water, with

temperatures of approximately 4-7^{O}C. Although not as commonly occurring, glendonites have also been observed within the succession (Maher et al., 2004; Price & Nunn, 2010). Glendonite is a calcite pseudomorph of ikaite ($CaCO_3 \cdot 6H_2O$), which is a hydrated form of calcium carbonate (Suess et al., 1982). Glendonite most commonly occurs on cold water shelves, and its formation is therefore largely linked to cool temperatures (Selleck et al., 2007). The occurrence of glendonites in conjunction with ice rafter debris within the Lower Cretaceous succession (Dalland, 1977; Pickton, 1981) thus suggests influx of cold polar water, rather than solely warm climatic conditions (Price & Nunn, 2010; Hurum et al., 2016 A; Vickers et al., 2017; Grundvåg & Olaussen, 2017).

Summarizing the abovementioned climatic indicators, it becomes apparent that there is no consensus with regards to which climatic conditions dominated during the Cretaceous period in Svalbard. Changes in climatic conditions, possibly due to the emplacement of the HALIP, and the presence of indicators of both warm and cold palaeo-climatic conditions have been observed. This suggest that the Early Cretaceous period in Svalbard may have been influenced by fluctuating and possibly seasonal climatic changes. As the Svalbard archipelago offers a near-complete Lower Cretaceous succession, it holds a great potential with regards to palaeo-climate studies of higher latitude regions in the Mesozoic.

As the characteristics of palaeosols can reflect the climatic conditions under which they were formed, they are potentially powerful palaeo-climatic proxies (Cecil & Dulong, 2003; Sheldon & Tabor, 2009). The co-occurrence of coal-seams and palaeosols within the heterolithic Glitrefjellet Member of the Helvetiafjellet Formation therefore potentially offers new means of investigation with regards to the Early Cretaceous palaeo-climate in Svalbard. Climatic indicators observed within the palaeosols could thus contribute to the ongoing debate with regards to the Cretaceous climatic fluctuations, and the various interpretations provided by different proxies. Due to the generally poor exposure quality and low accessibility in the field, the palaeosols in the Glitrefjellet Formation have never previously been described in detail. A noble exception is provided by Nemec, (1992), but this study was entirely based on macro-scale outcrop investigations and focused on the sedimentological context of the palaeosols. In his article, Nemec, (1992) stated that the overall conditions with regards to both climate and the ground-water table favoured the formation and accumulation of

organic material. The general lack of thick coal seams within the Helvetiafjellet Formation was therefore interpreted as a consequence of the large input of clastic sedimentary deposits. This is discussed further in this thesis.

In this study, selected palaeosols within the Glitrefjellet Member are investigated by combining core descriptions with petrographic analysis and X-ray diffraction data, thus providing observations at a level of detail not achievable by outcrop studies alone.

1.2 Objectives

In this thesis, the described cores are used as a basis for a petrographic characterisation of palaeosols within the Glitrefjellet Member of the Helvetiafjellet Formation. The purpose of this study is to document and classify palaeosols within the formation and to combine core descriptions with thin section and X-ray diffraction analysis in order to determine if the observed palaeosols are eligible as palaeo-climatic proxies. Thin sections collected throughout the Helvetiafjellet Formation are also used to highlight changes in mineralogical composition in relation to interpreted facies associations. Based on the various investigations of the two cores DH-1 and DH-1A, the specific aims of this thesis is to:

- Describe and physically characterise selected palaeosols in the Glitrefjellet Member.
- Classify the palaeosols and interpret in what depositional environments they possibly formed.
- Highlight petrographic changes within the succession and highlight changes related to pedogenic processes.
- Assess whether or not the palaeosols are valid palaeo-climatic indicators.
- Discuss the potential formations and climatic impact of iron ooids within the Helvetiafjellet Formation.

2 Geological setting

The Svalbard archipelago represents the uplifted and exposed NW corner of the Barents Shelf (Steel & Worsley, 1984; Worsley, 2008; Grundvåg, et al., 2017). The archipelago consists of several islands, where Spitsbergen is the largest. In the west, the area is bounded by a sheared margin while in the north, it is bounded by a passive continental margin (Faleide et al., 1984; Grogran et al., 1999). In the south and east the area is bounded by the Baltic Shield and Novaya Zemlya, respectively (Steel & Worsley, 1984; Dallmann, 2015; Grundvåg et al., 2017). The timing and causes for uplift of the archipelago and the Barents Shelf is debated, but has been suggested to be the result of tectonic and magmatic activity during the Mesozoic and the Cenozoic (Maher, 2001).

Today, the different islands are situated between 74 to 81^{O}N, and 10 to 35^{O} E (Steel & Worsley, 1984; Senger et al., 2014; Fig. 1). The sedimentary record in Svalbard contains sediments ranging from Devonian to Eocene in age (Harland et al., 1976; Grogran et al., 1999; Grundvåg & Olaussen, 2017; Fig.1).

2.1 Introduction to the Mesozoic

The Mesozoic Era can be divided into the Triassic, Jurassic and Cretaceous periods, and extends from 252 Ma–66 Ma (Cohen et al., 2013; Fig. 5). This was an Era dominated globally by both climatic and tectonic changes. During the Mesozoic, Svalbard was a part of an intracratonic sag basin, which was covered by an epicontinental sea (Midtkandal et al., 2007; Midtkandal & Nystuen, 2009; Hurum et al., 2016; Grundvåg & Olaussen, 2017). Epicontinental seas are often recognized as being relatively shallow, generally with a depth of less than 200 m. Another characteristic feature is a gently dipping ramp shelf morphology, typically lacking a pronounced shelf-break. The dip of these shelves can be as little as 0.001–1^{o}, often steepening slightly towards the central part of the basin (Midtkandal & Nystuen, 2009). The gentle gradient of the ramp shelf makes epicontinental seas very sensitive to sea-level change (Midtkandal et al., 2008; Midtkandal & Nystuen, 2009). The exposure of the Mesozoic deposits in Svalbard are illustrated in Fig. 1. These deposits are generally well preserved.

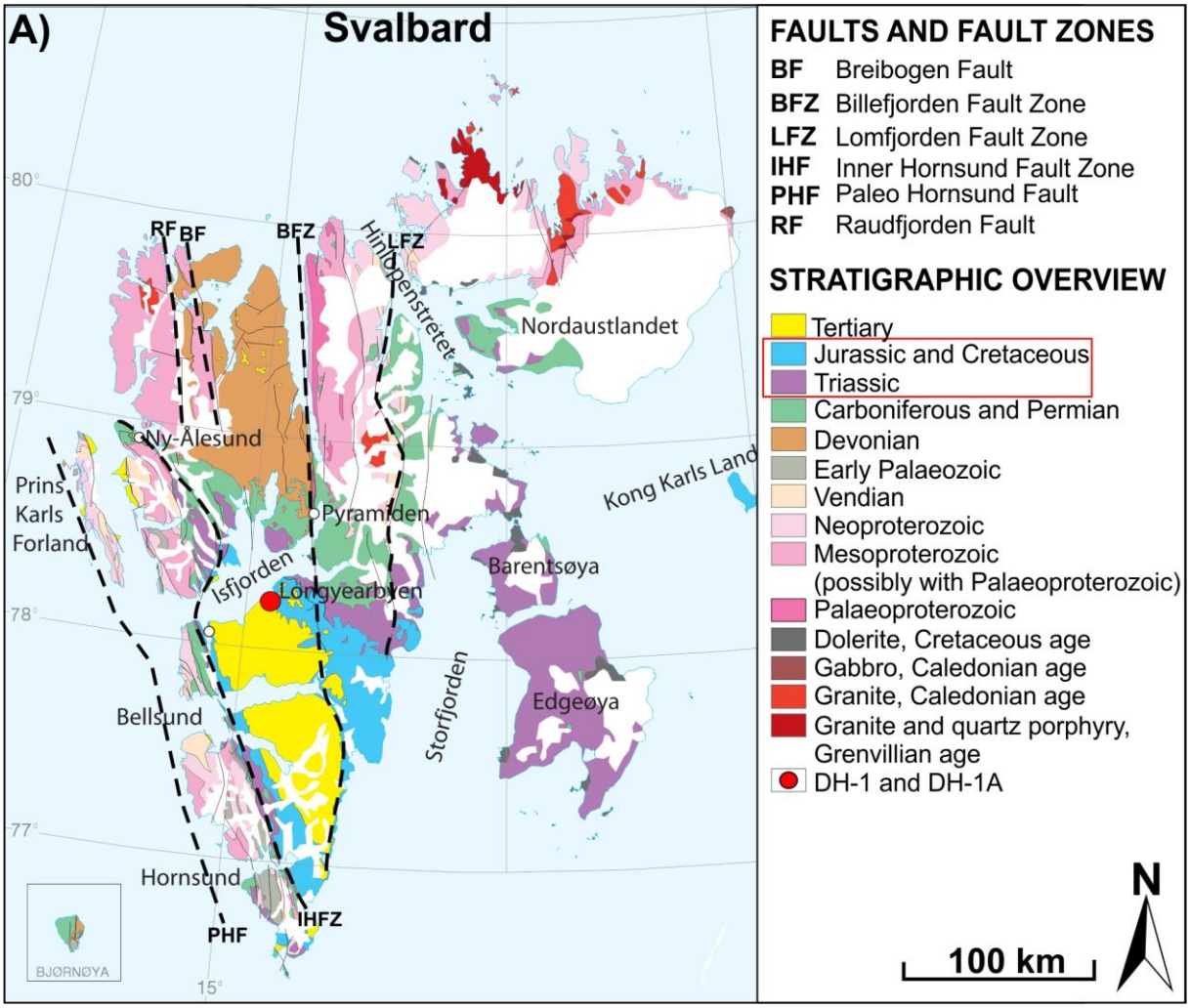

Figure 1: Geological map illustrating the distribution of sediments deposited during the various periods in Spitsbergen. The red rectangle indicates the deposits of the Mesozoic Era (252.17-66 Ma). The deposits of the Triassic period are represented by a purple colour, while the deposits of the Jurassic and Cretaceous periods are represented by a light blue colour. The red circle indicates the approximate position of cores DH-1 and DH-1A. The figure is modified from Elvevold et al., (2007).

2.1.1 Triassic (252.17—201.3 Ma)

Triassic is the first period of the Mesozoic Era. It extends from 252.17—201.3 Ma (Cohen et al., 2013; Fig. 5). The period can be further subdivided into the Early, Middle and Late Triassic epochs. The Triassic period in Svalbard was characterised by stable shelf conditions and a fluctuating sea-level (Buchan et al., 1965; Mørk et al., 1982; Faleide et al., 1984; Mørk et al., 1999; Fig. 2). As a result, the Triassic succession largely consists of both marine and non-marine shales, siltstones and sandstones (Buchan et al., 1965; Nakrem et al., 2008). The Triassic deposits display a varying thickness, changing from a maximum thickness of approximately 1000 m, to a minimum of around 200 m (Buchan et al., 1965). In Svalbard, the Lower to Middle Triassic deposits are represented within the Sassendalen Group, while the Upper Triassic succession belongs to the Kapp Toscana Group.

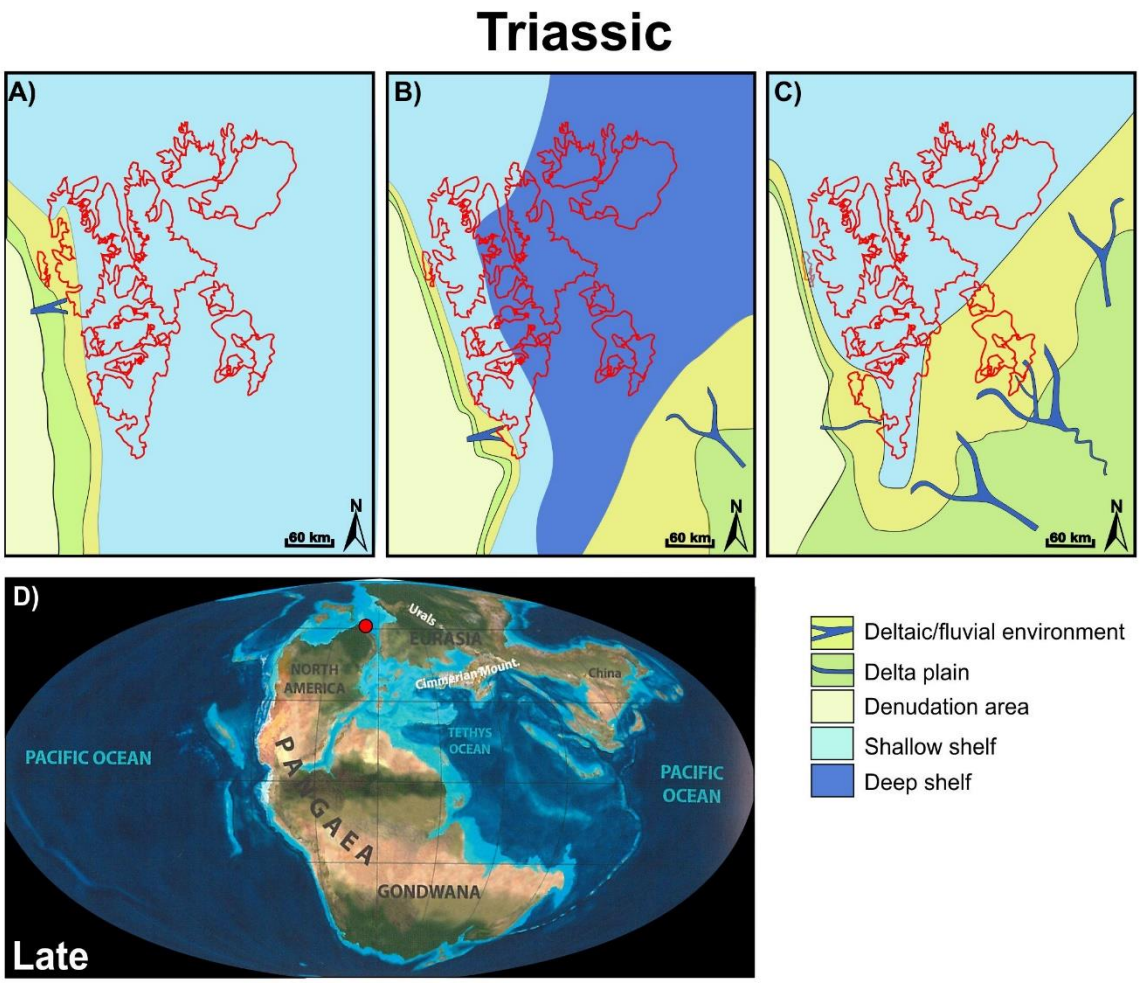

*Figure 2: Illustration of the fluctuating sea-level conditions throughout Early (**A**), Middle (**B**) and Late (**C**) Triassic in Svalbard. The variations in depositional conditions throughout the Triassic period has resulted in a variety of deposits such as shales, siltstone and sandstone. Palaeogeography during Late Triassic is illustrated in image **D**. The approximate position of Svalbard is indicated with a red circle. The figure is not to scale, and is modified from Dallmann (2015).*

2.1.2 Jurassic (201.3—145.0 Ma)

The Jurassic period is the middle period of the Mesozoic Era. The period extends from 201-3—145.0 Ma, and can be further subdivided into the Early and Late Jurassic epochs (Cohen et al., 2013; Fig. 5). The dissolution of the supercontinent Pangea began during Early Jurassic. By the end of Late Jurassic, two continents were fully formed; Laurasia in the north, and Gondwana in the south (Dallmann, 2015). This is illustrated in Fig. 3.

The Jurassic period as a whole was dominated by several cycles of eustatic sea-level rise and subsequent fall. In the final stages of the Late Jurassic, the sea-level rose once more. This led to the formation of an epicontinental sea in the Svalbard region. The seafloor topography of an epicontinental sea is not ideal for ocean currents, and in combination with high CO_2 levels, large amounts of organic matter were produced and stored (Dallmann, 2015). The

shales observed in the Upper Jurassic succession suggests anoxic shelf environments (Smelror, 1994). Today, the Upper Jurassic succession has been proven as a valuable source rock on the Barents Shelf (Steel & Worsley, 1984; Ramberg et al., 2013; Dallmann, 2015).

In the rock record in Svalbard, the Lower Jurassic succession is represented within the Kapp Toscana Group, while the Upper Jurassic deposits can be seen within the Adventdalen Group. For further discussion on the Adventdalen Group and the formations in which it includes, please see chapter *2.3*.

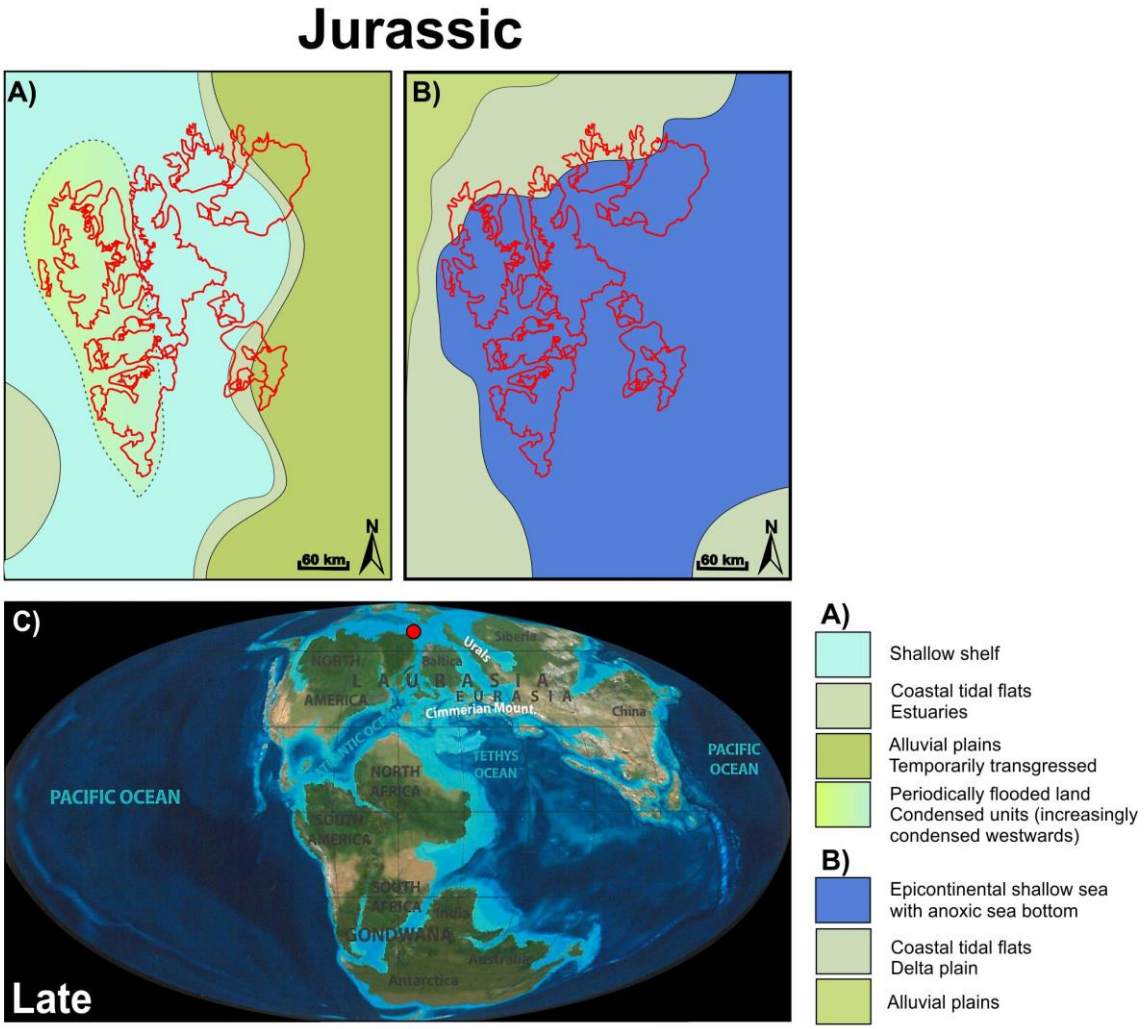

*Figure 3: Illustration of the development of Svalbard during the Jurassic period. Several cycles of eustatic sea-level rise and subsequent fall have been documented throughout both the Early (**A**) and Late (**B**) Jurassic periods. The Jurassic period culminated in a relative sea-level rise, which today can be observed as thick shale successions within the rock record. Global palaeogeography during the Late Jurassic period is illustrated in image **C**. The approximate position of Svalbard is indicated with a red circle. The figure is not to scale, and is modified from Dallmann, (2015).*

2.1.3 Cretaceous (145—66 Ma)

The Cretaceous period is the final period of the Mesozoic Era. Deposits observed within the rock record with an age ranging from 145 Ma to 66 Ma are considered to have been deposited in the Cretaceous period. The period is subdivided into the Early Cretaceous (145 Ma–100.5 Ma) and the Late Cretaceous epochs (100.5 Ma–66 Ma) (Cohen et al., 2013; Fig. 5). In Svalbard, regional uplift took place during the Late Cretaceous, thus effectively removing the Upper Cretaceous strata (Harland, 1969; Faleide et al., 1984; Steel & Worsley, 1984). As a result, only the Lower Cretaceous succession is preserved in Svalbard. Therefore, only the sediments deposited during the Early Cretaceous will be discussed further.

The opening of the Canada Basin, as well as the later parts of the Ameriasian Basin took place during the Cretaceous period (Grantz et al., 2011). This led to volcanic activity and the following emplacement of the High Arctic Large Igneous Province (HALIP) (Maher, 2001; Maher et al., 2004; Brekke & Olaussen, 2013; Senger et al., 2014). The HALIP activity caused uplift of the strata, which has been interpreted as most severe in the NW area of the Svalbard archipelago (Dörr et al., 2011; Fig. 4). As a result, the sedimentary package of the Lower Cretaceous decreases in thickness towards the north (Parker, 1967; Nagy, 1970). A change from a more than 1000 m thick sedimentary package in the south, to an approximate thickness of 300 m in the north can be observed.

In Svalbard, the Lower Cretaceous succession is accompanied by the Upper Jurassic deposits within the Adventdalen Group. For the lithostratigraphic features of the Adventdalen Group, please see chapter *2.3*.

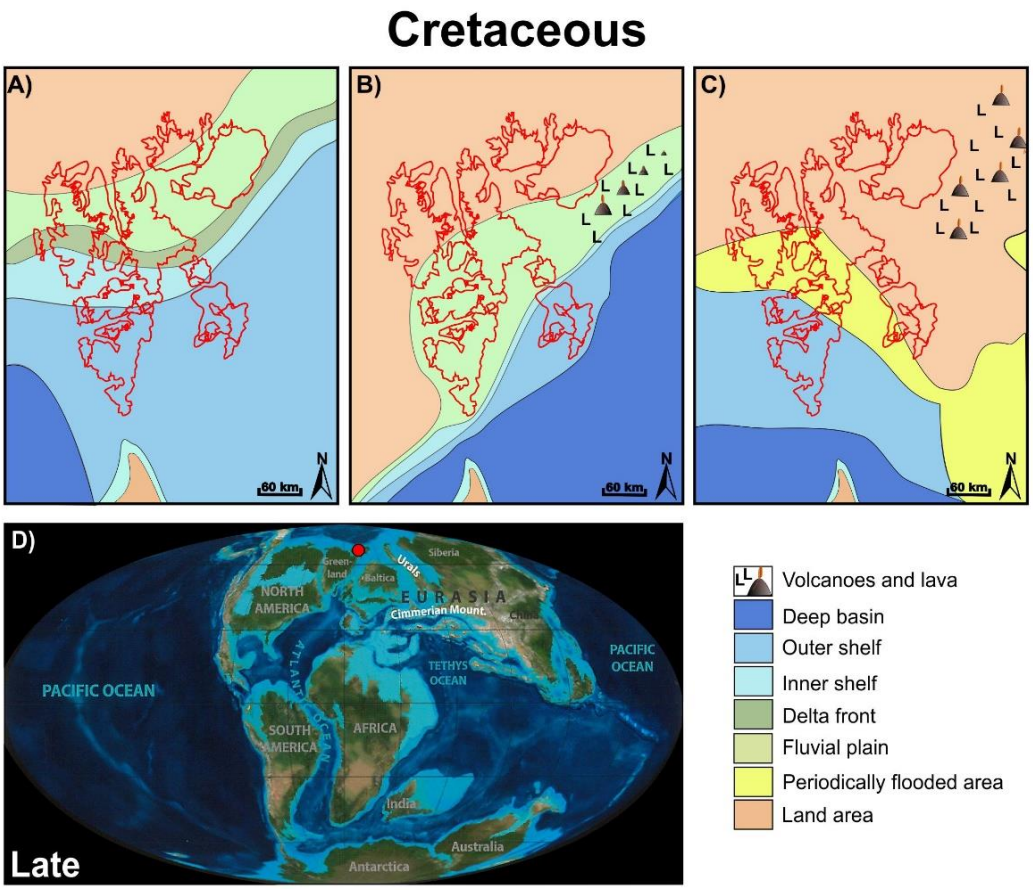

*Figure 4: Illustration of the dominating depositional environments of the Early Cretaceous period. Images **A-C** represent a palaeogeographic reconstruction of the Rurikfjellet Formation (**A**), the Helvetiafjellet Formation (**B**), and the Carolinefjellet Formation (**C**). A regional uplift occurred during the Late Cretaceous, which was caused by crustal doming and HALIP activity. This is interpreted to have caused the removal of the Upper Cretaceous succession. Global palaeogeography during Late Cretaceous is illustrated in image **D**. The approximate position of Svalbard is indicated by a red circle. The figure is not to scale, and is modified from Dallmann (2015).*

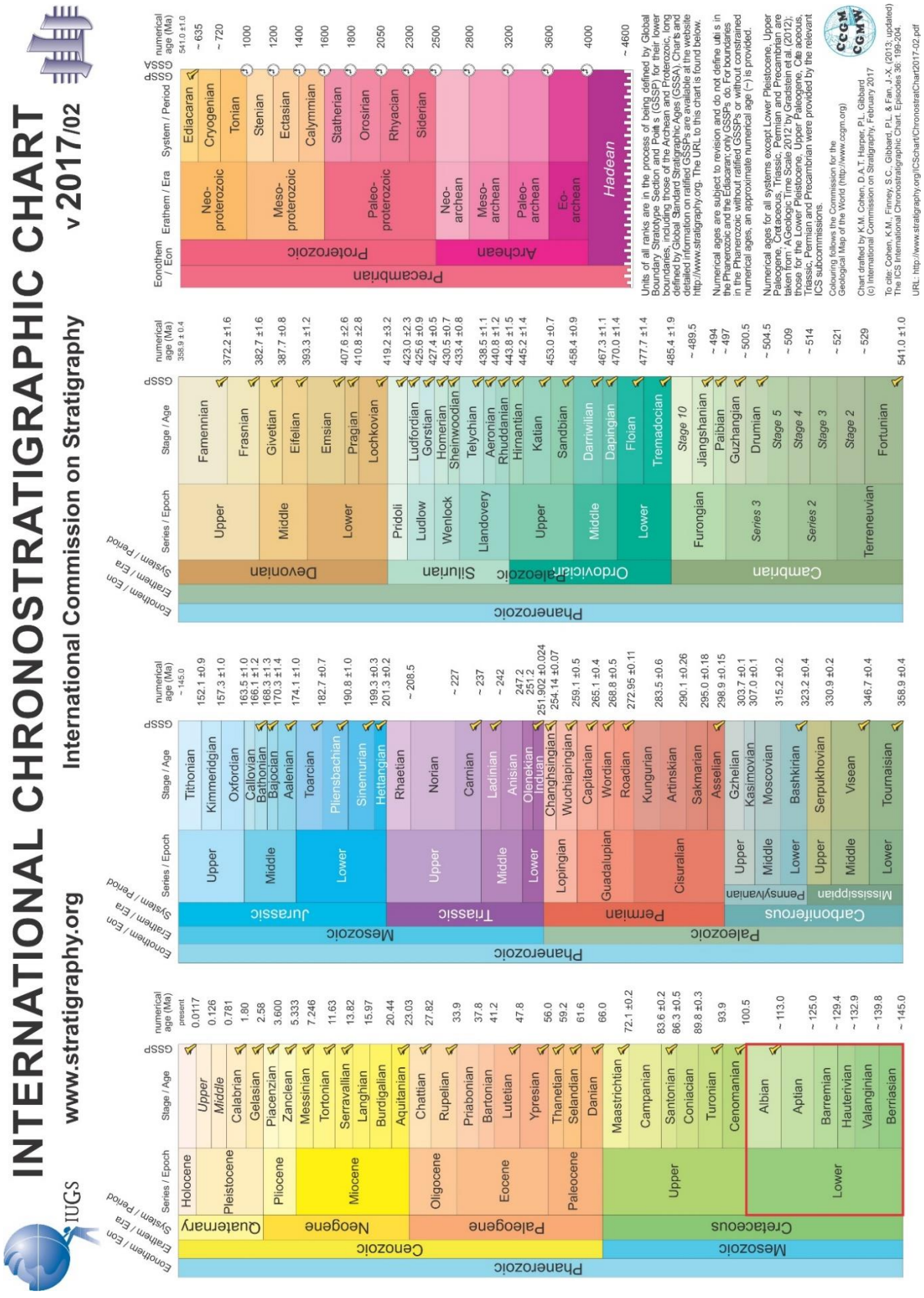

Figure 5: Chronostratigraphic chart which offers an overview of the different eons, eras, periods, epochs and stages that together make up the geological time scale. The Early Cretaceous epoch (marked with a red square) is subdivided into the stages (from oldest to youngest): Berriasian, Valanginian, Hauterivian, Barremian, Aptian and Albian. Retrived from Cohen et al., (2013).

2.2 Tectonic framework

2.2.1 Structural evolution

The collapse of the early Paleozoic orogen during Early Devonian marks the beginning of the structural evolution that would later result in the uplift and exposure of the Svalbard archipelago (Dallmann, 1999). After the collapse, several basins were formed due to extensional rifting (Steel & Worsley, 1984; Grogran et al., 1999). With the onset of the Svalbardian orogen in the Late Devonian, the rift basins that formed during the Early Devonian were compressed. Although the area has been documented as more stable from here on out, the Middle Carboniferous period (and locally throughout Permian) was dominated by discrete regional extensional events (Nøttvedt et al., 1992; Grogran et al., 1999).

Regional uplift in the Late Cretaceous and Tertiary periods also led to the reactivation of older fault systems. These were primarily the Lomfjorden/Agardhbukta and Billefjorden Fault Zones during the Cretaceous (Onderdonk & Midtkandal, 2010), and the Inner Hornsund and the Palaeo-Hornsund Fault Zones during the Tertiary period (Steel & Worsley, 1984; Grogran et al., 1999; Fig. 1). The uplift of Spitsbergen, which was caused by the reactivation of the fault systems led to erosion during the Late Cretaceous (Dörr et al., 2011).

The most recent major tectonic event in the structural evolution in Svalbard is the Paleogene development of the West Spitsbergen Fold Belt (WSFB) (Harland, 1969; Steel & Worsley, 1984; Steel et al., 1985; Figs. 1 & 9). The WSFB is NNW-SSE trending, and extends along the western coast of Svalbard for approximately 300 km. The belt is approximately 50 km wide (Steel & Worsley, 1984). The onset of the WSFB is interpreted to be related to the opening of the Norwegian-Greenland Sea, seen as a major continental transform fault (Harland, 1969; Steel & Worsley, 1984; Dörr et al., 2011). An associated basin, the Central Tertiary Basin, consists of a relatively broad NNW-SSE trending syncline and formed as a foreland basin of the West Spitsbergen Fold Belt (Müller & Spielhagen, 1990; Dörr et al., 2011). As a result, the Lower Cretaceous succession can be observed as relatively steeply dipping to the east along the western coast of Spitsbergen, whereas to the east of Spitsbergen (and in the rest of Svalbard), the strata is observed as relatively horizontal.

2.2.2 HALIP (High Arctic Large Igneous Province) activity

In association with fast-moving sea-floor spreading and the opening of the Canada Basin, the magmatic activity rose. As a result, the basaltic Alpha Ridge formed during Early Cretaceous (Lane, 1997; Grogran et al., 1999; Maher, 2001). The High Arctic Large Igneous Province (HALIP) was also emplaced during the Early Cretaceous (Maher, 2001; Corfu et al., 2013; Senger et al., 2014). Such igneous provinces are generally characterised as very large, predominantly mafic magmatic bodies (Coffin & Eldholm, 1994; Corfu et al., 2013). They can be observed as both extrusive and intrusive units. In Svalbard, the HALIP can be observed as predominantly sills, but also occasionally as dykes and as basalt flows in the east (Maher, 2001; Senger et al., 2014; Polteau et al., 2016; Fig. 4).

The extensive intrusion caused by the HALIP emplacement led to crustal updoming (Maher, 2001). Therefore, it is likely that tectonic activity was not the only cause for the uplift of Svalbard and the northern margin of the Barents Shelf in the Early Cretaceous. The crustal updoming due to HALIP activity is interpreted as the cause of the tectonically forced regression that led to the formation of the Barremian subaerial unconformity at the boundary between the Rurikfjellet and the Helvetiafjellet formations (Gjelberg & Steel, 1995; Maher, 2001).

2.3 Lithostratigraphy of the Adventdalen Group

The Adventdalen Group consists of four formations. These are the Agardhfjellet, the Rurikfjellet, the Helvetiafjellet and the Carolinefjellet formations (Parker, 1967; Fig. 7). In this section, the characteristics of these four formations will be highlighted. Special attention will be given to the Helvetiafjellet Formation and its members, as they are the focus of this study.

2.3.1 The Agardhfjellet Formation (Middle Jurassic to earliest Cretaceous)

The Agardhfjellet Formation is the oldest unit within the Adventdalen Group. The formation is Middle Jurassic to earliest Cretaceous in age, and is commonly subdivided into four members. The lowermost member is the Oppdalen Member, which is dominated by silty sediments (Dypvik, et al., 1991; Koevoets et al., 2018). The overlying member is mainly organic-rich sediments, known as the Lardyfjellet Member (Dypvik, et al., 1991; Koevoets et al., 2018). The overlying member is the Oppdalssåta Member, which primarily consist of sandstone and siltstone (Koevoets et al., 2018). Similarly to the Lardyfjellet Member, the

uppermost member of the formation is also dominated by organic-rich mudstone (Dypvik, et al., 1991; Druckenmiller et al., 2012). This member is known as the Slottsmøya Member, and is dated to be of Tithonian age (Harland & Kelly, 1997; Olaussen, 2015; Koevoets et al., 2016).

The Agardhfjellet Formation varies in thickness throughout the Svalbard archipelago. This can be observed as a decrease in thickness when moving in a W-E direction. Where the formation is approximately 250 m thick in the central part of Spitsbergen in the west, it is reduced to a unit that is less than 50 m thick on Kong Karls Land in the east. This change in thickness is interpreted to have been caused by erosion prior to the deposition of the Early Cretaceous Helvetiafjellet Formation (Collignon & Hammer, 2002; Olaussen, 2015). Because the Agardhfjellet Formation contains large quantities of organic material, it has proven to be an important source rock for hydrocarbon formation. An example here is in the time and lateral equivalent Hekkingen Formation, which is found within in several basins on the SW Barents Shelf (Mørk et al., 1999).

The boundary between the Agardhfjellet Formation and the overlying Rurikfjellet Formation is generally recognized as a light coloured claystone bed, known as the Myklegardfjellet Bed (Dypvik et al., 1991; Collignon & Hammer, 2002; Smelror & Dypvik, 2006). However, this bed is can be poorly developed, thus making it difficult to distinguish the two formations from one another. Where this is the case, the two formations are combined and referred to as the Janusfjellet Subgroup (Parker, 1967; Dypvik et al., 1991; Grundvåg et al., 2017).

2.3.2 The Rurikfjellet Formation (Valanginian to early Barremian)

The Rurikfjellet Formation is the second unit in the Adventdalen Group, and the lowermost unit of the Lower Cretaceous succession. The formation is Valanginian to Barremian in age (Grøsfjeld, 1992), and has a recorded maximum thickness of up to 400 m (Midtkandal & Nystuen, 2009). The formation can also be referred to as a part of the Janusfjellet Subgroup in areas where the Myklegardsfjellet Bed is not present and separation from the Agardhfjellet Formation is problematic (Parker, 1967; Dypvik et al., 1991). The Rurikfjellet Formation has two recognized members. The lowermost member is the shaley Wimanfjellet Member (Dypvik et al., 1991). This is overlain by the Kikutodden Member, which is primarily dominated by sandstone and siltstone (Midtkandal et al., 2008).

2.3.3 The Helvetiafjellet Formation (Barremian to early Aptian)

The Helvetiafjellet Formation (Parker, 1967; Fig. 7) has two recognized members; the basal Festningen Member and the overlying Glitrefjellet Member (Parker, 1967; Midtkandal et al., 2007; Fig. 7). The formation primarily consists of coarse grained braidplain deposits in its lowermost member, transitioning upwards into coastal plain and shallow marine facies in its uppermost member (Steel & Worsley, 1984; Gjelberg & Steel, 1995; Nemec, 1992). There is an abrupt erosional contact between the Rurikfjellet Formation and the overlying Helvetiafjellet Formation, which can be seen as a change in lithologies from a marine to a fluvial influenced environment (Birkenmajer, 1984; Grundvåg et al., 2017). This boundary is recognized as a Barremian subaerial unconformity (Parker, 1967; Nemec, 1992; Midtkandal & Nystuen, 2009; Midtkandal et al., 2016; Fig. 7). This unconformity represents a sudden drop in relative sea-level, interpreted to be a result of the tectonic uplift related to the HALIP activity (Maher, 2001). The unconformity is regionally extensive and can be observed throughout Svalbard (Nemec et al., 1988; Gjelberg & Steel, 1995; Maher, 2001; Midtkandal & Nystuen, 2009; Grundvåg & Olaussen, 2017). The architecture and facies stacking of the formation reflects a long-term transgression (Nemec, 1992; Gjelberg & Steel, 1995; Grundvåg & Olaussen, 2017).

The Helvetiafjellet Formation has a varying thickness, from up to 150 m in S-SE Spitsbergen to approximately 40 m in the NE (Gjelberg & Steel, 1995; Brekke & Olaussen, 2013). The formation is diachronous and is observed as progressively younger towards the north (Steel & Worsley, 1984; Gjelberg & Steel, 1995; Midtkandal & Nystuen, 2009).

2.3.3.1 The Festningen Member

The lowermost unit of the Helvetiafjellet Formation is the Festningen Member (Parker, 1967). The base of the member is defined by a Barremian subaerial unconformity which is dated at 127 Ma (Parker, 1967; Edwards, 1976; Midtkandal & Nystuen, 2009). It is commonly agreed upon that the deposits of the Festningen Member are primarily fluvial in origin (Steel, 1977; Nemec, 1992; Mørk et al., 1999). The deposition of the Festningen Member is interpreted to have commenced as a result of relative sea-level rise during Early Cretaceous and the creation of continental accommodation space that followed (Midtkandal & Nystuen, 2009). Despite the clastic input being relatively high, the deposition took place in a backstepping manner (Nemec, 1992; Gjelberg & Steel, 1995; Midtkandal & Nystuen, 2009).

The large-scale tabular and trough cross-beds that are observed in the sandstone units within the member are interpreted to owe their geometry to the migration of composite sand and gravel bars in a fluvial braidplain setting (Birkenmajer, 1984; Nemec, 1992). The fluvial facies may locally alternate or interfinger with floodplain, crevasse splay, bay head delta deposits or fluvial mouth bars (Midtkandal et al., 2008). The Festningen Member generally consist of medium to very coarse-grained sandstone and conglomerates. These deposits are interpreted to have been deposited in a low-gradient braidplain setting (Nemec, 1992; Midtkandal et al., 2007; Midtkandal & Nystuen, 2009; Grundvåg et al., 2017). The lower units of the Festningen Member display a lateral variation in thickness, indicating that the sediment deposition was controlled by an incised valley topography (Midtkandal & Nystuen, 2009; Grundvåg et al., 2017). The top of the Festningen Member is typically recognized by a relatively thin, regionally extensive coal seam (Grundvåg & Olaussen, 2017).

2.3.3.2 The Glitrefjellet Member

Overall, the Glitrefjellet Member primarily consists of interbedded silty shales with thin coal seams, coarse-grained sandstone units with both tabular and trough cross-bedding and ripple cross-lamination, an abundance of plant debris and subordinate conglomerates (Parker, 1967; Birkenmajer, 1984). Within cores DH-1 and DH-1A, the sandstone units were the most commonly observed deposits (Figs. 23 & 24). The sedimentary units of the Glitrefjellet Member are interpreted to have been deposited as a part of a delta plain, under overall transgressive conditions due to basinal subsidence, and a relative rise in sea-level (Gjelberg & Steel, 1995; Midtkandal et al., 2008; Chap. *2.4*). Therefore, the marine influence generally increases upwards within the succession, towards the upper boundary to the overlying Carolinefjellet Formation. At the boundary between the two formations, there is an abrupt deepening across a regional marine flooding surface of early Aptian age (Midtkandal et al., 2016; Grundvåg et al., 2017).

2.3.4 The Carolinefjellet Formation (Aptian to Albian)

The Carolinefjellet Formation is the youngest formation of the Adventdalen Group. The formation is Aptian to Albian in age, and has a maximum recorded thickness of 850 m (Nagy, 1970; Steel & Worsley, 1984; Dypvik et al., 2002). The formation consists of five units; the Dalkjegla, the Innkjegla, the Langstakken, the Zillberget and the Schönrockfjellet members. The members alternate between being dominated by sandstone and mudstone,

respectively. The formation is interpreted to have been deposited in a more marine influenced environment than the underlying Helvetiafjellet Formation (Nagy, 1970; Gjelberg & Steel, 1995; Maher et al., 2004; Grundvåg, 2015; Hurum et al., 2016 A). Traditionally, the boundary between the Helvetiafjellet Formation and the base of the overlying Carolinefjellet Formation has been described as gradational (e.g. Gjelberg & Steel, 1995; 2012). However, in more recent studies a relatively thick (approx. 10—30 m) black shale unit of early Aptian age has been suggested as the transition between the two formations (Midtkandal et al., 2016; Grundvåg et al., 2017). This unit has been recognized across the majority of the outcrop window in Spitsbergen. The upper parts of the Carolinefjellet Formation is truncated by the Palaeocene unconformity. This is interpreted as a consequence of uplift and erosion. The truncation corresponds to a major hiatus in sedimentation, equivalent to the Late Cretaceous to earliest Tertiary time interval. Therefore, no Upper Cretaceous strata is present in Svalbard (Grundvåg, 2015; Hurum et al., 2016 A; Smelror & Larssen, 2016).

2.4 Depositional architecture of the Helvetiafjellet Formation

The Helvetiafjellet Formation was first named by Parker, (1967) with its subdivision into the Festningen Member and the overlying Glitrefjellet Member. Gjelberg and Steel, (1995) found it difficult to use this subdivision of the formation in many of the locations in Spitsbergen because the boundary between the two members was observed as being repeated, interfingering and generally difficult to define. The Helvetiafjellet Formation records a gradual facies change upwards, reflecting a transgressive setting (Gjelberg & Steel, 1995). As a result, Mørk et al., (1999) revoked the Festningen Members formal status as a member of the Helvetiafjellet Formation. In their article, the unit is referred to as the informal Festningen sandstone member. Midtkandal et al., (2008) re-established the Festningen Member as the formal lower member of the Helvetiafjellet Formation.

Several authors have discussed the regional depositional system of the Helvetiafjellet Formation. These are summarized in Fig. 6. The first depositional model was presented by Parker, (1967) and later modified by Nagy, (1970). It is known as the layer-cake model. This model suggests that the basal deposits of the Helvetiafjellet Formation were deposited with a sheet-like geometry at a very low-angle shelf or platform. As Fig. 6 illustrates, the units are interpreted to have covered large areas of Spitsbergen (Midtkandal & Nystuen, 2009). However, the model did not take into account how the system developed outside of the

outcrop window. Several attempts have been made to illustrate this development, however many problems with regards to stratigraphic correlation were encountered. This led to the abandonment of this model.

A regressive-transgressive model (Steel & Worsley, 1984; Nemec, 1992; Fig. 6) explains how the Rurikfjellet and Helvetiafjellet formations are stratigraphically linked by the transition between braided stream and mouth bar deposition. This leads to an overall transgressive development. Based on this, a more complex transgressive diachronous model was suggested by Gjelberg & Steel, (1995; Fig. 6). This model is similar to the regressive-transgressive model, but provides a better understanding of the backstepping trend with inferred delta lobes pinching out within the outcrop window. This model contains a shoreline a possible shelf-break and a maximum regression point just south of the present-day coastline in Svalbard. The self-break model also suggests thick, sandy basin-floor fans offshore (Steel et al., 2000).

Midtkandal & Nystuen, (2009) also argued for a model (Fig. 6). This model has many similar characteristics to the previously described layer-cake model. The model illustrates large-scale aggradation of facies belts, with a regression-transgression point that is interpreted to be present somewhere out on the Barents Shelf.

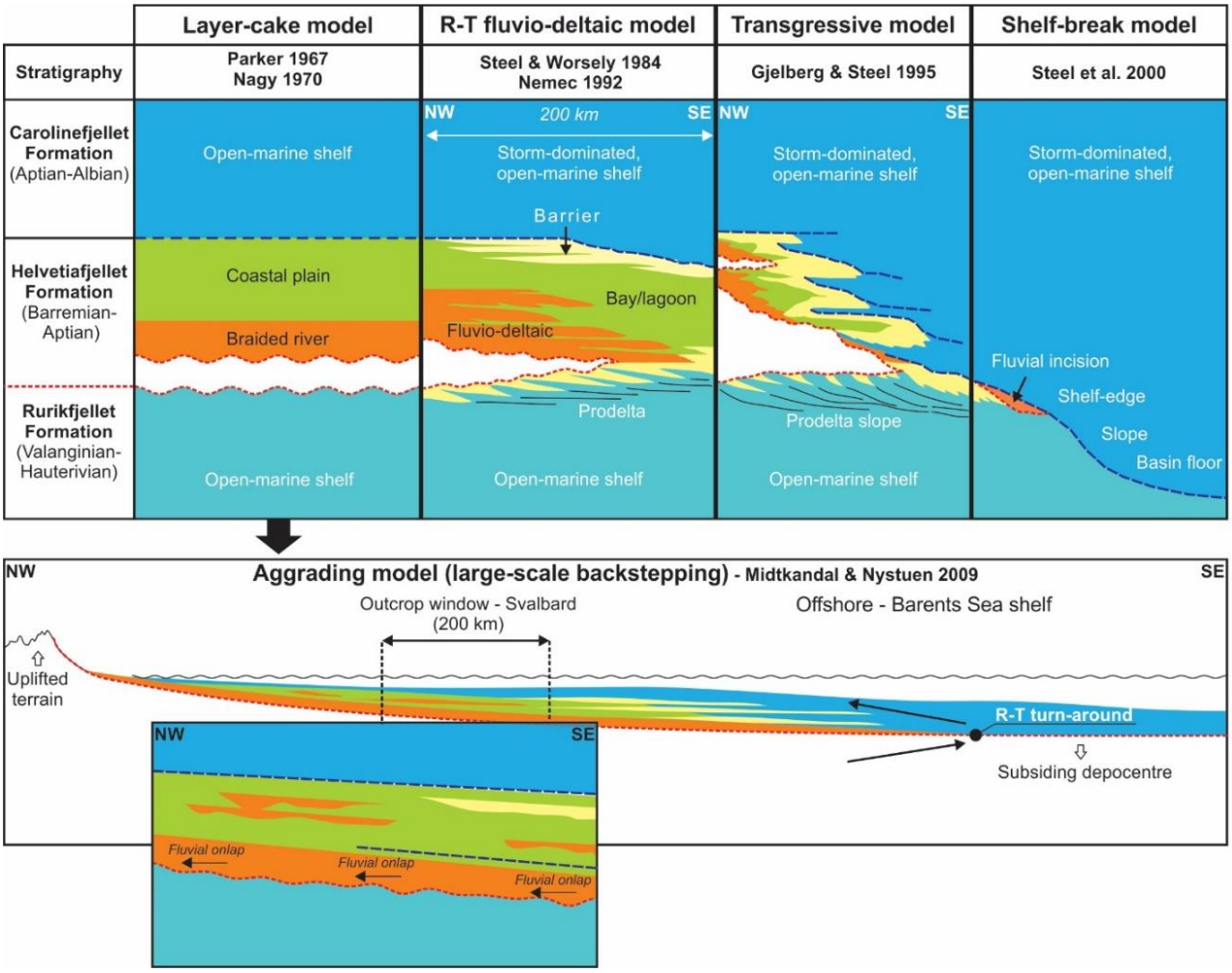

Figure 6: Simplified summary of the previous depositional models illustrating the development of the Helvetiafjellet Formation. Modified from Nemec et al., (1988), Nemec, (1992), Gjelberg & Steel, (1995), Steel et al., (2000), Midtkandal & Nystuen, (2009) and Grundvåg & Olaussen, (2017). Please see chapter 2.4 for further details.

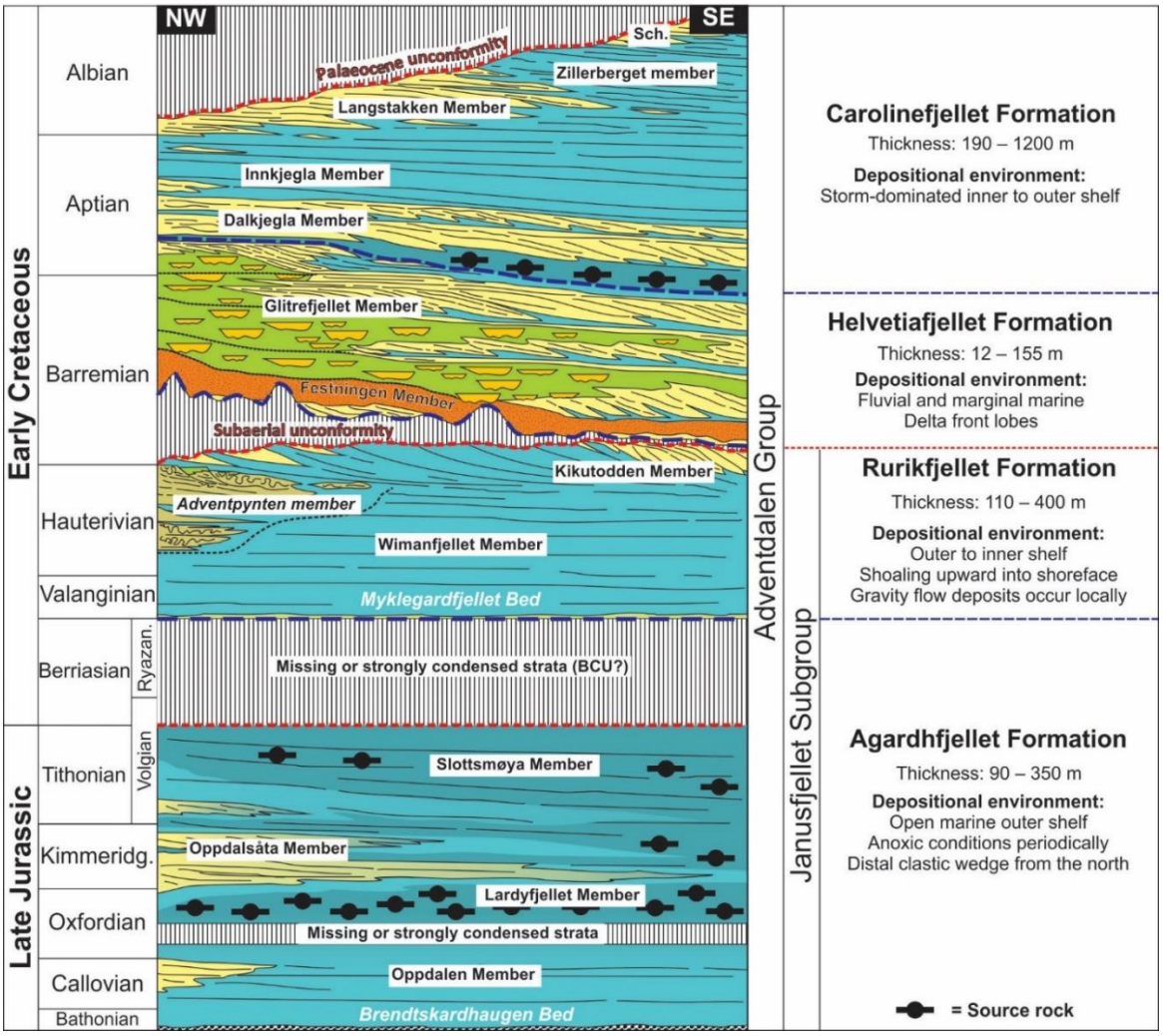

Figure 7: NW-SE trending cross-section illustrating the current lithostratigraphic understanding of the Rurikfjellet, Helvetiafjellet and Carolinefjellet formations. Retrieved from Grundvåg & Olaussen, (2017).

2.5 Age of the Helvetiafjellet Formation

The age of the Lower Cretaceous succession in Svalbard has been a long-standing problem with regards to geological age (Parker, 1967; Grøsfjeld, 1992; Hurum et.al, 2016; Midtkandal et al., 2016). Biostratigraphy is regarded as the traditional way to date a sedimentary succession. Within the Helvetiafjellet Formation however, macrofossils are scarce, thus making the dating of the succession problematic. Therefore, it was until recently common practice to use lithostratigraphy and relative ages as the primary tool for defining the age of Helvetiafjellet Formation. Plant and microfossils and dinoflagellates were also used where possible (Århus, 1992; Grøsfjeld, 1992; Hurum et.al, 2016). The discovery of bentonite within the Helvetiafjellet Formation offered a more precise way to determine the age of the formation (Corfu et al., 2013; Midtkandal et al., 2016; Polteau et al., 2016; Vickers et al.,

2017). In this section, the age of the Helvetiafjellet Formation will be discussed with references to both biostratigraphy and bentonite dating.

Parker, (1967) was the first to mention the age of the Helvetiafjellet Formation. In the article, the formation was assigned a Barremian age based on dating of ammonites and bivalves within the over and underlying formations. Lower Cretaceous dinoflagellate assemblages were detected in both the underlying Rurikfjellet Formation as well as within the Helvetiafjellet Formation (Grøsfjeld, 1992). Though the dinoflagellate assemblage could not be used to date the Helvetiafjellet Formation directly, it contributed to defining the age of the underlying formation. The age of the Rurikfjellet Formation was determined to be Valanginian and Valanginian to Hauterivian, as well as early Barremian in its uppermost parts (Grøsfjeld, 1992; Midtkandal et al., 2008; Grundvåg et al., 2017). Knowing that the overlying Carolinefjellet Formation was Aptian in age, a Barremian age was suggested for the Helvetiafjellet Formation (Grøsfjeld, 1992). Based on biostratigraphic data, the subaerial unconformity that defines the boundary between the Rurikfjellet and the Helvetiafjellet formations is interpreted to be earliest Barremian in age (Grøsfjeld, 1992; Grundvåg et al., 2017). It is therefore commonly referred to as a Barremian subaerial unconformity.

A bentonite layer was discovered in several of the onshore CO_2 wells in Svalbard (e.g. wells DH-3 and DH-5R; Fig. 9) within the upper part of the Helvetiafjellet Formation, in close proximity to the lithostratigraphical contact between the Helvetiafjellet and the Carolinefjellet formations (Fig. 7). This provided a more reliable method of dating for the formation. The bentonites found within the Helvetiafjellet Formation were dated to an age of 123.3+/-0.2 Ma, indicating a Barremian age for the formation (Corfu et al., 2013; Midtkandal et al., 2016; Polteau et al., 2016; Vickers et al., 2017). The boundary between the Helvetiafjellet and the Carolinefjellet formations was not as easily dated, and therefore has a broader age of Barremian-Aptian transition. This corresponds to an approximate age of 121-122 Ma (Midtkandal et al., 2016).

2.6 Palaeo-climatic indicators in the Lower Cretaceous succession

The Cretaceous period is known as one of the warmest periods recorded in Earth's history (Nemec, 1992; Harland & Kelly, 1997). This is interpreted to be related to overall greenhouse conditions on Earth, which prevented permanent ice caps from forming in polar areas (Nemec, 1992; Grundvåg & Olaussen, 2017). Consequently, the eustatic sea-level rose. In the Early Cretaceous period, the Svalbard archipelago was located at 63 to 66 ^{o}N (Torsvik et al., 2012; Hurum et al., 2016). The area was dominated by a relatively warm climate when considering its latitude at the time, with a mean temperature of 7-10^{o}C (Hurum et al., 2016 A; Grundvåg & Olaussen, 2017).

During the Barremian, the temperature gradients were low and the overall climate was relatively humid. This is supported by observations of coal seams, seatearths and transported tree remains, which also suggests abundant vegetation (Nemec, 1992; Harland et.al., 2007). Traces from several different dinosaur species have also been observed within the Lower Cretaceous succession (Heintz, 1962; Hurum et al., 2016). Examples here are Ornithopod and Iguanodon traces, observed within the Festningen Member of the Helvetiafjellet Formation. This furthermore supports the theory that the Early Cretaceous in Svalbard was dominated by abundant vegetation, which was luxuriant enough to support a herbivore dinosaur population (Heintz, 1962; Nemec, 1992; Hurum et al., 2016).

However, there has been some debate with regards to the climate in the Early Cretaceous in Svalbard. Despite the abovementioned indicators of an at least seasonally warm climate, observations that contradict this have also been made. Belemnites have been reported within the Lower Cretaceous succession in Svalbard, and were identified as Arctic belemnites (Harland & Kelly, 1997; Price & Nunn, 2010). Glendonites ($CaCO_3 \cdot 6H_2O$), which are calcite pseudomorphs of the mineral ikaite (Suess et al., 1982), alongside observations of potential ice rafted debris are both indicative of cold, polar oceanic conditions (Harland & Kelly, 1997; Price & Nunn, 2010; Hurum et al., 2016 A). This suggests that the shelf area of Svalbard was at least periodically influenced by polar water during the Early Cretaceous, rather than solely being dominated by warm climatic conditions (Price & Nunn, 2010; Grundvåg & Olaussen, 2017).

In his article, Nemec, (1992) proposes three main factors that control vegetation growth in an area. These are climate, ground-water conditions and clastic environment. Based on the abovementioned observations, the climate appears to have been relatively favourable with regards to plant growth. Because parts the Helvetiafjellet Formation are interpreted to have been deposited in alluvial plain environments, it is fair to assume that the ground-water levels were relatively high. A regional transgression, accompanied by a relative sea-level rise also contributed to an interpreted high ground-water table. These factors also accommodate plant growth.

However, although the climatic and ground-water conditions are interpreted to have been favourable in the Early Cretaceous period in Svalbard, thick coal deposits are lacking within the succession. This could potentially be caused by the third controlling factor on plant growth; the rate of sediment supply in a clastic environment. In an alluvial plain environment the sediment input can be very high, therefore inhibiting thick accumulations of organic material. Changes in sea-level can also affect sediment deposition. Nemec, (1992) describes the periods of time with less clastic sedimentary input as local “windows”. It is within these windows of relatively low sedimentary input that organic material was allowed to accumulate in larger quantities.

The accumulation of organic material is an important factor to consider when discussing palaeo-climatic indicators. This is because the palaeosols that can develop in relation to this accumulation are regarded as important indicators of past climates, because they can preserve evidence of the climatic conditions under which they were formed (Bown & Kraus, 1987; Mack & James, 1994). As a detailed study of the palaeosols that occur within the Glitrefjellet Member has never previously been conducted, the palaeosols potentially hold new information with regards to the dominating palaeo-climatic conditions during the Early Cretaceous period.

2.7 Palaeosol theory

In this section, some general theory with regards to palaeosols and what their development is dependent on will be covered.

2.7.1 The definition of a palaeosol

A palaeosol can be defined as a fossil soil, which was created by the soil forming processes that occurred on an ancient surface (Mack et al., 1993; Kraus, 1999; Retallack, 2001; Sheldon & Tabor, 2009). Palaeosols are most commonly observed in sedimentary rocks (Kraus, 1999), but have also occasionally been observed in weathered basement rocks (Mohanty & Nanda, 2015). Palaeosols were first recognized in the Quaternary record (Kraus, 1999), but are now observed in strata dating back to Precambrian (Gay & Grandstaff, 1980; Gall, 1992).

From the surface moving down into the subsurface, different factors such as sunlight, water and bioturbation will influence the soil in varying degree. It is therefore common to see layering within a soil profile. These are often referred to as soil horizons (Mack et al., 1993; Retallack, 2001; Buol et al., 2011). Continuous deposition will over time bury the underlying soil profiles. Burial of the soil profiles effectively inhibits further influence of soil forming processes. The soil forming processes are thus terminated and a palaeosol is formed. Because palaeosols form relatively quickly and their characteristics are largely dependent on climatic factors, palaeosols are regarded as excellent palaeo-climatic indicators (Cecil & Dulong, 2003; Sheldon & Tabor, 2009).

Although the definition of a palaeosol is relatively clear, there is however, some disagreement as to what the definition of a soil is. The term soil is often used in day-to-day speech. Consequently, the term has various definitions. In geology, a relatively wide definition is often used. Retallack (2001) defines a soil as "*material forming the surface of a planet or similar body and altered in place from its parent material by physical, chemical and biological processes*". This definition of a soil is wide enough to include almost all landmasses. The exceptions here are river and lakes, as well as areas that recently have been under the influence of erosion. For this thesis, the definition of a soil presented by Retallack, (2001) will be used.

2.7.2 Factors influencing soil formation

Many different factors can be influential when soils are forming. The maturity of a soil is a measurement of the degree of alteration that the parent sediment or bedrock has undergone (Mack et al., 1993; Kraus & Aslan, 1999). In the following sections, some of the most important factors with regards to soil formation are described.

2.7.2.1 Water

Water is one of the most important factors with regards to soil formation. The amount of water that is present within a specific environment is dependent on a number of factors. The most significant are rainfall, ground-water level, soil-drainage and evaporation (Retallack, 2001). An overview of the relationship between the overall climate in an area and the number of wet months was made by Cecil & Dulong, (2003). Here, a wet month is defined as a month where rainfall exceeded evaporation. The authors defined the amount of rainfall required in a month to be approximately 100 mm. Cecil et al., (2003) then developed an overview of which soils are likely to form based on the number of wet months. By linking the two models together, it is possible to predict which type of palaeosol is likely to form in an area based on the dominating climatic conditions. The two models are presented in Fig. 8.

However, the two models presented in Fig. 8 have been interpreted as most representative for tropical to subtropical areas. A requirement is that the area has to be free of frost the majority of the year, with the exception of in mountainous areas. Because the Cretaceous period is known as a greenhouse period, and Svalbard was located further south than it is today, at 63-66 ^{O}N (Hurum et.al. 2016; Hurum et al., 2016 A; Grundvåg & Olaussen, 2017), it is fair to assume the principles presented in Fig. 8 are valid for palaeosols found in the Cretaceous succession in Svalbard.

Model A (Fig. 8 A) provides an overview of the most common climates the Earth can be subdivided into, with arid being the driest and perhumid being the wettest. Model B (Fig. 8 B) displays the different palaeosols that are expected to develop depending on the number of wet months that occur in a year. Following the model, it becomes apparent that entisols and inceptisols can develop almost regardless of number of wet months, while for instance the development of an aridisol is dependent on few wet months.

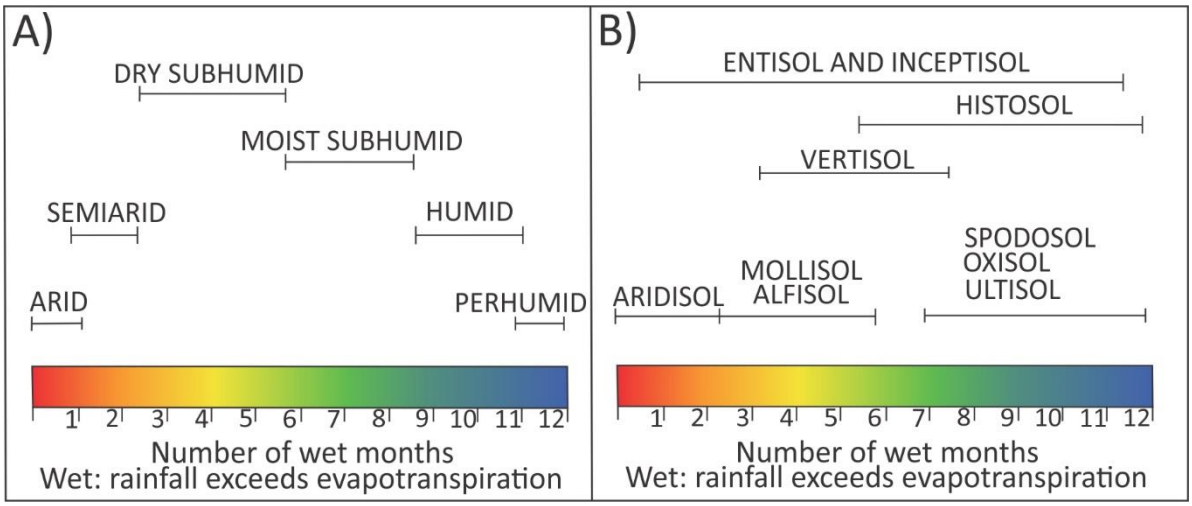

*Figure 8: Model describing (**A**) different climatic conditions and (**B**) the expected palaeosols developed based on number of wet months in an area. Retrieved from Cecil et al., (2003).*

2.7.2.2 Temperature

The temperature of an area in which a soil is forming can have a drastic impact on the rate of soil formation. For example, if the temperature of an area was raised by 10^{O}C, the rate of the chemical processes taking place would multiply (Retallack, 2001). Such a change in temperature would thus significantly influence the rate of soil development and soil maturity. This can also be seen in present time, where soils that are formed in warmer climates near equator tend to be more developed than soils developing in colder regions (Retallack, 2001).

2.7.2.3 Time

The amount of time the soil forming processes are allowed to rework the parent material will also greatly influence the maturity of a soil. Different characteristics within a soil profile develop in a varying time-span. For example, vertic fractures can be expected to form after tens of years, while distinguishable horizons within the profile can take thousands of years to develop (Wright, 1992). Generally speaking, the longer the soil forming processes are allowed to rework the parent material, the more developed and mature the soil will become (Bown & Kraus, 1987).

2.7.3 Climatic influence on soil formation

Climate is typically defined as the average weather that occurred over a period of 30 years (Retallack, 2001). While weather can change over a matter of hours, a change in climate can take several thousand years to become apparent. Kottek et al., (2006) developed a system, commonly referred to as the world classification of climate. This system is based on temperatures and seasonality, and is a common way to classify the different climate zones on Earth. As it is stated above, it becomes clear that several climatic factors, such as precipitation and temperature, are significant in determining the rate of the soil forming process that take place. Therefore, the dominating climate in an area will influence both the rate of soil formation and the characteristics of the soil that is formed. Due to this close link, palaeosols are considered as important sources of information in palaeo-climatic reconstruction (Mack & James, 1994; Sheldon & Tabor, 2009).

3 Methods

3.1 Study area

Seven wells were drilled in the Adventdalen area, in relatively close proximity to Longyearbyen (Fig. 9). The wells were drilled in relation to the CO_2 sequestration and capture project (Braathen et al., 2012). The main target of the wells was an inferred reservoir consisting of Jurassic and Upper Triassic deposits. The Lower Cretaceous succession, including the Helvetiafjellet Formation were cored as well. The location of the different drill hole sites are indicated in Fig. 9 C.

Lower Cretaceous strata is generally well preserved, and is primarily exposed in the south and west of Svalbard (Fig. 1). As a result of the West Spitsbergen Fold Belt (WSFB), the exposed strata is observed dipping steeply on the western coast of Spitsbergen (Parker, 1967; Fig. 9 B). Despite the fact that the drill sites for DH-1 and DH-1A are located near the WSFB, the Lower Cretaceous succession is still approximately horizontal. A semi-regional detachment zone can be recognized at the bottom of the Lower Cretaceous strata in the study area (Braathen et al., 2012). Based on previous palaeogeographic reconstructions of the deposition the Helvetiafjellet Formation, the clastic source area has been interpreted to have been located in the W-NW (Steel & Worsley, 1984; Worsley, 1986; Gjelberg & Steel, 2012). Therefore, the sediments within cores DH-1 and DH-1A are interpreted to represent the proximal areas of the Helvetiafjellet Formation.

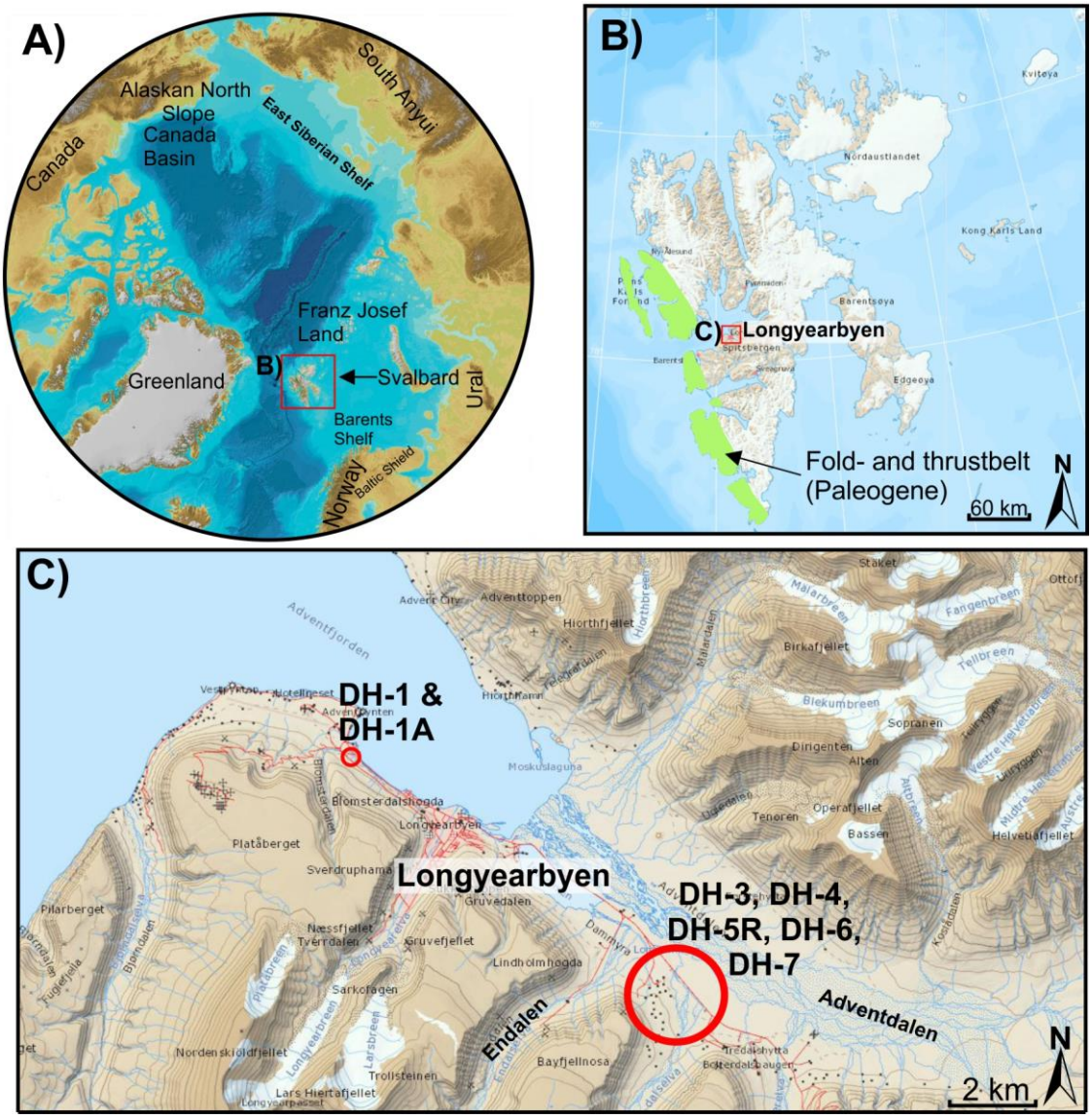

*Figure 9: **A)** Bathymetry map indication the location of the study area. The map is retrieved from IBCAO (https://www.ngdc.noaa.gov/mgg/bathymetry/arctic/maps/version3_0/) **B)** Map of Svalbard, the location of the investigated cores indicated with a red square. **C)** Topographic map that indicates the location of the drill hole sites drilled in the Adventdalen area. In this thesis, cores DH-1 and DH-1A were used. The image is retrieved from http://toposvalbard.npolar.no/.*

3.2 Data collection and analysis

For this thesis, cores DH-1 and DH-1A were logged from 216–144 meters and 214–142 meters below the present day surface, respectively. One sedimentary log (1:50 cm) was produced for each of the cores. These logs illustrate the observed lithological changes, sedimentary structures and facies variations occurring within the Helvetiafjellet Formation, and are presented in their entirety in Appendix A.

The cores were stored in a container at UNIS in Longyearbyen, Spitsbergen. The logging took place from September 24th to October 2nd, with guidance from supervisor Assoc. Prof. Sten-Andreas Grundvåg (UiT) and co-supervisor Prof. Snorre Olaussen (UNIS). The equipment that was used in the logging process was a tool for grain size measurement, a folding rule, graph paper, a geological hammer, a hand lens and a camera.
The cores were logged in 1:50 cm scale. Grain size, primary and secondary sedimentary structures, bed thickness, colours, boundaries, and degree of bioturbation were thoroughly noted, thus forming the basis for the detailed facies analysis presented in Thesis 1 by Thea Engen. In relation to Thesis 2, special attention was given to the identification of coal seams and associated root structures, and from this identify potential palaeosols. Palaeosols were described and classified according to the nomenclature and standards proposed by Retallack, (1988).

For the thin section analysis in this study, twenty-four rock samples were collected by using a hammer and a chisel. All samples were collected from core DH-1. In addition, four samples were collected for XRD-analysis from one of the chosen palaeosols (PS 2) observed within the core. Sixteen of the samples were taken in relatively even intervals throughout the entire Helvetiafjellet Formation, or where significant lithological changes were observed. Where the potential palaeosols occurred, the samples were taken at a closer sampling interval for a more detailed analysis. Eight samples were taken in total for this purpose. The stratigraphic levels from which the samples were taken are indicated in Figs. 23, 27 & 33.

The samples used for petrographic analysis were cut into smaller pieces using a rock saw, and thin sections were produced at the laboratory at the Department of Geosciences at UiT, The Arctic University of Norway. All thin sections were successfully produced, with the exception of thin section 21, which was the uppermost sample collected from Palaeosol 2.

The sample was prone to breaking due to internal pressure and as a result, it was not possible to glue the sample on to a glass plate and further produce it into a thin section.

3.3 Post data collection work

One presentation log (1:200 cm; Figs. 23 & 24) for each of the cores was made based on the observations noted in the original raw logs. Two of the potential palaeosols observed within core DH-1 are presented in logs of a more detailed scale (1:10 cm; Figs. 27 & 33). All logs are presented in the following chapters. CorelDraw was used in order to produce the best visualization of all figures presented in this thesis.

3.3.1 Optical microscopy

The microscope used for the petrographic study was a Leica DMLP Polarizing Microscope. Both plane and cross-polarized light was used to determine the mineralogical composition of the thin sections. In the seven successfully produced thin sections from potential palaeosols, special attention was also given to the identification of root structures, organic material and minerals that could be telling with regards to climatic conditions at the time of deposition.

The microscope had a Leica DFC450 Digital Microscope Camera attached to it. This allowed for detailed photomicrographs to be taken where interesting features were observed within the thin sections. This was a valuable resource when describing and interpreting the palaeosols found in core DH-1, as well as documenting the change in mineralogical composition occurring throughout the core.

3.3.2 XRD-analysis

XRD is short for x-ray powder diffraction. The method was developed based on the assumption that the reflection produced by an x-ray when it comes into contact with a crystal surface will depend upon the crystalline structure. Therefore, different minerals will produce different reflection patterns thus allowing us to distinguish individual minerals within a sample (Cullity, 1978).

The XRD-analysis was performed by EARTHLAB at the University of Bergen. Prior to the samples being sent to Bergen, they were crushed into a suitable grain size. Because the samples were extracted from solid rock cores, the crushing process was divided into two steps. First, the samples were crushed into relatively coarse grains and rock fragments. This was executed using the Retsch Jaw Crusher. This machine has the ability to reduce material

of up to 90 mm down to an individual grain size of around 3 mm.
For XRD-analysis however, a grain size of 5 µm or less is desirable. Therefore, further preparation was required. To achieve such a fine grain size the Retsch Planetary Ball Mill PM 100 was used. In this apparatus, one sample at a time was placed into a hollow cylindrical container along with small steel balls. The number of balls is dependent on the volume of the sample. The container was then secured onto the Planetary Ball Mill, and the machine began to rotate. The rotating speed was set to 475 rounds per minute, and the duration varied from fifteen to twenty-five minutes in order to obtain the desired grain size. The cylinder was then thoroughly cleaned and the process was repeated for each of the four samples.

4 Results

4.1 General petrographic observations of the Helvetiafjellet Formation

In the following section, the various minerals and materials observed in the thin sections collected from core DH-1 are accounted for. Because the drill sites for cores DH-1 and DH-1A were only 20 m apart, it is fair to assume that the interpretations made with regards mineralogical characteristics observed within cores DH-1 are also valid within core DH-1A.

4.1.1 Monocrystalline quartz

Description

Plane polarized light

The mineral is transparent in colour and has a low positive relief (Fig. 10 PPL). The mineral grains vary in size within each investigated thin section throughout the core. Grain shape also varies throughout the Helvetiafjellet Formation, where sub-angular to sub-rounded grains are most frequently observed. An anhedral crystal shape is typically observed regardless of the individual grain size. No apparent cleavage is observed.

Cross-polarized light

When observed through cross-polarized light, the mineral appears to be optically uniaxial. The mineral also displays weak birefringence, changing from white to grey in colour (Fig. 10 XPL). For some grains, the colour-change is instantaneous for the entire grain. In other grains however, the colour-change shifts as the grain is rotated. This results in different sections of a single grain being blackish grey while the remainder of the grain is still white. Some overlapping along the crystal margins is also observed where the crystals appear to be tightly packed. This can be observed in both plane and cross-polarized light, but is more easily detected in the latter of the two (Fig. 10 XPL).

Interpretation

Based on the observations made in both plane and cross-polarized light, this mineral fits well with the characteristics of quartz, as they are presented by Nesse, (2012). Due to the fact that the quartz occurs as single grains, it can be further classified as monocrystalline quartz. In general, most sandstones are composed of around two-thirds quartz (Boggs, 2009). This is largely due to the resistant nature of quartz. As other minerals are removed or altered due to physical and chemical weathering, the quartz remains relatively unaltered (Boggs, 2009).

This fits well with observations in DH-1 and DH-1A (Fig. 23 & 24), where quartz-rich sandstones were abundant. The observation of quartz is also consistent with previous studies of the formation (Edwards, 1979; Prestholm & Walderhaug, 2000; Maher et al., 2004). The authors have all described quartz as the dominant detrial mineral within the formation. In the units where the quartz content was estimated to be >95%, the rocks are defined as quartz arenites. The gradual colour-change observed in some quartz grains when viewed in cross-polarized light is interpreted as undulose extinction, as described by Maher et al., (2004).

The overlapping observed along the margins of some quartz grains is interpreted as quartz overgrowth, which is an effect of pressure solution and re-cementation (Waugh, 1970). The compaction and increase in temperature that occurs with post-depositional burial can cause the quartz grains to react with each other, thus precipitating quartz cement, which is also referred to as quartz overgrowth. Compaction and overgrowth will typically lower the pore space within a sedimentary rock (Waugh, 1970; Worden & Burley, 2003).

Previous studies have also observed the presence of quartz overgrowths within the Helvetiafjellet Formation (Edwards, 1979; Prestholm & Walderhaug, 2000). Prestholm & Walderhaug, (2000) described quartz overgrowths as the most commonly occurring diagenetic phase within the formation. Where packing was tight and little matrix was present, quartz overgrowth was more extensive. Examples of monocrystalline quartz and quartz overgrowth, both in plane and cross-polarized light are presented in Fig. 10.

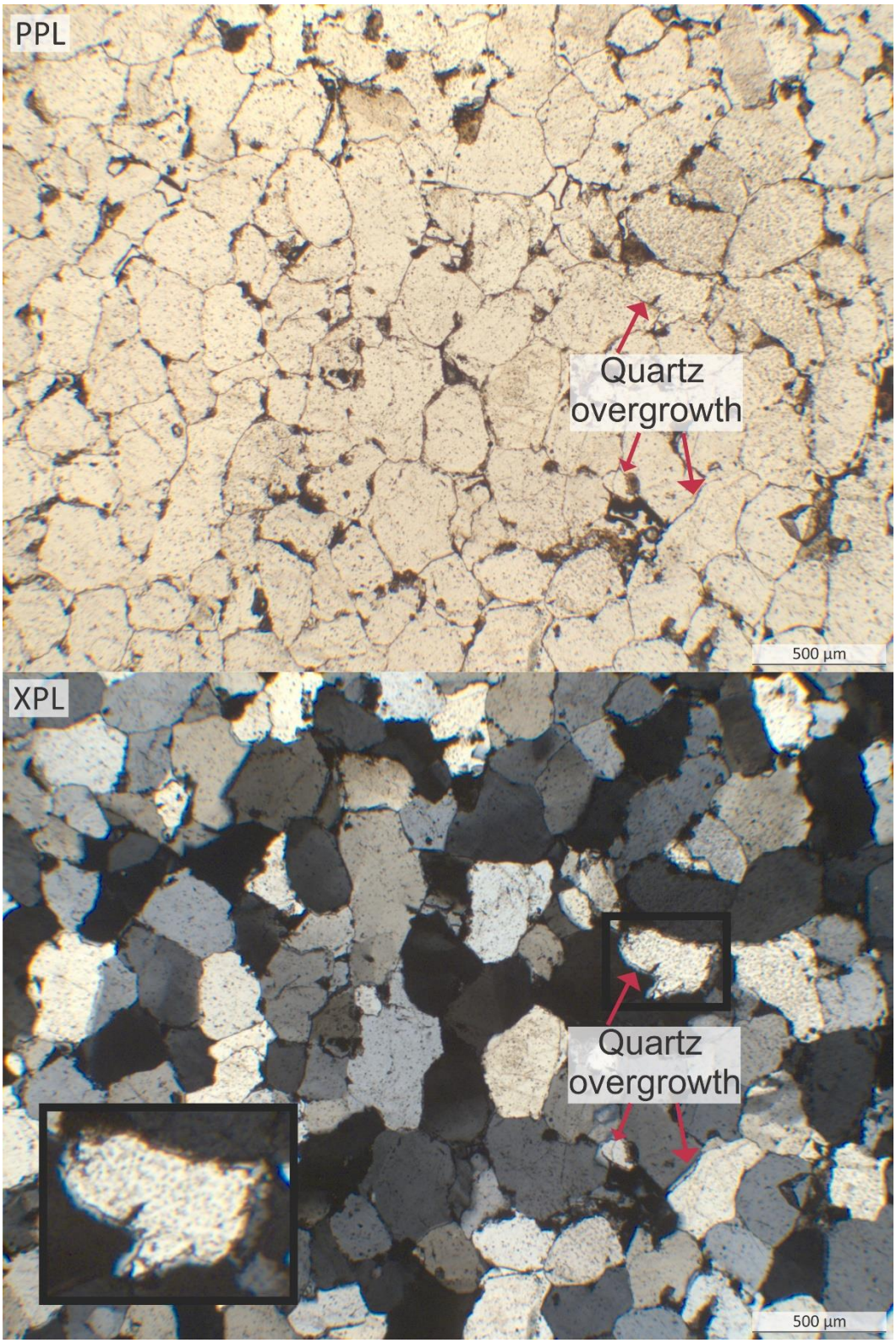

Figure 10: Representative photomicrograph of the monocrystalline quartz observed in the Helvetiafjellet Formation. PPL stands for plane polarized light and XPL stands for cross-polarized light. The red arrows point to some of the places where quartz overgrowth occurs, as a result of diagenesis. The quartz overgrowth around an individual quartz grain is also highlighted in the lower left-hand corner. The quartz in this photomicrograph was observed in thin section 10, and its location within the Helvetiafjellet Formation can be seen in Fig. 23. The quartz present in this thin section was well cemented, and little matrix was present. Throughout this thesis, all thin section images are oriented with the correct way up, in accordance with the samples occurrence within the core DH-1.

4.1.2 Polycrystalline quartz

Description

Plane polarized light

The crystal shape of the mineral is primarily anhedral. The mineral is mainly transparent, but is occasionally observed with a very light brown colour. The grains have a low positive relief. No apparent cleavage is observed. However, the mineral can commonly be recognized by a distinct, grainy texture on the surface of the grains (Fig. 11 PPL).

Cross-polarized light

The mineral is optically uniaxial. The grains show weak birefringence. When the mineral is rotated in cross-polarized light, different areas of the grain changes from white to grey at different positions (Fig. 11 XPL). Its appearance is comparable to many small crystals confined within a larger grain. As described for monocrystalline quartz, the outer perimeter of some of the crystals are irregular in shape and can occasionally be observed overlapping each other.

Interpretation

Overall, the mineral has many characteristics in common with monocrystalline quartz (Chap. *4.1.1*), with the exception of its distinctive appearance when viewed in cross-polarized light, and the grainy texture observed in plane polarized light. The mineral is therefore interpreted as polycrystalline quartz. Polycrystalline quartz can be defined as quartz grains that are composed of two or more quartz crystals. It can also be referred to as composite quartz (Boggs, 2009). Similarly to monocrystalline quartz, polycrystalline quartz is a relatively common mineral in sandstones, and was observed by both Edwards, (1979) and Prestholm & Walderhaug, (2000) within the Helvetiafjellet Formation. Some quartz overgrowth as a result of pressure solution and re-cementation was also observed in association with the polycrystalline quartz. An example of both the observed polycrystalline quartz and quartz overgrowth is presented in Fig. 11.

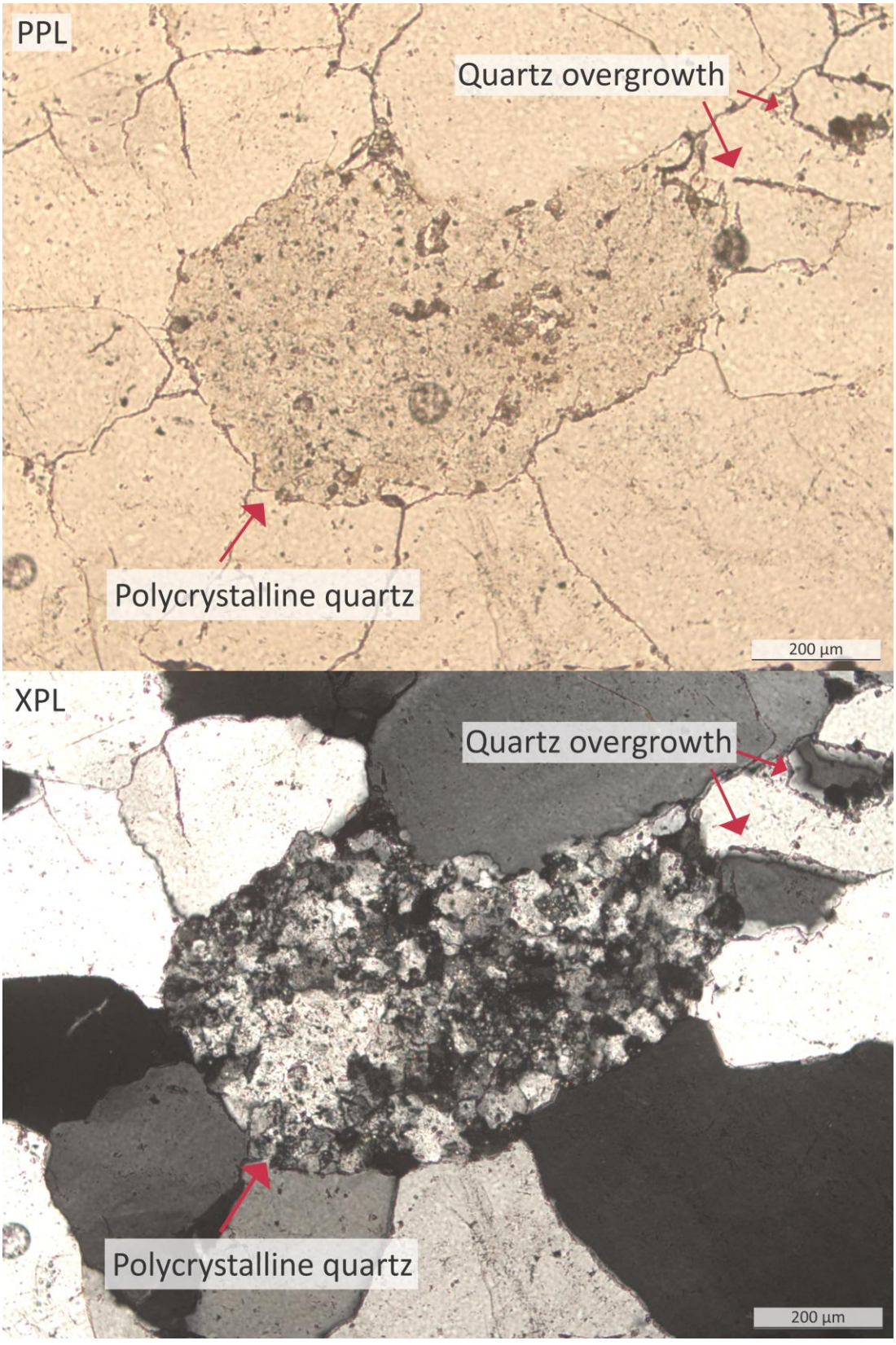

Figure 11: The mineral in the centre of the photomicrograph is interpreted as polycrystalline quartz, which is recognized as quartz grains that are composed of two or more crystals. In the figure, PPL stands for plane polarized light, and XPL stands for cross-polarized light. Examples of quartz overgrowth are also highlighted. This quartz grain was observed in thin section 24, and its location within the Helvetiafjellet Formation is indicated in Fig. 23.

4.1.3 Plagioclase feldspar

Description

Plane polarized light

The grains of the mineral are typically relatively small and an anhedral crystal shape is typically observed. The mineral is transparent in colour and displays a low, positive relief (Fig. 12 PPL). No cleavage is observed. When observing the mineral through plane polarized light, it bares many similarities to the previously described monocrystalline quartz (Chap. *4.1.1*).

Cross-polarized light

The grains of the mineral displays black and white parallel lineations as the thin section is rotated. The lineations are very straight and parallel (Fig 12 XPL). The change in colour from black to white is relatively abrupt.

Interpretation

The lineations observed within the mineral are interpreted as lamellar twinning. Due to the very parallel nature of the observed twinning, the mineral is interpreted as plagioclase feldspar (Nesse, 2012). Plagioclase feldspar is also an important component in many sandstones (Boggs, 2009). This is consistent with the observation of previous studies, where plagioclase feldspar was observed as the dominant feldspar within the Helvetiafjellet Formation (Edwards, 1979; Prestholm & Walderhaug, 2000; Maher et al., 2004). Sandstone with a strong plagioclase feldspar component has previously been observed within the Helvetiafjellet Formation, and has been linked to the emplacement of the HALIP (Maher, 2001; Maher et al., 2004; Senger et al., 2014).

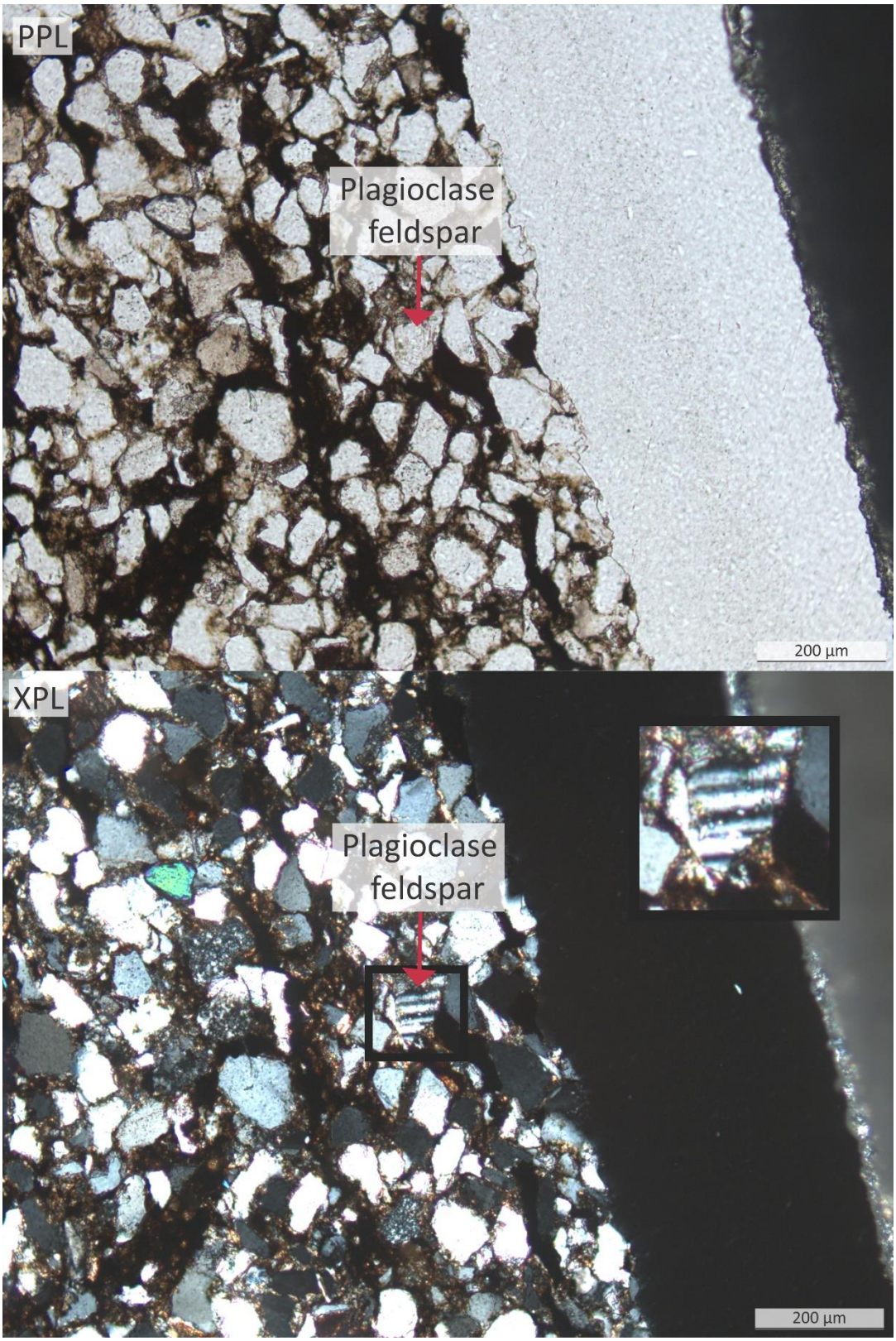

Figure 12: Representative photomicrograph of plagioclase feldspar observed during thin section analysis. The mineral was largely identified based on the presence of lamellar twinning. The plagioclase feldspar is indicated with a red arrow, but is also enhanced in the upper right-hand corner. In the image, PPL stands for plane polarized light, and XPL stands for cross-polarized light. This example of plagioclase feldspar was observed in thin section 2, and its location within the Helvetiafjellet Formation is indicated in Fig. 23. The large white (PPL)/black (XPL) area seen on the right-hand side indicated the margin of the thin section. This area is void of lithic material.

4.1.4 Potassium feldspar

Description

Plane polarized light

The mineral is composed of irregular shaped grains and is typically observed with an anhedral crystal shape. The mineral is transparent in colour and has a low positive relief (Fig. 13 PPL). No apparent cleavage is observed. Overall, this mineral is very similar to the previously described monocrystalline quartz (Chap. *4.1.1*) when viewed in plane polarized light.

Cross-polarized light

When the thin sections is rotated under cross-polarized light, relatively thin lineations are observed. The lineations form relatively parallel to each other, but are somewhat uneven in shape. The lineations are spaced relatively close together (Fig. 13 XPL).

Interpretation

The relatively parallel lineations observed in cross-polarized light are interpreted as examples of simple twinning. Based on the characteristics presented by Nesse (2012), the mineral is interpreted as potassium feldspar (K-feldspar). This mineral group can also be referred to as alkali feldspar (Boggs, 2009). Based on the relatively parallel nature of the twinning, the K-feldspar presented in Fig. 13 is likely to be monoclinic. The most likely minerals in this category are sanidine or orthoclase. Previous petrographic studies of the Helvetiafjellet Formation have revealed the presence of small amounts of K-feldspar within the formation (Edwards, 1979; Prestholm & Walderhaug, 2000).

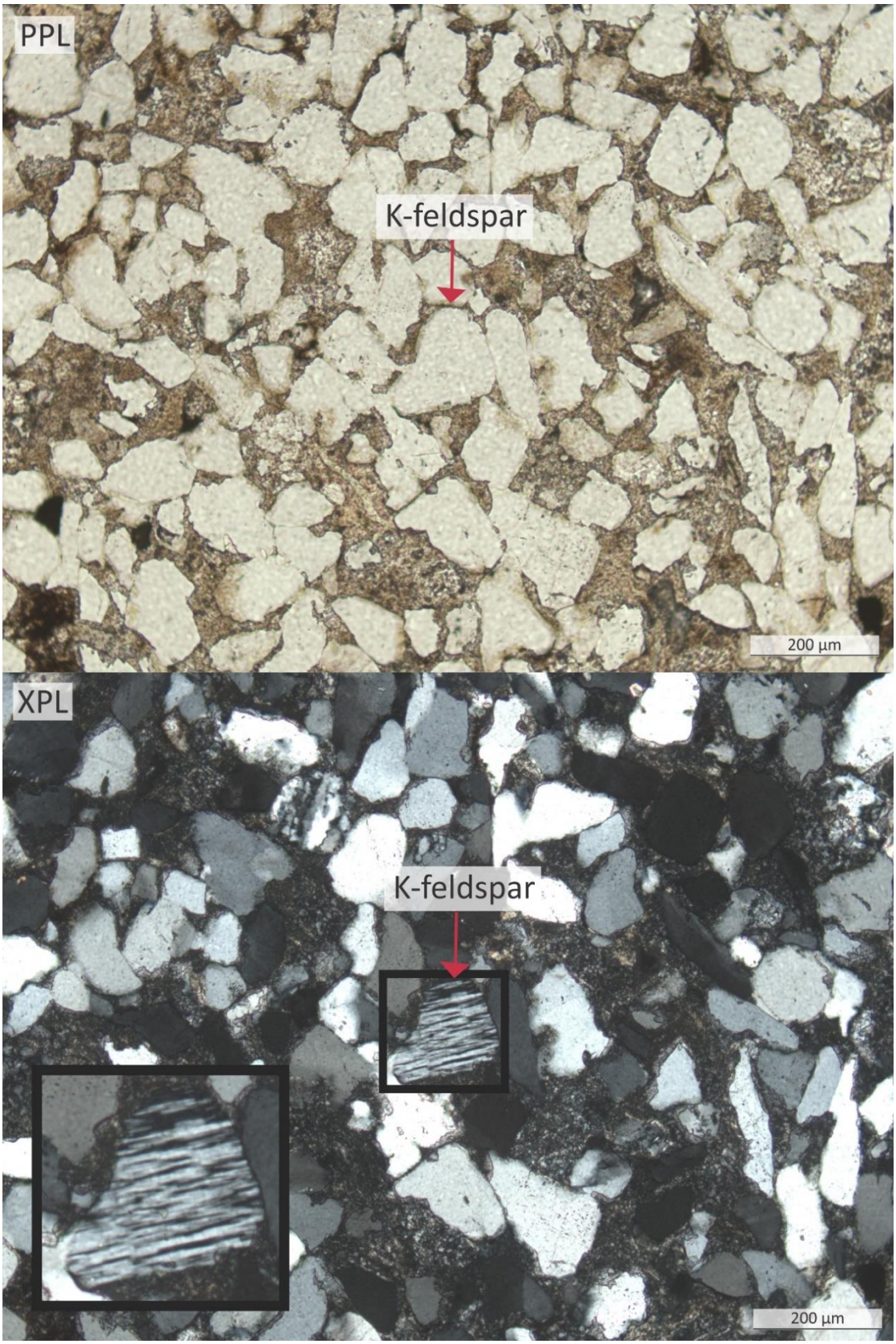

Figure 13: Representative photomicrograph of K-feldspar observed during thin section analysis. The K-feldspar is indicated with a red arrow. PPL stands for plane polarized light, and XPL stands for cross-polarized light. This K-feldspar grain was observed in thin section 18, and its location within the Helvetiafjellet Formation is indicated in Fig. 23. The K-feldspar grain is also enlarged in the lower left-hand corner of the figure (XPL).

4.1.5 Micas

Description

Plane polarized light

The observed mineral is typically transparent or light brown in colour. The crystal shape is subhedral to euhedral. The mineral stands out when compared to most other minerals within the thin section, which suggests a higher relief. The mineral can also be recognized by a perfect cleavage in one direction (Fig. 14 PPL & 15 PPL).

Cross-polarized light

The mineral displays a strong birefringence. Throughout the thin sections, the mineral was observed with blueish green to yellow colours (Fig 14 XPL.) while in other thin sections, it is dominated by red, golden and orange colours (Fig 15 XPL). When referencing to the Michel-Lévy Interference Color Chart (Appendix B), such colours are consistent with second-order interference colours.

Interpretation

Based on the crystal shape, the perfect cleavage in one direction and strong birefringence, this mineral is interpreted as mica. However, the colour of the mica is observed to vary throughout the different thin sections. As a result, two different sub-categories of mica have been identified within the Helvetiafjellet Formation. Pink, yellow and blue interference colours are often seen in muscovite (Nesse, 2012; Fig. 14 XPL), while a red to orange colour is more common for biotite (Nesse, 2012; Fig. 15 XPL).

Muscovite has previously been described as the most commonly occurring mica within the Helvetiafjellet Formation, while biotite has been less frequently observed (Prestholm & Walderhaug, 2000; Maher et al., 2004). This is consistent with the observed mineralogical composition of cores DH-1 and DH-1A (Table 1). Mica is relatively common in sandstones, especially if the sandstone is regarded as immature. When the occurrence of mica is observed to be around 1%, as it generally was in the thin sections of the present study, the mineral can be defined as an accessory mineral (Boggs, 2009).

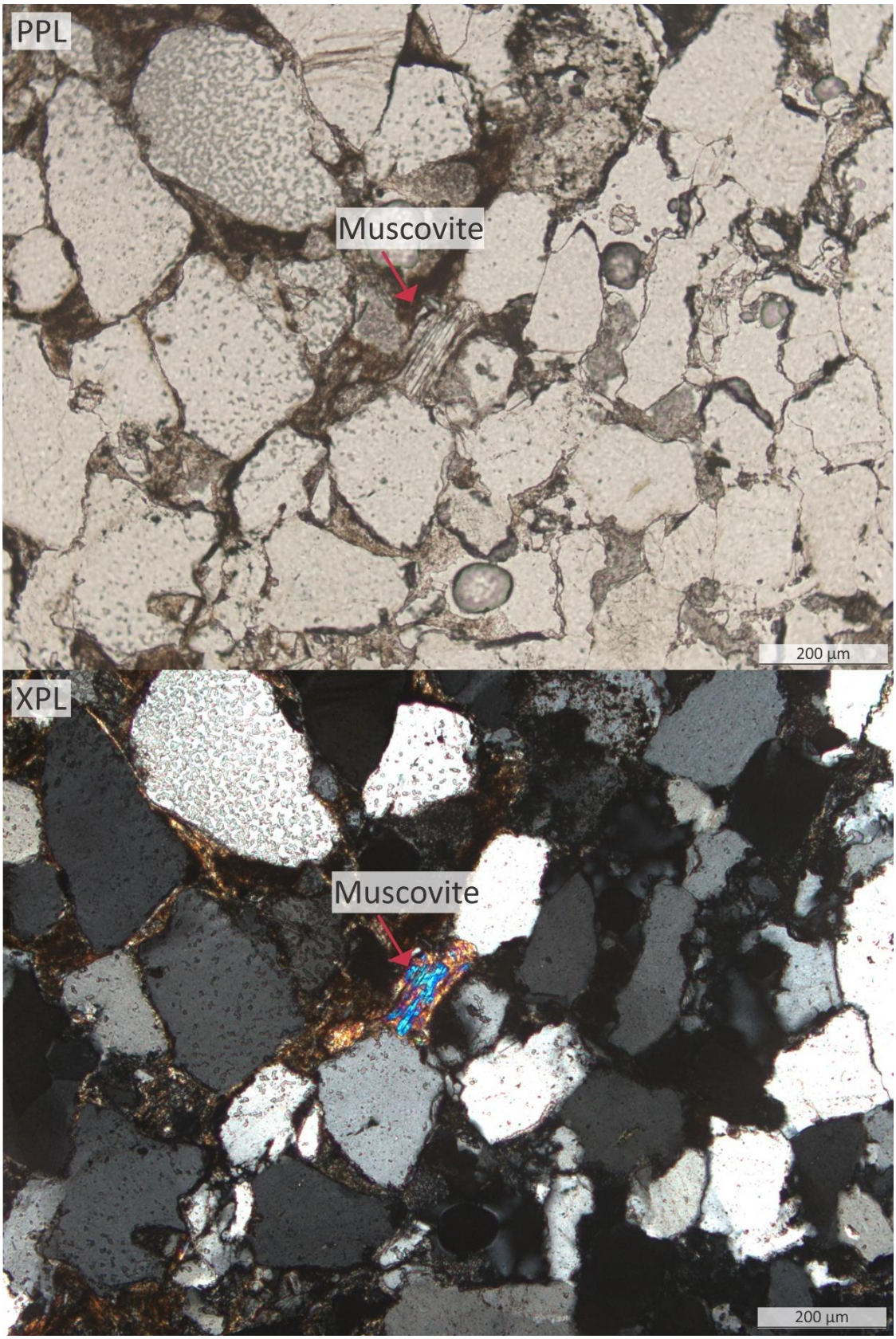

Figure 14: Representative photomicrograph of mica observed within the Helvetiafjellet Formation, indicated with a red arrow. Based on its colour when viewed in cross-polarized light, the mineral was interpreted as muscovite. PPL stands for plane polarized light, and XPL stands for cross-polarized light. This mineral was observed in thin section 11, and its location within the formation can be seen in Fig. 23.

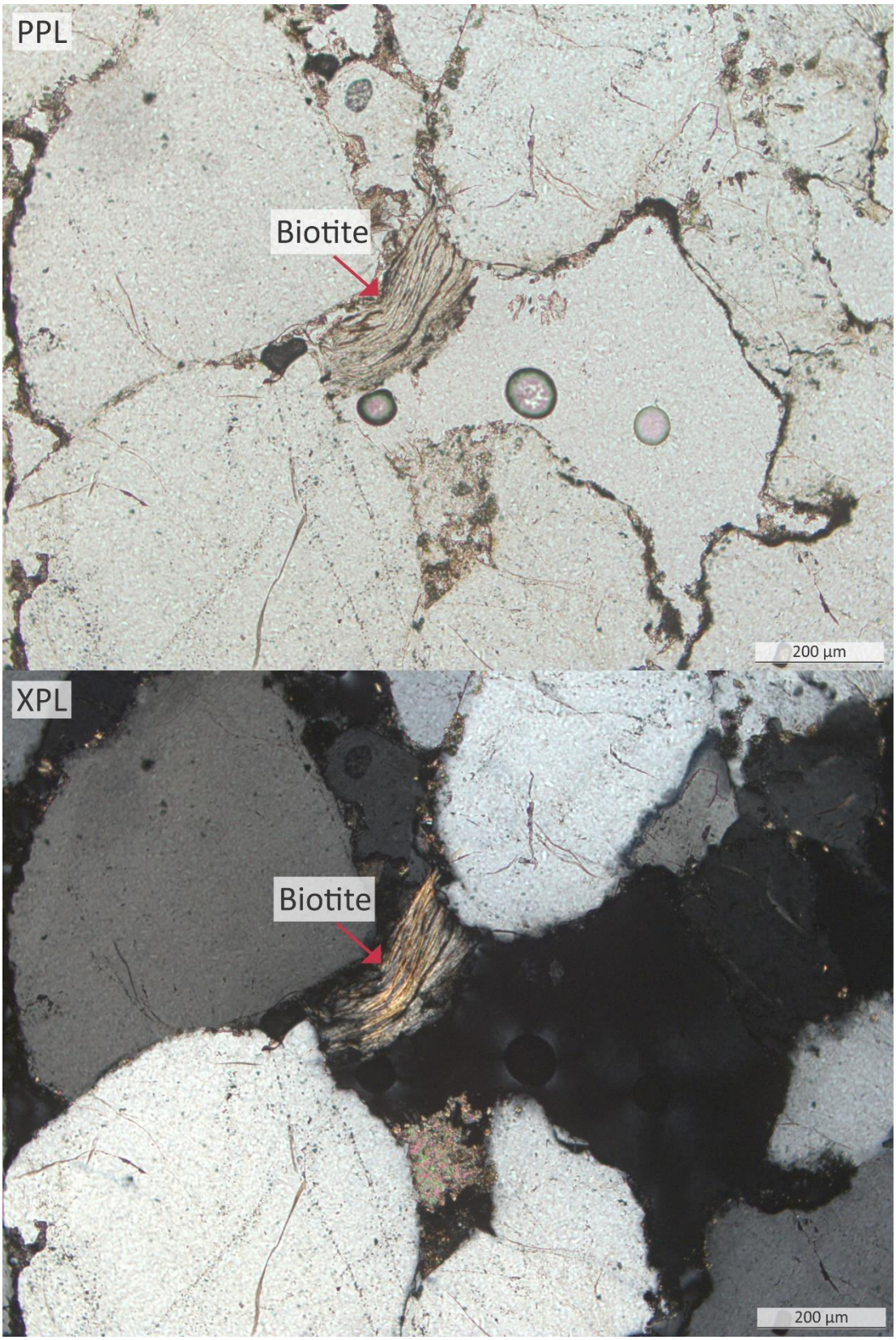

Figure 15: Example of mica observed within the Helvetiafjellet Formation. Based on its colour when viewed in cross-polarized light, the mineral is interpreted at biotite. PPL stands for plane polarized light, and XPL stands for cross-polarized light. The biotite is indicated with a red arrow. This photomicrograph is taken from thin section 12, and its location within the formation can be seen in Fig. 23.

4.1.6 Kaolinite

Description

Plane polarized light

The mineral is observed as very small clasts and as a result, the crystal shape is difficult to determine. The mineral is light brown in colour and has a low, positive relief (Fig. 16). In the thin section, the mineral is observed enclosing the much larger monocrystalline quartz grains, filling in the voids between the dominant mineral of the sample.

Cross-polarized light

When viewed in cross-polarized light, the colour of the mineral is relatively unaltered compared to its appearance in plane polarized light (Fig. 16). This corresponds roughly to first-order interference colours when referencing the Michel-Lévy Interference Color Chart (Appendix B). Due to the very small grain size of the mineral, other optical characteristics are difficult to distinguish.

Interpretation

Based on its petrographic characteristics, including crystal shape, size and colour, the mineral fits well with the characteristics of clay minerals, as they are presented by Nesse, (2012). As seen in Fig. 16, the interpreted clay appears to be filling up the voids between the larger quartz grains. Authigenetic kaolinite has previously been described as an important pore-filling clay within the Helvetiafjellet Formation (Edwards, 1979; Prestholm & Walderhaug, 2000). Therefore, the pore-filling clays observed during thin section analysis are interpreted as kaolinite.

Clay formation occurs when silicate rocks and water interact. Another condition for clay formation are relatively low temperature gradients. Therefore, clays tend to form relatively close to the sediment surface, where kaolinite is regarded as a product of the early stages of diagenesis (Milliken, 2003; Nesse, 2012). As close proximity to the sediment surface is a condition of formation, kaolinite is often associated with soil forming processes (Miranda-Tervino & Coles, 2003).

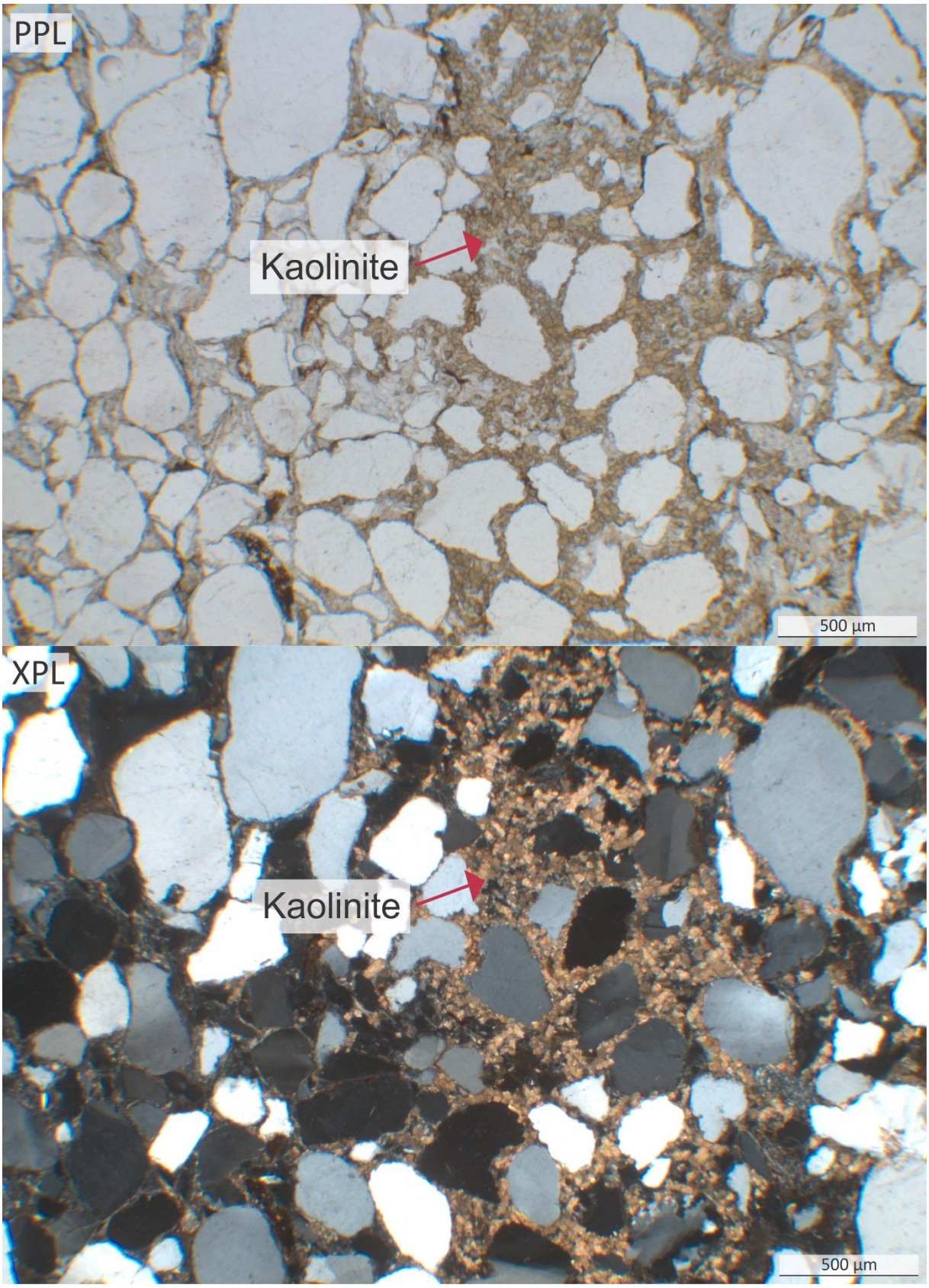

Figure 16: Photomicrograph of kaolinite observed within the Helvetiafjellet Formation. The kaolinite grains can be recognized as being very small and brown in colour, and are indicated in the photomicrograph by a red arrow. PPL stands for plane polarized light and XPL stands for cross-polarized light. This example of kaolinite was observed in thin section 4, and its location within the Helvetiafjellet Formation is indicated in Fig. 23.

4.1.7 Carbonate

Description

Plane polarized light

The mineral is transparent in colour and is dominated by an anhedral crystal shape. The surface of the mineral is observed as relatively grainy, which indicates high relief. A rhombohedral cleavage is observed (Fig. 17).

Cross-polarized light

The mineral displays relatively strong birefringence. The majority of the mineral is white, but where colour is present, it is pearlescent (Fig. 17 XPL). According to the Michel-Lévy Interference Color Chart (Appendix B), this suggests very high interference colours.

Interpretation

Based on the observations made through both plane and cross-polarized light, the mineral is interpreted to be a carbonate. This interpretation is based on the minerals high relief, its pearlescent colour in cross-polarized light and its cleavage, which are all consistent with the expected characteristics of carbonate, as presented by Nesse, (2012). Calcite has in previous studies been described as the primary carbonate cement observed within the Helvetiafjellet Formation (Edwards, 1979; Prestholm & Walderhaug, 2000). It is therefore likely that the observed carbonate in this study is also calcite, but this is difficult to determine with confidence without further analysis.

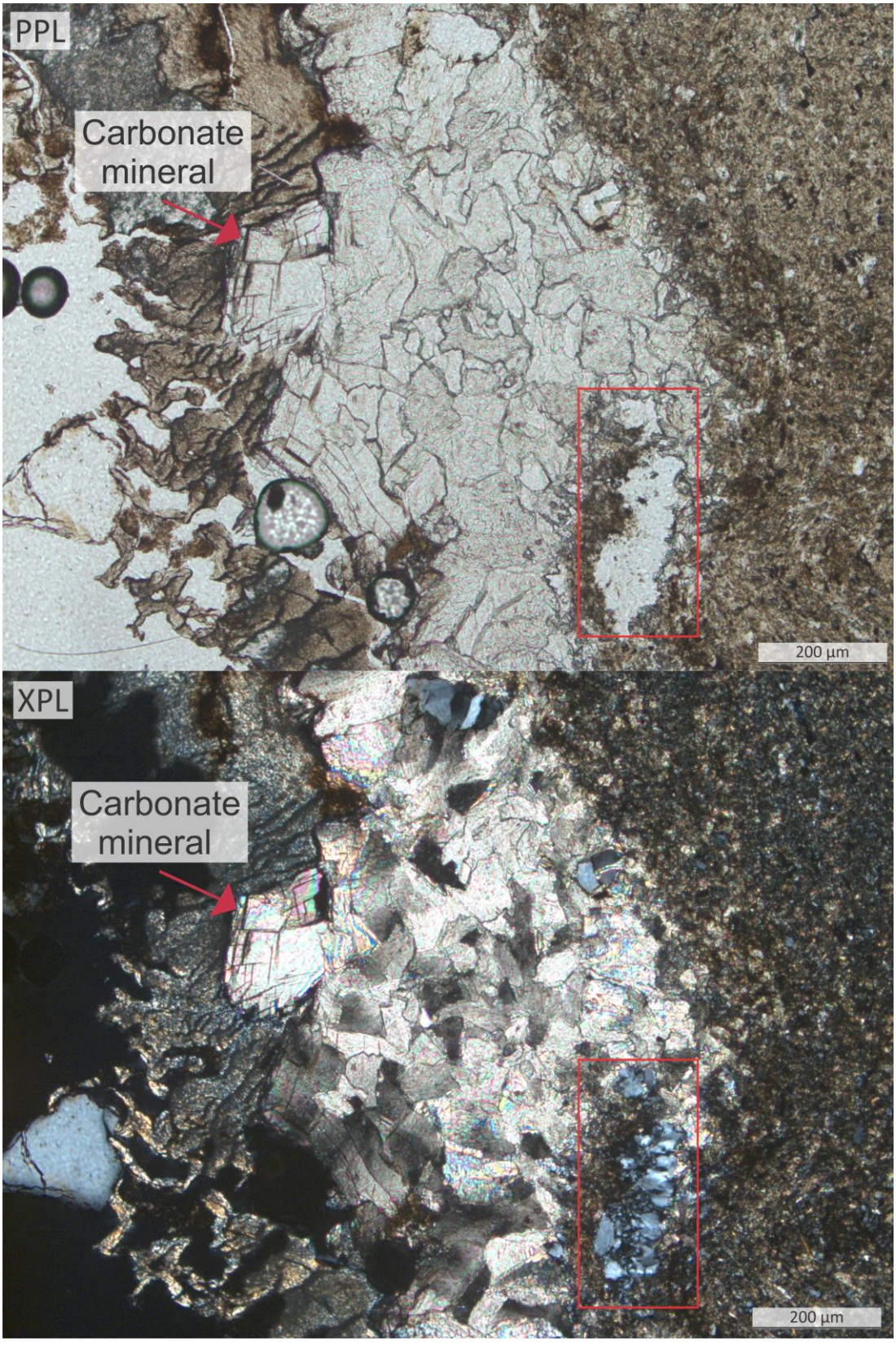

Figure 17: The carbonate mineral seen in thin section 14 is indicated with a red arrow. High interference colours and a rhombohedral cleavage can be observed. PPL stands for plane polarized light, and XPL stands for cross-polarized light. Where thin section 14 was extracted from within the Helvetiafjellet Formation can be seen in Fig. 23. Please also note the quartz cement present in the photomicrograph which can be seen in the lower right hand corner of the figure, indicated with a red square.

4.1.8 Non-crystalline minerals – Organic components

Description

Plane polarized light

The clast size of this amorphous mineral varies greatly throughout the observed thin sections, ranging from very small fragments, to elongated ribbons (Fig. 19), to relatively large and irregular clasts (Fig. 18). The material is deep red to orange in colour, but black patches also occasionally occur. The relief appears to be relatively high. No apparent cleavage is observed. Occasionally, a fibrous to cellular texture is observed (Fig. 19).

Cross-polarized light

No birefringence is observed in the material when the thin section is rotated under cross-polarized light. The colour of the amorphous mineral is typically consistent when viewed in both plane and cross-polarized light (Figs. 18 & 19).

Interpretation

Based on the colour and fibrous texture observed during petrographic analysis, this component is interpreted to be coalified organic material. The small quantities, shape and distribution of the organic material suggests that it represents transported material, rather than in-situ coal. The exception is in the horizons where rootlets are present.

Both fragments of coalified plant fragments and rootles have been described in previous studies of the Helvetiafjellet Formation (Edwards, 1979; Nemec, 1992). Examples of the organic material observed throughout the thin sections of the Helvetiafjellet Formation are presented in Figs. 18 & 19.

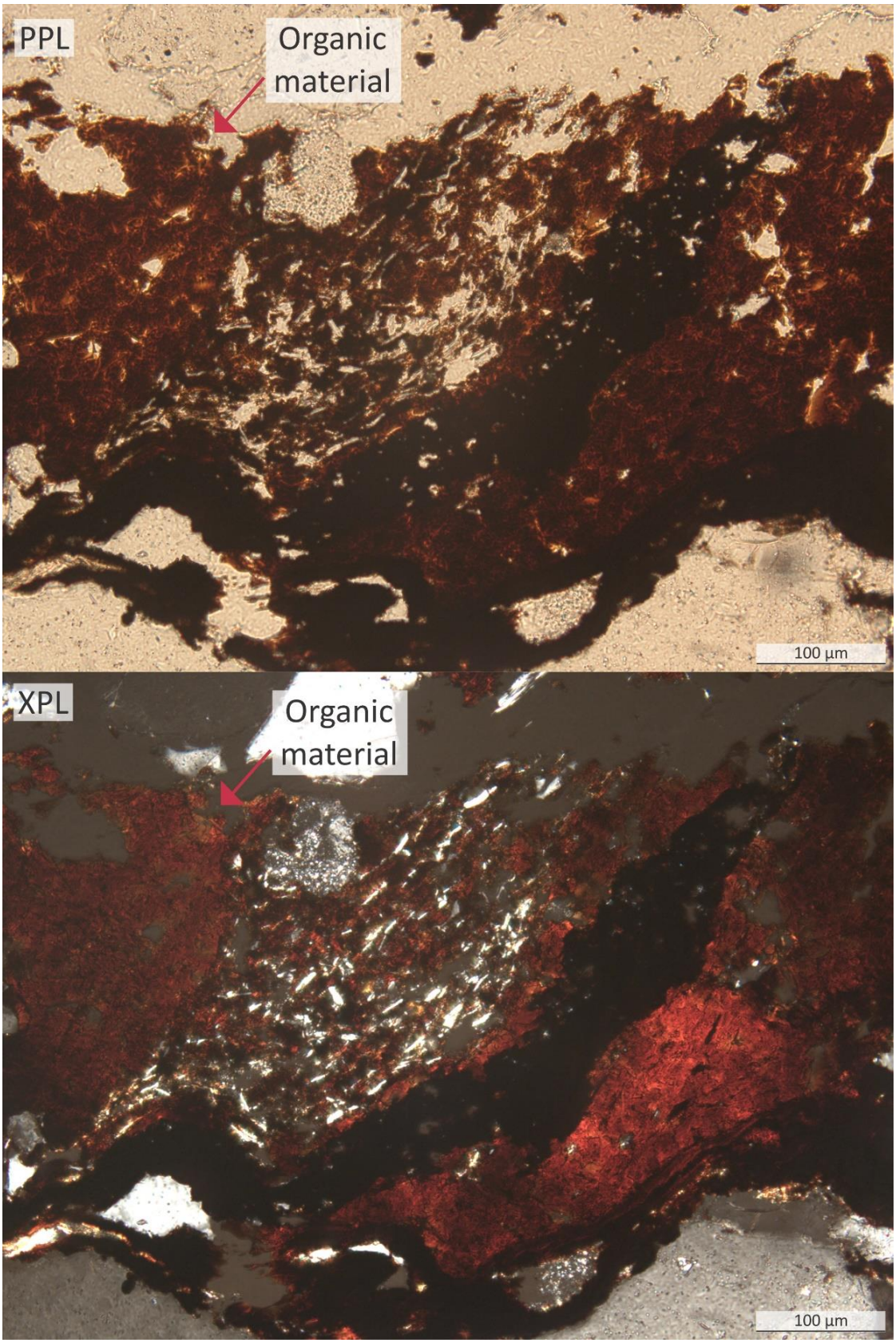

Figure 18: Photomicrograph of coalified organic material observed within the Helvetiafjellet Formation. The colour of the organic matter remains a vibrant red colour in both plane polarized light (PPL) and cross-polarized light (XPL). The bands of a black amorphous mineral are also interpreted as coalified organic matter. The organic matter in this photomicrograph was observed in thin section 24. Its location within the Helvetiafjellet Formation is indicated in Fig. 23.

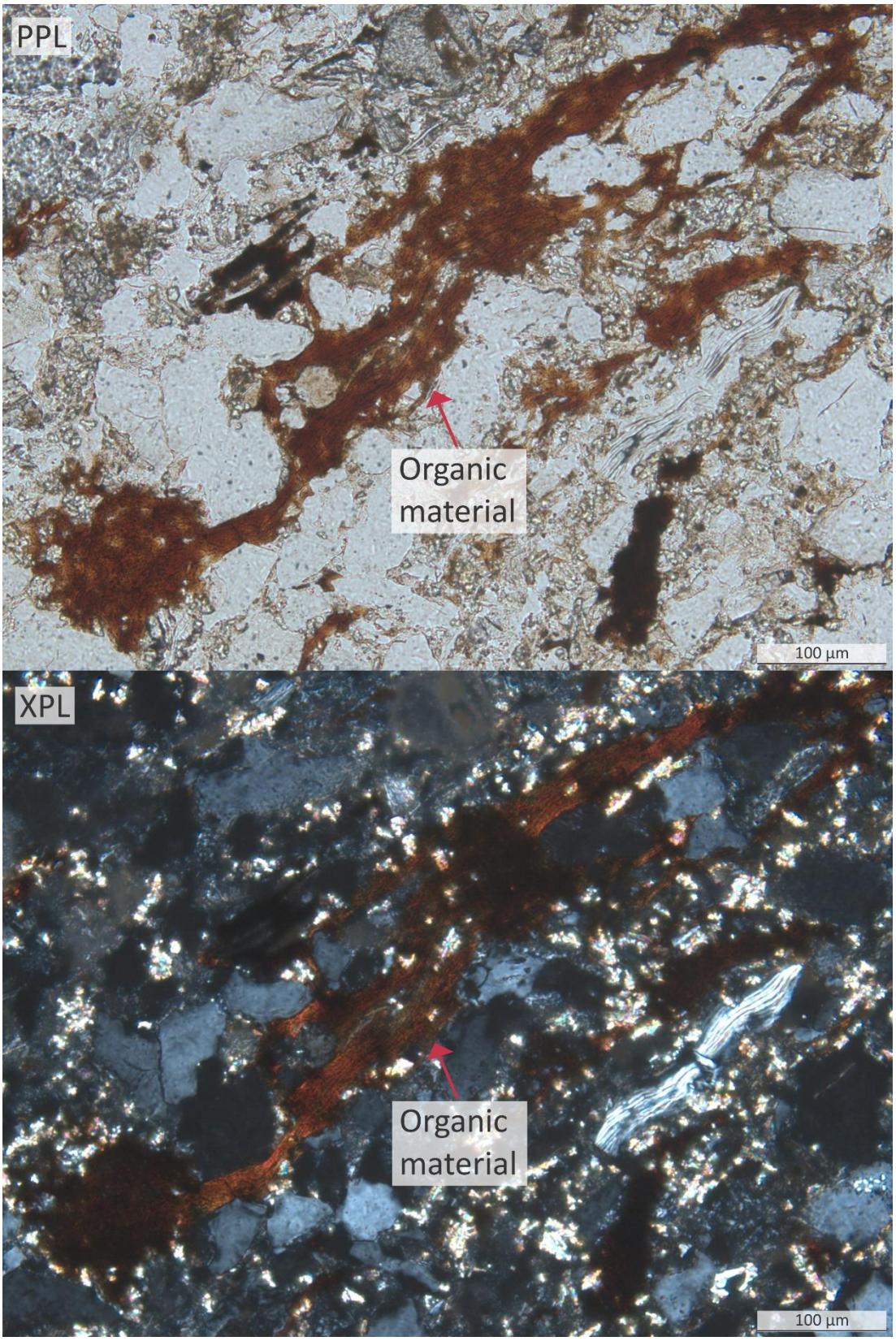

Figure 19: Another example of organic material observed within the Helvetiafjellet Formation. The organic matter is indicated in the figure with a red arrow, and can be recognized by its vibrant red colour in both plane polarized light (PPL) and cross-polarized light (XPL). In this photomicrograph, the fibrous texture of the organic material is highlighted. This example of organic material was observed in thin section 6, and its location within the Helvetiafjellet Formation is indicated in Fig. 23.

4.1.9 Carbonate clasts – iron ooids

Description

Plane polarized light

The mineral appears to be composed of several subspherical grains (Fig. 20). The grains appear to be composed of a transparent or brown coloured nucleus, surrounded by concentric laminae (Fig. 21). The laminae is typically brown in colour. The pore space between the subspherical grains appears to be infilled by a colourless mineral (Fig. 21 PPL).

Cross-polarized light

The internal structure of the subspherical grains is more distinct in cross-polarized light. The laminae displays a variety of colours, from dark grey, to black, to redish brown, to dark green. The nucleus is generally brown or dark grey in colour (Fig. 20). The inclusions display a weak birefringence. The mineral that surround the subspherical grains also displays a weak birefringence, changing from white to grey. This mineral has a much more distinctive appearance in cross-polarized light compared to when viewed in plane polarized light. The grains of the mineral are too small to be seen, but a fibrous texture can be observed (Fig 21 XPL).

Interpretation

Based on the characteristics of the subspherical grains described above, they are interpreted as ooids. Internally, ooids are composed of a nucleus which is surrounded by a cortex of laminae through precipitation (Simone, 1981; Young & Taylor, 1989; Collin et al., 2005). The nucleus of an ooid can have varying lithological characteristics, such as mud clasts, quartz grains and fragments of organic material (Simone, 1981). The nucleus of the ooids observed in this study are interpreted to predominantly consist of quartz and mud clasts. Broken fragments of other ooids can also function as a nucleus, which suggests several growth cycles (Mutrux et al., 2008). The ooids observed within the thin section share many of the characteristics of the iron ooids described by Mutrux et al., (2008). These iron ooid were observed within the overlying Carolinefjellet Formation. Therefore, the ooids within the thin section are interpreted as iron ooids. Based on the colour of the cement in both plane and cross-polarized light, the weak birefringence and fibrous texture in cross-polarized light, it is interpreted as chalcedony. Chalcedony can be recognized as fibrous quartz crystals of

microscopic to submicroscopic size (Allaby, 2013). Similarly to the nucleus material, the general shape of an ooid can vary greatly. Both primary shapes, where the shape of the ooid reflects the shape of the nucleus (Collin et al., 2005) and more irregular shapes due to deformation (Mutrux et al., 2008) are commonly observed. The ooids presented in Fig. 20 are interpreted to primarily reflect primary shapes. Iron ooids have previously been observed within the overlying Carolinefjellet Formation (Mutrux et al., 2008), but never before within the Helvetiafjellet Formation.

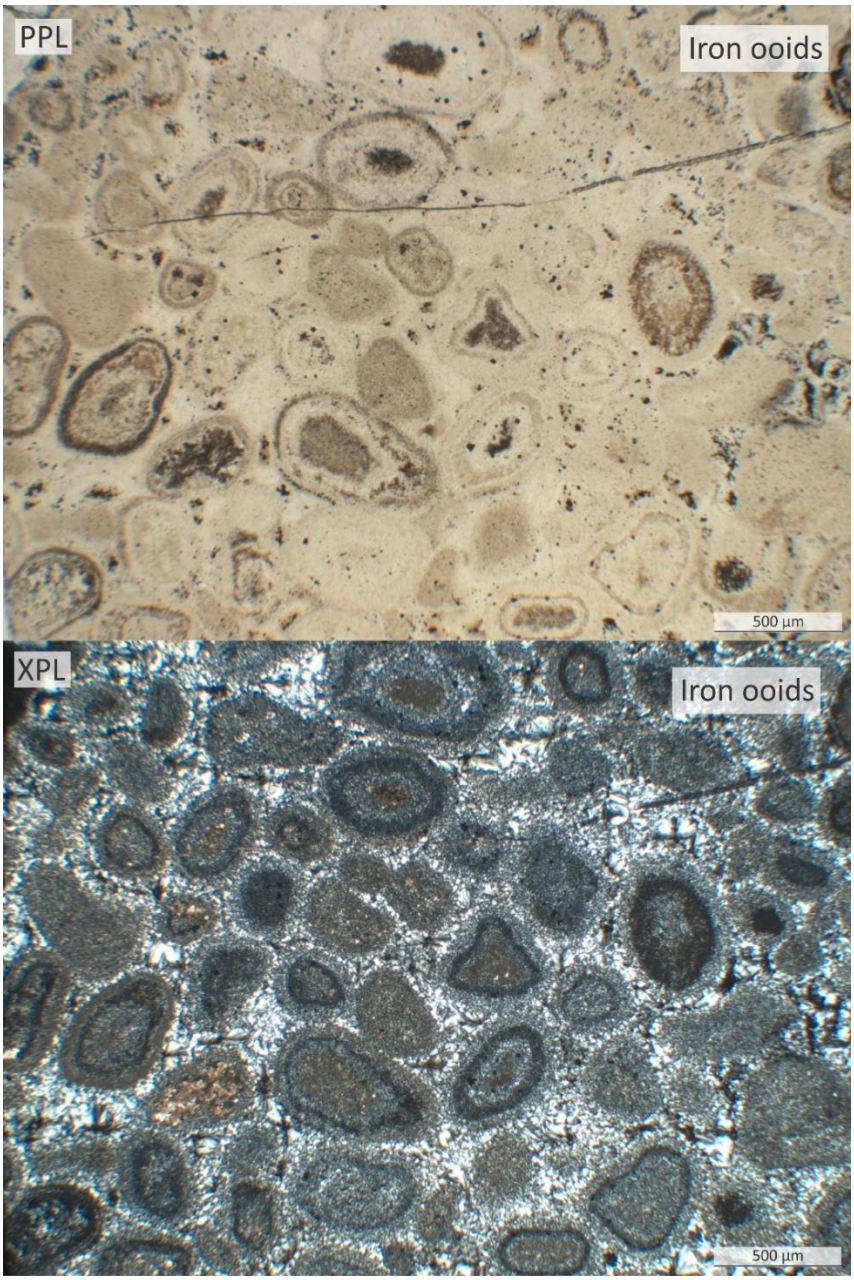

Figure 20: Photomicrograph of the iron ooids observed within thin section 16. A nucleus surrounded by concentric laminae is observed. The iron ooids were observed on the transition between the Helvetiafjellet and the Carolinefjellet formations (Fig. 23). PPL stands for plane polarized light, and XPL stands for cross-polarized light.

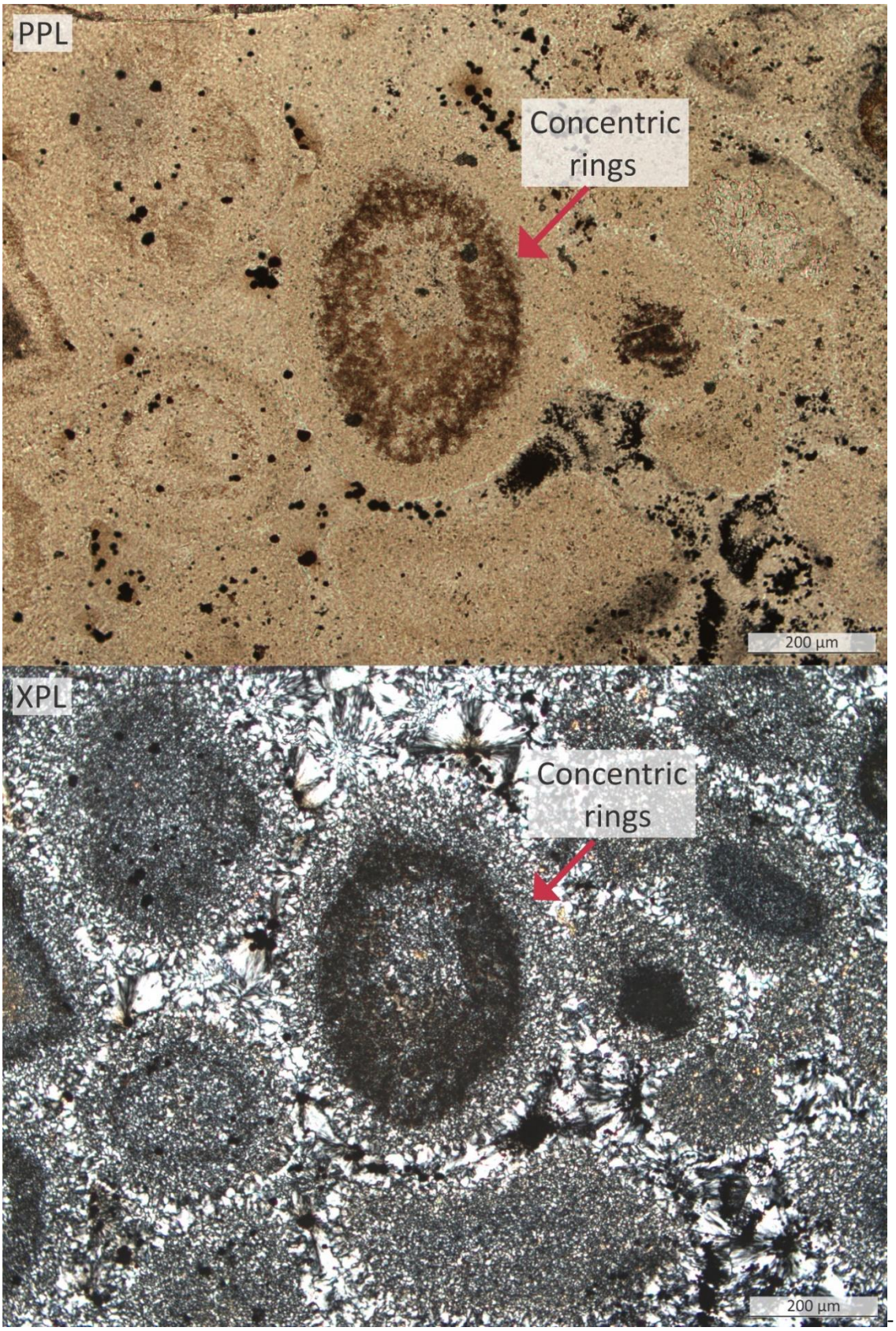

Figure 21: A closer look at one of the iron ooids observed within the Helvetiafjellet Formation. In this photomicrograph, the concentric rings of the ooid are easily distinguished from the surrounding cement. Within the thin section, the shape of the laminae typically reflects the shape of the nucleus. Please also note the fibrous texture of the cement, which is interpreted as chalcedony. PPL stands for plane polarized light, and XPL stands for cross-polarized light.

4.1.10 Lithic clasts – Biogenic chert

Description

Plane polarized light

The mineral is observed within a relatively well-rounded clast. The mineral is brown in colour in plane polarized light, with light brown to transparent inclusions occurring throughout the clast (Fig. 22 PPL). The individual grain size appears to be very small, and it is therefore difficult to distinguish crystal shapes through thin section analysis. The inclusions vary in shape from relatively spherical to more needle shaped (Fig. 22 PPL). A relatively low, positive relief is observed.

Cross-polarized light

The white inclusions display a low birefringence, changing from white to grey in colour. The brown mineral surrounding the white inclusions appear to have a slightly higher birefringence, displaying white, light brown and grey colours (Fig. 22 XPL). According to the Michel-Lévy Interference Color Chart (Appendix B) this is consistent with first-order interference colours.

Interpretation

Although the dominant brown mineral within the clast is much more fine-grained than previously seen, it is otherwise consistent with many of the characteristics previously described for quartz (Chap. *4.1.1*). This includes the low positive relief and weak birefringence. Based on the indistinguishable grains of the mineral, the clast is interpreted as a chert, which is a mineral predominantly composed of microcrystalline quartz (Nesse, 2012). The occurrence of chert within the Helvetiafjellet Formation is consistent with previous studies of the formation (Edwards, 1979; Prestholm & Walderhaug, 2000; Maher et al., 2004).

Based on their shape, the white inclusions are interpreted as spicules. Their difference in shape can be due to the angle in which they were cut when the thin section was produced. The largest spicules appear to be infilled with silica, giving them their transparent appearance in plane polarized light. When a mineral is composed largely of such spicules, it is commonly referred to as a spiculite (Maher et al., 2004; Allaby, 2013). On Spitsbergen, the Upper Permian Kapp Starostin Formation is known to contain spiculite (Ezaki et al., 1994). As

this clast was found within the conglomerate in the transition between the Helvetiafjellet and the Carolinefjellet formations, it is possible that it originated within the significantly older Upper Permian Kapp Starostin Formation. Spiculite is a very hard sedimentary rock, thus suggesting that the observed degree of rounding is indicative of prolonged transportation and abrasion.

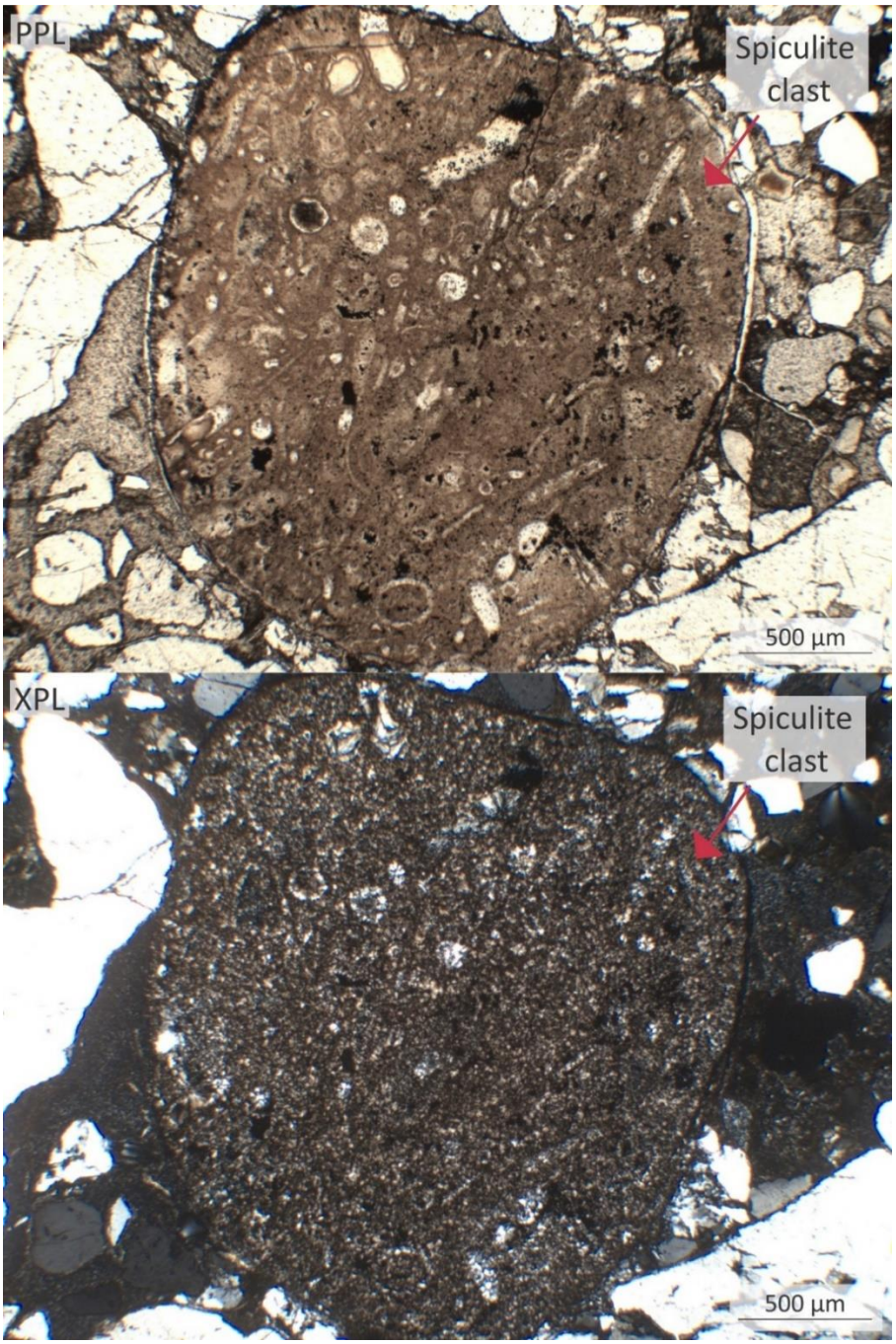

Figure 22: The spiculite clast observed within the conglomerate on the transition between the Helvetiafjellet and the Carolinefjellet formations can be seen in the centre of the photomicrograph, indicated with a red arrow. The degree of rounding suggests prolonged transportation. PPL stands for plane polarized light, and XPL stands for cross-polarized light. The clast was observed in thin section 16, and its location within the logged section is indicated in Fig. 23.

4.1.11 Overview of the mineralogical composition of the Helvetiafjellet Formation

A summary of the mineralogical composition of thin sections 1-24 is presented in Table 1. This provides an overview of the mineralogical changes that occur throughout the Helvetiafjellet Formation within cores DH-1 and DH-1A. As it can be seen from the table, quartz, both as lithic grains and cement overgrowth, was the most commonly occurring mineral within the formation. Where the quartz grains were tightly packed and little matrix was present, quartz overgrowths were more commonly observed. Quartz was the dominating mineral in most thin sections, with the exception of thin section 5 and 15. Their location within core DH-1 is indicated in the presentation log (Fig. 23).

K-feldspar, plagioclase feldspar and variations of mica were all relatively common as accessory minerals, though they were never observed in large quantities within the thin sections. The clay content was according to observations relatively low. Carbonate cement was observed in relatively small amounts, often as infill between quartz grains. Organic matter was present in several thin sections, presenting itself either as dispersed clasts or root structures. The spiculite clast and the iron ooids were only present in thin section 16.

*Table 1: Table presenting the mineralogical composition of thin sections (TS) 1 to 24. M.qrtz = monocrystalline quartz. Qrz.cem = quartz cement. P.qrtz = polycrystalline quartz. K-fls = K-feldspar. Pla.fls = plagioclase feldspar. Kaol. = Kaolinite. Org.mat = organic matter. I.ooids = iron ooids. Spic. = Biogenic chert. In the thin sections where quartz cement is indicated by an **(X)**, there were only small amounts of quartz cement observed. Larger amounts of quartz cement was typically related to tightly packed quartz grains. As thin section 21 was not successfully produced, no mineralogical composition is available.*

TS	M.qrtz	Qrz.cem	P.qrtz	K-fls	Pla.fls	Mica	Kaol.	Carb.	Org.mat	I.ooids	Spic.
TS 1	**X**	**X**	**X**			**X**					
TS 2	**X**	**(X)**	**X**		**X**	**X**			**X**		
TS 3	**X**	**(X)**	**X**	**X**		**X**			**X**		
TS 4	**X**		**X**				**X**				
TS 5	**X**		**X**		**X**	**X**					
TS 6	**X**				**X**	**X**	**X**		**X**		
TS 7	**X**	**(X)**	**X**			**X**			**X**		
TS 8	**X**	**X**	**X**						**X**		
TS 9	**X**					**X**			**X**		
TS 10	**X**	**X**	**X**	**X**	**X**				**X**		
TS 11	**X**	**X**	**X**						**X**		
TS 12	**X**	**(X)**	**X**	**X**	**X**			**X**			
TS 13	**X**		**X**		**X**	**X**	**X**		**X**		
TS 14	**X**	**X**	**X**		**X**			**X**	**X**		
TS 15	**X**								**X**		
TS 16	**X**	**X**	**X**	**X**						**X**	**X**
TS 17	**X**					**X**	**X**		**X**		
TS 18	**X**	**(X)**	**X**	**X**		**X**			**X**		
TS 19	**X**	**X**	**X**		**X**				**X**		
TS 20	**X**	**X**	**X**	**X**		**X**			**X**		
TS 21	-	-	-	-	-	-	-	-	-	-	-
TS 22	**X**	**X**	**X**		**X**			**X**	**X**		
TS 23	**X**	**X**	**X**			**X**		**X**	**X**		
TS 24	**X**	**X**	**X**						**X**		

4.2 Sedimentary logs from the Helvetiafjellet Formation

As it can be observed in Figs. 23 & 24, there are many similarities in the characteristics of cores DH-1 and DH-1A. This is not surprising as the cores were drilled only 20 meters apart (Fig. 9). Two lithologies are predominantly observed in both core DH-1 and DH-1A; very fine to coarse-grained sandstone and shale. Some sections also contain coaly shale and thin coal seams.

The dominating primary structures within core DH-1 and DH-1A are observed as both dipping and cross-cutting units of varying magnitude. Where the units are less than 1 cm in thickness, they are referred to as laminae. Where laminae is observed cross-cutting each other, they are interpreted as the internal structure of ripples. Within the cores, these structures are observed as being asymmetrical, and is therefore interpreted as current ripple cross-lamination (Reineck & Singh, 1980; Tucker, 2011). When cross-cutting is observed in units thicker than 1 cm, this is interpreted as trough cross-bedding. Based on the size of the sets, these trough cross-bedded units are interpreted to be the result of migrating three dimensional dunes (Collinson et al., 2006). Sub-parallel dipping beds of varying thickness are also observed throughout both core DH-1 and DH-1A. These are interpreted as tabular cross-beds, which are common internal structures within two dimensional dunes (Collinson et al., 2006).

Throughout the Helvetiafjellet Formation, foremost within the Glitrefjellet Member, abundant bioturbation is observed. The bioturbation is interpreted to be largely the result of root structures displacing the loose sediments (Nemec, 1992). Root traces and fossilised roots, which are both present throughout the formation, are clear indicators of subaerial exposure and soil formation (Retallack, 1988; Buol et al., 2011). The two palaeosols chosen for this thesis are discussed further in chapter *4.3*. The placement of the palaeosols within core DH-1 is indicated in Fig. 23.

The lower boundary of the Helvetiafjellet Formation, which is defined by a Barremian subaerial unconformity, is present within both core DH-1 and DH-1A. This contact can be observed as an abrupt transition from a dark coloured very fine-grained sandstone, to a relatively coarse-grained conglomerate. The Festningen Member, which is the lowermost member within the Helvetiafjellet Formation, is observed to be approximately 12 and 16

meters thick in cores DH-1 and DH-1A, respectively. In both cores, the transition from the basal Festningen Member to the overlying Glitrefjellet Member is indicated by a dark-coloured shale unit. The upper boundary of the Helvetiafjellet Formation is defined by a lower Aptian flooding surface (Midtkandal et al., 2016; Grundvåg et al., 2017). This is observed in both cores as a conglomerate, overlain by a thick black shale unit.

A series of samples intended for thin section analysis were collected from core DH-1 during the logging process. Where the samples were collected from within the core is indicated in Fig. 23. The mineralogical composition of the different samples was presented in Table 1, and gives an overview of the mineralogical changes that occur throughout the Helvetiafjellet Formation.

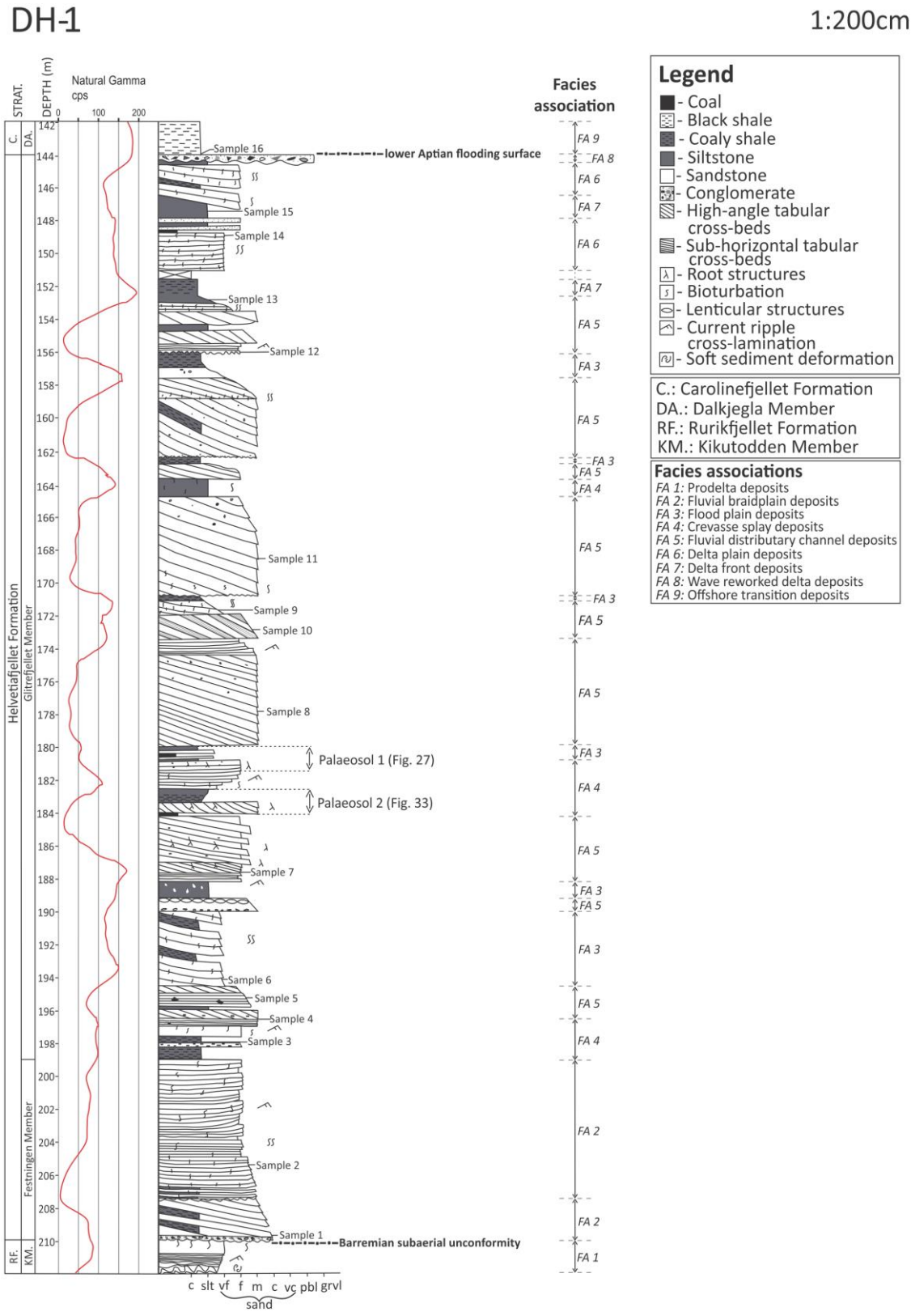

Figure 23: Presentation log based on the logged section of core DH-1. Scale is set to 1:200 cm. The natural gamma measurements indicates the radioactivity of the deposits in the logged section. The upper and lower boundaries of the Helvetiafjellet Formation, a lower Aptian flooding surface and a Barremian subaerial unconformity, respectively, are indicated in the figure. The samples collected for thin section analysis are indicated in the figure, and named sample 1 to 16. The palaeosols which are presented in chapter 4.3 *are indicated in the figure. The facies associations defined in Thesis 1 are also indicated in the figure. Their characteristics are presented in Table 2.*

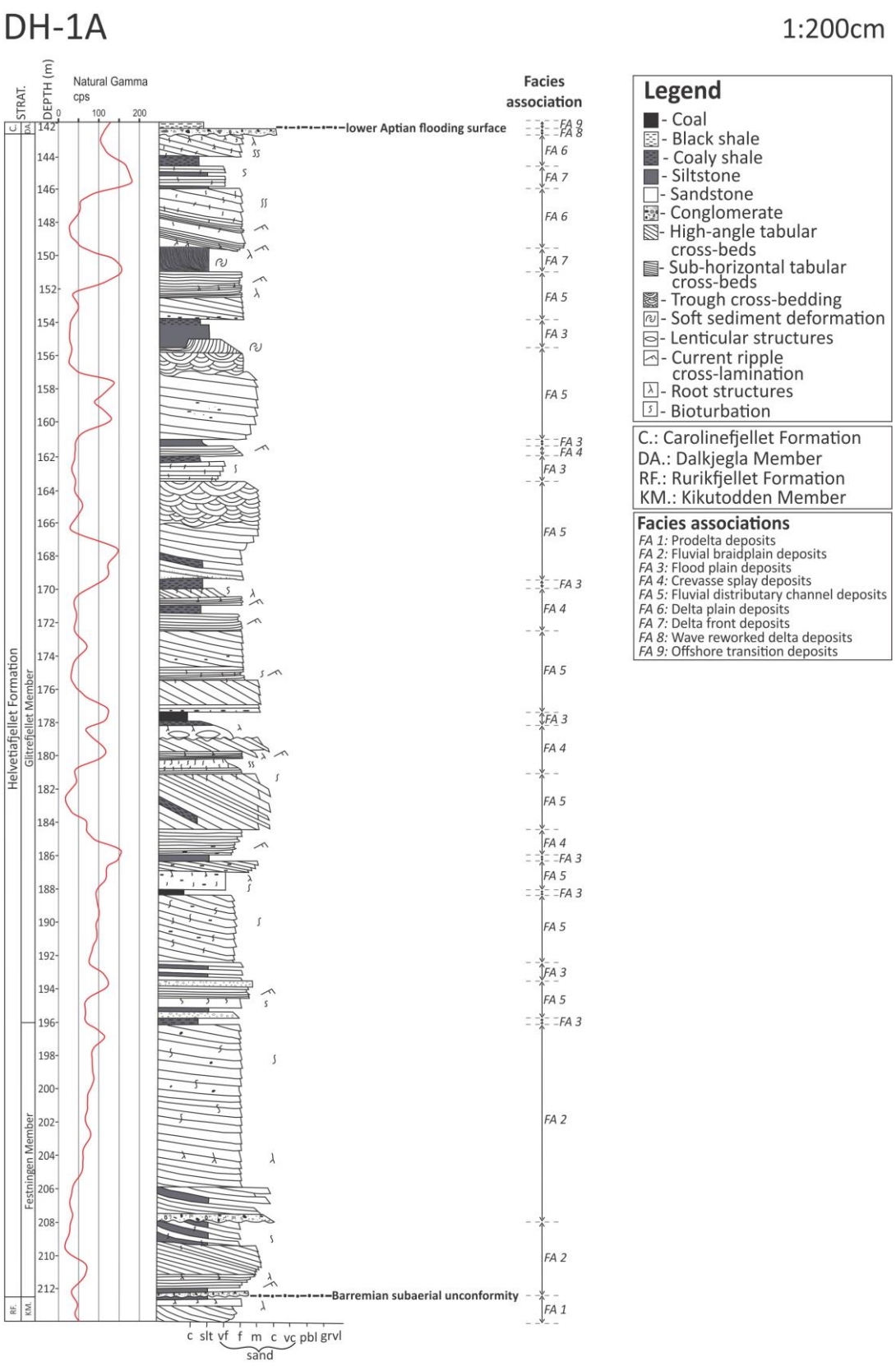

Figure 24: Presentation log based on the logged section of core DH-1A. Scale is set to 1:200 cm. The natural gamma measurements indicates the radioactivity of the deposits of the logged section. The upper and lower boundaries of the Helvetiafjellet Formation, a lower Aptian flooding surface and a Barremian subaerial unconformity, respectively, are indicated within the figure. The interpreted facies association, defined in Thesis 1 are also indicated in the figure. Their characteristics are presented in Table 2.

4.2.1 Thin section characteristics in relation to interpreted facies associations

In Table 2, the facies associations and their general characteristics, as defined by Thea Engen in Thesis 1, are presented. In the following subchapters, thin section characteristics are compared to the expected characteristics of the deposits within each facies association, observed through logging. No thin section represents the deposits of the Rurikfjellet Formation (FA 1) as the deposits of the Helvetiafjellet Formation are the focus of this thesis. The different facies associations and their corresponding thin sections are presented in Table 2 below. The occurrence of the facies associations within the Helvetiafjellet Formation zre indicated in Figs. 23 & 24.

Table 2: The facies associations and their interpreted characteristics based upon logged sections of the Helvetiafjellet Formation. The occurrence of the different facies associations is indicated in the presentation logs in Figs. 23 & 24. As the uppermost section of the Rurikfjellet Formation and the lowermost section of the Carolinefjellet Formation were included when logging, these are represented by facies associations 1 and 9, respectively. Several thin sections were collected from the varying facies associations. These are also presented in the table.

Facies association (FA)	**FA characteristics**	**Thin sections (TS)**
FA 1 (*Prodelta deposits*)	Grain size varies from siltstone to coarse-grained sandstone. The deposits are relatively well-sorted. Units are <1 m. Observed features are tabular cross-beds, ripple cross-lamination and structureless units. Roots, bioturbation and coal clasts are occasionally observed.	-
FA 2 (*Fluvial braidplain deposits*)	Grain size varies from siltstone to coarse-grained sandstone. Where conglomerate is present, pebbles are observed. The deposits are generally well-sorted, with the exception of conglomerate deposits. Units are <80 cm. Observed features are tabular cross-beds, ripple cross-lamination and structureless units. Some bioturbation is also present.	1, 2
FA 3 (*Floodplain deposits*)	Grain size is typically claystone to siltstone. The deposits are overall well-sorted. The units are generally <50 cm. The deposits are homogeneous to weakly laminated. A shiny texture and high organic content is observed in some deposits.	6

FA 4 (*Crevasse splay deposits*)	Grain size varies from claystone to coarse-grained sandstone. The deposits are homogeneous to weakly laminated. Ripple cross-lamination is also observed. The deposits are relatively well-sorted. Some coalified organic material is observed.	3, 10
FA 5 (*Fluvial distributary channel deposits*)	Grain size varies from claystone to coarse-grained sandstone. Pebbles are present within the conglomerate. The deposits are relatively well-sorted, with the exception of the conglomerate deposits. Roots and coal clasts are present. Other observed features are structureless units, trough cross-beds, tabular cross-beds and ripple cross-lamination.	4, 5, 7, 8, 9, 11, 12, 13
FA 6 (*Delta plain deposits*)	Grain size varies from claystone to coarse-grained sandstone. The deposits are relatively well-sorted. High organic content and bioturbation is occasionally observed. Other observed features are tabular cross-beds, heterolithic beds and homogeneous to weakly laminated units.	14
FA 7 (*Delta front deposits*)	Grain size is typically claystone to siltstone. Units are <50 cm. The deposits are well-sorted. The organic content is interpreted as relatively high. The deposits are typically homogeneous to weakly laminated.	15
FA 8 (*Wave-reworked delta deposits*)	Conglomerate consisting of fine-grained sandstone to gravel sized clasts. The unit is typically <20cm. The deposits are chaotic to poorly sorted.	16
FA 9 (*Offshore transition deposits*)	Grain size is typically equivalent to claystone or siltstone. The unit is <1 m. High organic content is observed. The deposits are homogeneous to weakly laminated.	16

As seen in Table 2, the majority of the thin sections were collected from facies association 5 (FA 5; *fluvial distributary channel deposits*). This is likely because FA 5 has been interpreted as the most frequently occurring facies association within the Helvetiafjellet Formation (Figs. 23 & 24).

4.2.1.1 Facies association 2 (FA 2) – Fluvial braidplain deposits

Macro-scale observations

The deposits of FA 2 are dominated by grain sizes varying from siltstone to coarse-grained sandstone. Conglomerate is also observed within the facies association. Where a conglomerate is present, gravel sized clasts are also observed. With the exception of conglomerates, the deposits are relatively well-sorted. Commonly observed primary structures are tabular cross-bedding, ripple cross-lamination and structureless units. Some bioturbation is also present (Fig. 25 A).

Micro-scale observations

Thin sections collected from FA 2 deposits are primarily quartz dominated. The grain size is generally equivalent to very fine to medium-grained sandstone. The matrix content is varying. When the quartz grains are packed tight, the matrix content is low and when the packing is not as tight, more matrix is present. Coalified organic material observed as plant debris and potential root structures is also observed (Fig. 26 A). The grain size within the individual thin sections is relatively uniform (Fig. 26 A).

Interpretation

Based on the grain size, organic content and degree of sorting observed in both macro and micro-scale observations and the presence of both tabular cross-bedding and ripple cross-lamination in macro-scale observations, FA 2 is interpreted as fluvial braidplain deposits (Jones & Hartley, 1993; Table 2; Figs. 23 & 24). Units consistent with the characteristics of fluvial braidplain deposits have previously been described within the Helvetiafjellet Formation (Steel et al., 1978; Nemec, 1992; Midtkandal et al., 2007; Midtkandal & Nystuen, 2009).

4.2.1.2 Facies association 3 (FA 3) – Floodplain deposits

Macro-scale observations

The deposits of FA 3 are dominated by grain sizes equivalent to claystone and siltstone (Fig. 25 B). The deposits are typically well-sorted. A dark colour and high organic content is commonly observed. The deposits are typically homogeneous (Fig. 25 B), or weakly laminated.

Micro-scale observations

The thin section collected from facies association 3 is dominated by quartz grains equivalent to siltstone to very fine-grained sandstone, that are enclosed by large quantities of muddy matrix (Fig. 26 B). The grain size throughout the thin section is relatively uniform. Fragments of coalified plant debris are also observed (Fig. 26 B).

Interpretation

Based on the large fraction of fine-grained sediments observed through both macro and micro-scale observations, the occasional lamination and the presence of organic material, FA 3 is interpreted as floodplain deposits (Berner et al., 2011; Table 2; Figs. 23 & 24). Deposits that are consistent with the characteristics of floodplain deposits have previously been documented within the Helvetiafjellet Formation (Steel et al., 1978; Midtkandal et al., 2007).

4.2.1.3 Facies association 4 (FA 4) – Crevasse splay deposits

Macro-scale observations

The deposits of FA 4 are dominated by grain sizes varying from claystone to coarse-grained sandstone. The sediments are typically relatively well-sorted (Fig. 25 C). Throughout the logged sections, varying characteristics are observed. Examples are both interlaminated and interbedded sandstones, ripple cross-lamination and homogeneous (Fig. 25 C) to weakly laminated units. The organic content varies.

Micro-scale observations

Thin sections collected from FA 4 are generally rich in quartz (Fig. 26 C). Where the quartz grains are larger (fine-grained sandstone), the grains are packed tighter, and the matrix content is lower (Fig. 26 C). The opposite is true when the quartz grains are smaller (siltstone). Fragments of coalified organic material are also observed (Fig. 26 C).

Interpretation

Based on the varying grain size observed in both macro and micro-scale observations, the presence of ripple cross-lamination and the observation of coalified plant debris, FA 4 is interpreted as crevasse splay deposits (Mjøs et al., 1993; Table 2; Figs. 23 & 24). Deposits that are consistent with the expected characteristics of crevasse splay deposits have previously been documented within the Helvetiafjellet Formation (Steel et al., 1978; Gjelberg & Steel, 1995; Midtkandal et al., 2007).

4.2.1.4 Facies association 5 (FA 5) – Fluvial distributary channel deposits

FA 5 is the most frequently occurring facies association within the logged sections of the Helvetiafjellet Formation.

Macro-scale observations

The grain size of the deposits typically varies from claystone to coarse-grained sandstone. Conglomerate deposits are also observed within the facies association. In such deposits, pebble to gravel-sized clasts are also observed. With the exception of the conglomerate, the deposits are relatively well-sorted (Fig. 25 D). Roots and coal clasts are also present. The units are often characterised by trough cross-bedding, tabular cross-bedding (Fig. 25 D), ripple cross-lamination or a structureless appearance.

Micro-scale observations

The thin sections collected from FA 5 are predominantly quartz dominated (Fig. 26 D). However, relatively large quantities of muddy matrix is also observed. Root structures and coalified organic material is also observed within several thin sections (Fig. 26 D). The grain size within each individual thin section is relatively uniform.

Interpretation

Quartz grains and muddy matrix dominates the deposits of FA 5. Root structures and coalified organic material is documented through both macro and micro-scale observations. Trough cross-bedding, tabular cross-bedding and ripple cross-lamination is observed through macro-scale observations. Based on these observations, the deposits of FA 5 are interpreted as fluvial distributary channel deposits. Deposits with similar characteristics have previously been documented within the Helvetiafjellet Formation (Steel et al., 1978; Gjelberg & Steel, 1995; Midtkandal et al., 2007; Table 2; Figs 23 & 24).

4.2.1.5 Facies association 6 (FA 6) – Delta plain deposits

Macro-scale observations

The deposits of FA 6 are dominated by grain sizes ranging from claystone to coarse-grained sandstone. The deposits are typically observed in units of <50 cm. In some deposits, bioturbation (Fig. 25 E) and high organic content is observed. The units are typically dominated by tabular cross-bedding or heterolithic bedding (Fig. 25 E). Homogeneous to weakly laminated units are also observed.

Micro-scale observations

The thin section collected from FA 6 deposits is predominantly composed of quartz grains, with an overall grain size that is equivalent to fine to medium-grained sandstone (Fig. 26 E). Significant amounts of muddy matrix fills up the voids between the quartz grains (Fig. 26 E). Some fragments of coalified plant debris are also observed.

Interpretation

Based on the presence of both quartz grains and large amounts of muddy matrix, the occasionally high organic content and the presence of both homogeneous units as well as tabular cross-bedding, the deposits of FA 6 are interpreted as delta plain deposits (Coleman, 1976; Coleman & Prior, 1981; Table 2; Figs. 23 & 24). Deposits that are consistent with the characteristics of delta plain deposits have previously been documented within the Helvetiafjellet Formation (Steel et al., 1978; Nemec, 1992; Gjelberg & Steel, 1995).

4.2.1.6 Facies association 7 (FA 7) – Delta front deposits

Macro-scale observations

The deposits of FA 7 are dominated by grain sizes equivalent to claystone and siltstone (Fig. 25 F). The deposits are generally very well-sorted, and can be observed in units <50 cm thick. The colour of the deposits is typically dark, and the organic content is often observed as relatively high (Fig. 25 F). The deposits are generally homogeneous (Fig. 25 F) to weakly laminated, and can be relatively fissile.

Micro-scale observations

The thin section collected from FA 7 is almost exclusively dominated by dark coloured, very fine-grained minerals, with a grain size equivalent to claystone and siltstone (Fig. 26 F). Due to the size of the grains, lithologies are difficult to determine through petrographic analysis. However, some of the larger silt-sized grains are interpreted as quartz (Fig. 26 F).

Interpretation

Based on the large fraction of fine-grained material observed through both macro and micro-scale observations, the observation of homogeneous to weakly laminated units and the relatively high organic content, the deposits of FA 7 are interpreted as delta front deposits. Deposits with similar characteristics have previously been documented within the Helvetiafjellet Formation (Steel et al., 1978; Nemec, 1992; Gjelberg & Steel, 1995; Table 2; Figs. 23 & 24).

4.2.1.7 Facies association 8 (FA 8) – Wave-reworked delta deposits

Macro-scale observations

The deposits of FA 8 consist of conglomerate deposits, composed of a muddy matrix and clasts with a grain size that ranges from fine-grained sandstone to gravel (Fig. 25 G). The clasts appear to be sub-angular to sub-rounded (Fig. 25 G). The unit is generally <20 cm. The deposits are typically chaotic and poorly sorted (Fig. 25 G).

Micro-scale observations

The clasts of the conglomerate are composed of varying lithologies, where quartz is the most commonly occurring mineral (Fig. 26 G). Spiculite clasts and iron ooids are also observed within the conglomerate. The clasts vary greatly in size, and are enclosed by a muddy matrix (Fig. 26 G).

Interpretation

Based on the characteristics of the clasts within the conglomerate and the poor sorting of the conglomerate itself, the deposits of FA 8 are interpreted as wave-reworked delta deposits. Such deposits can form as waves rework the delta front, and barrier bars are formed. Similar deposits have previously been described within the Helvetiafjellet Formation (Nemec et al., 1988; Table 2; Figs. 23 & 24).

4.2.1.8 Facies association 9 (FA 9) – Offshore transition deposits

Macro-scale observations

The deposits of FA 9 are typically composed of sediments with a grain size that is equivalent to claystone and siltstone (Fig. 25 H). The deposits are very well-sorted, and appear in units that are <1 m thick. The deposits are typically black in colour and as a result, the deposits appear homogeneous to weakly laminated (Fig. 25 H).

Micro-scale observations

The thin section collected from FA 9 is dominated by dark coloured sediments, with a grain size that is equivalent to claystone and siltstone (Fig. 26 H). As a result, mineralogical composition of the sediments and primary structures are difficult to distinguish through petrographic analysis.

Interpretation

Based on the grain size, dark colour and fissile nature of the sediments, the deposits of FA 9 are interpreted as offshore transition deposits. Such fine-grained sediments are typically transported for an extended period of time, and deposited when entering a low-energy settings (Berner et al., 2011). Deposits with similar characteristics have previously been described within the Carolinefjellet Formation (Nemec, 1992; Midtkandal et al., 2007; Table 2; Figs. 23 & 24).

Figure 25: Representative images of some of the macro-scale characteristics of the various facies associations (FA) interpreted for the Helvetiafjellet Formation. The occurrence of the samples (S) within the formation is indicated in the log in the right-hand side of the figure. The placement of the samples (S) is roughly equivalent to where the samples for thin section (TS) analysis were collected from, and should therefore represent the characteristics observed during micro-scale observations relatively well. Within the figure, ***FA 2*** *is characterised by fine to medium-grained sandstone, relatively horizontal bedding and some bioturbation.* ***FA 3*** *is characterised by claystone to siltstone and a homogeneous appearance. The sample is also well-sorted.* ***FA 4*** *is characterised by relatively homogeneous, well-sorted siltstone. The organic content is interpreted to be high.* ***FA 5*** *consists of medium-grained sandstone. Tabular cross-bedding is present.* ***FA 6*** *is composed of fine-grained sandstone to siltstone. Heterolithic bedding and bioturbation is observed.* ***FA 7*** *is characterised by homogeneous claystone to siltstone. The organic content is interpreted to be high.* ***FA 8*** *is interpreted as a chaotic conglomerate, with clasts ranging from fine-grained sandstone to gravel.* ***FA 9*** *is characterised by homogeneous to weakly laminated claystone to siltstone. The organic content is interpreted to be high.*

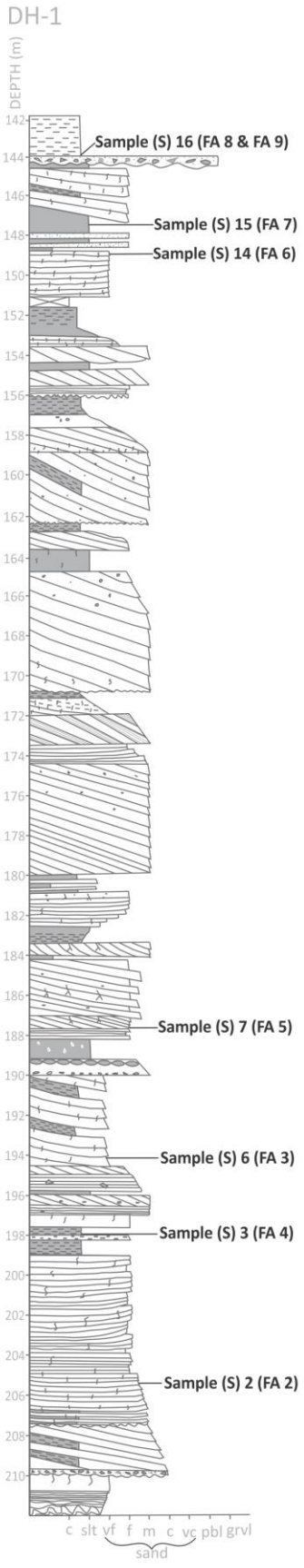

FA 2
- Fine to medium -grained sandstone
- Bioturbation

FA 3
- Claystone to siltstone
- Homogeneous
- Well-sorted

FA 4
- Siltstone
- Well-sorted
- Homogeneous
- Organic content

FA 5
- Medium-grained sandstone
- Tabular cross-bedding
- Relatively well-sorted

FA 6
- Fine-grained sandstone to siltstone
- Heterolithic bedding
- Bioturbation

FA 7
- Claystone to siltstone
- Well-sorted
- Homogeneous
- High organic content

FA 9
- Claystone to siltstone
- Homogeneous to weakly laminated
- High organic content

FA 8
- Conglomerate with fine-grained sandstone to gravel sized clasts
- Sub-angular to sub-rounded clasts
- Chaotic

Facies associations

FA 2: Fluvial braidplain deposits
FA 3: Flood plain deposits
FA 4: Crevasse splay deposits
FA 5: Fluvial distributary channel deposits
FA 6: Delta plain deposits
FA 7: Delta front deposits
FA 8: Wave reworked delta deposits
FA 9: Offshore transition deposits

Figure 26: Overview of the mineralogical characteristics of facies associations (FA) 2-9. Within the figure, each facies association is represented by one thin section (TS) photomicrograph. The placement of the various thin sections within the Helvetiafjellet Formation is indicated in Fig. 23. ***FA 2*** *has been interpreted as fluvial braidplain deposits. Image A (TS 2) represents the more fine-grained fraction of the FA. Potential root structures can also be observed.* ***FA 3*** *has been interpreted as floodplain deposits. Image B (TS 6) displays a large fraction of muddy matrix and quartz grains with a grain size equivalent to siltstone. Some coalified organic material is also present.* ***FA 4*** *has been interpreted as crevasse splay deposits. Image C (TS 3) illustrates the large quantities of quartz present, as well as a grain size equivalent to very fine-grained sandstone. Some organic material is also present.* ***FA 5*** *has been interpreted as fluvial distributary channel deposits. Image D (TS 7) displays quartz grains equivalent to fine to medium-grained sandstone. The thin section is well sorted. Clasts of coalified organic material is present.* ***FA 6*** *has been interpreted as delta plain deposits. Image E (TS 14) illustrates a relatively coarse-grained version of the deposits. Some muddy matrix and organic content is present.* ***FA 7*** *has been interpreted as delta front deposits. Image F (TS 15) displays grains with a grain size equivalent to siltstone and claystone.* ***FA 8*** *has been interpreted as wave-reworked delta deposits. Image G (TS 16) is composed of a relatively coarse-grained conglomerate.* ***FA 9*** *has been interpreted as offshore transition deposits. Image H (TS 16) displays deposits with a grain size equivalent to siltstone or claystone. The sample is very well sorted and the organic content is high.*

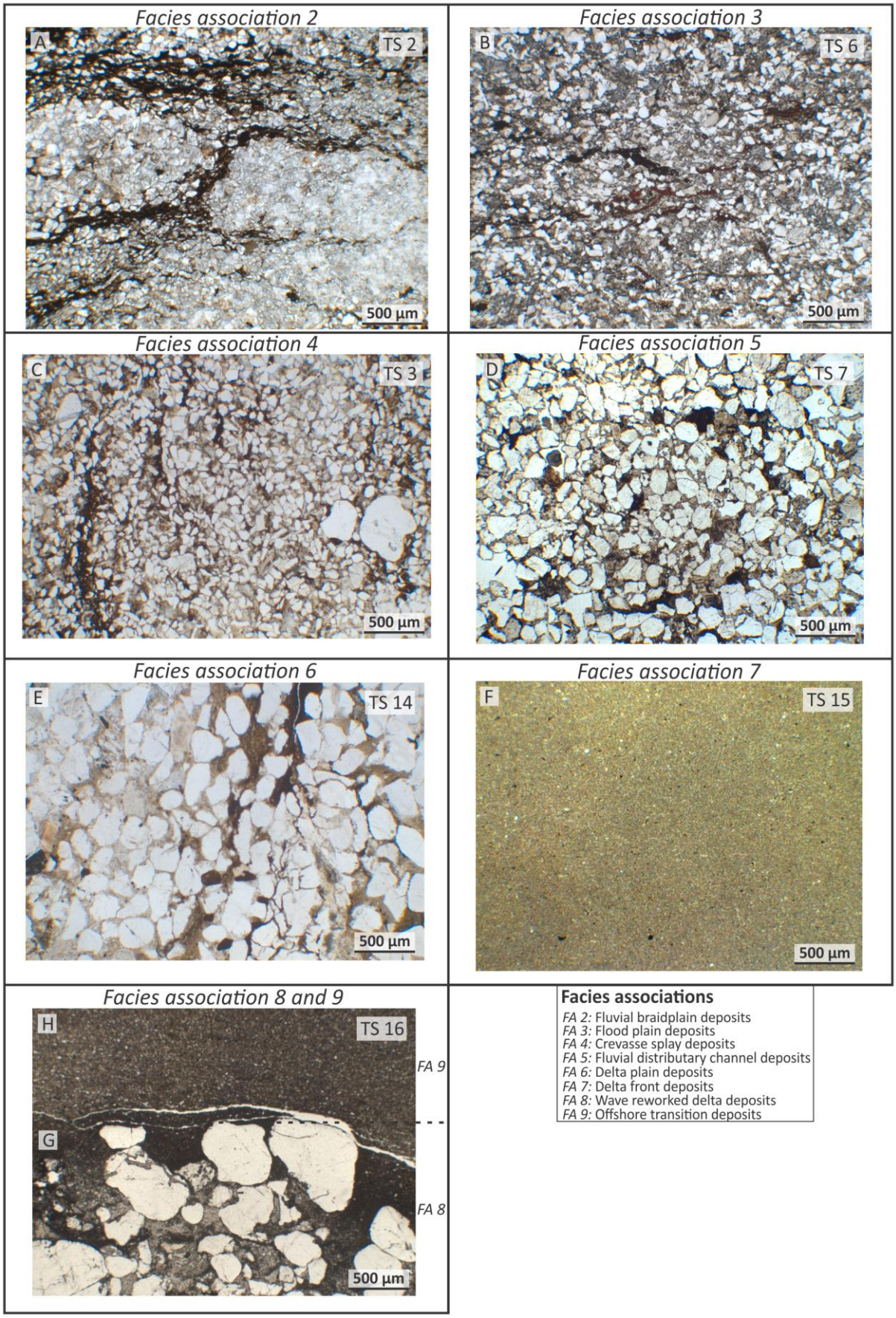
Facies association 2
A
TS 2
500 µm
Facies association 3
B
TS 6
500 µm
Facies association 4
C
TS 3
500 µm
Facies association 5
D
TS 7
500 µm
Facies association 6
E
TS 14
500 µm
Facies association 7
F
TS 15
500 µm
Facies association 8 and 9
H
TS 16
G
FA 9
FA 8
500 µm
Facies associations
FA 2: Fluvial braidplain deposits
FA 3: Flood plain deposits
FA 4: Crevasse splay deposits
FA 5: Fluvial distributary channel deposits
FA 6: Delta plain deposits
FA 7: Delta front deposits
FA 8: Wave reworked delta deposits
FA 9: Offshore transition deposits

4.3 Palaeosols within the Helvetiafjellet Formation

Palaeosols have previously been documented within the Helvetiafjellet Formation (Nemec, 1992). For this project, two palaeosols were selected for a more in-depth description: Palaeosol 1 and Palaeosol 2 herein. Two detailed logs were produced (Figs. 27 & 33), one for each palaeosol. Both the described palaeosols are located in core DH-1. Their stratigraphic position within the Helvetiafjellet Formation is indicated in Fig. 23.

Four thin sections from each palaeosol were also produced and investigated. Their stratigraphic position within the palaeosols is indicated in both detail logs (Fig. 27 & 33). However, as sample 21 was not successfully produced into a thin section, only three samples are indicated for Palaeosol 2. In addition, four samples were extracted from Palaeosol 2 for XRD-analysis. These are also indicated in Fig. 33.

In this section, the palaeosols will be classified according to the classifications of the US Soil Taxonomy (Soil Survey Staff, 1999). This will be done based on the observations that were made during logging of the cores, and the information gained from petrographic analysis. For Palaeosol 2, the XRD-analysis will also give an indication with regards to clay content.

4.3.1 Palaeosol 1 (PS 1)

4.3.1.1 Macro-scale observations

Palaeosol 1 has an approximate thickness of 2.05 meters, with its upper and lower boundaries at 180.1 m and 182.15 m below present day surface, respectively. A detailed 1:10 cm log of the palaeosol is presented in Fig. 27. Descriptive nomenclature for the palaeosols follows Retallack, (1988; 2001).

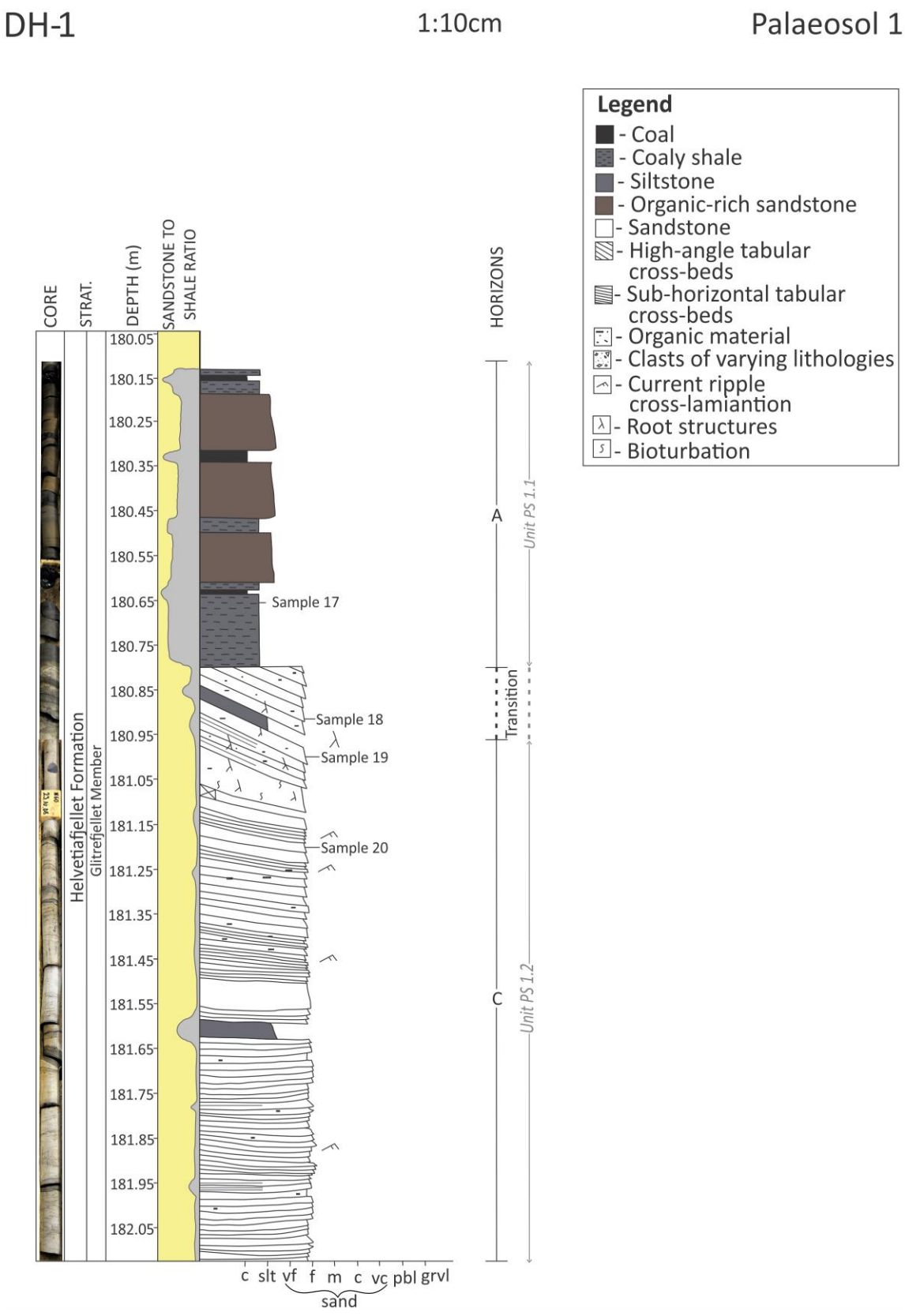

Figure 27: 1:10 cm detail log of Palaeosol 1. The palaeosol was observed in core DH-1, from 180.1 to 182.15 meters depth. To the very left of the figure, comparative images of the logged section can be seen. Sandstone to mudstone ratio is also added to illustrate the general composition of the palaeosol. The horizons on the right-hand side of the figure are interpretations based on the scheme presented by Retallack, (2001). For further details, please see Appendix C.

4.3.1.1.1 Unit PS 1.1 – Horizon A

The sediments in which unit PS 1.1 is composed of have been interpreted as floodplain deposits (Fig. 23; Table 2; FA 3).

Description

Unit PS 1.1 represents the upper 70 cm of Palaeosol 1, and can be recognized by grain sizes varying from very fine-grained sandstone to claystone and an overall dark colour (Fig. 28 A & 28 B). In hand samples, the sediments have a very brittle texture and are prone to breaking. The top of the unit is determined by a very sharp contact (Fig. 28 A). Within the upper 45 cm of this unit, three 8—10 cm thick beds are observed. These three beds stand out compared to the remaining part of the unit due to a slight increase in grain size (very fine-grained sandstone) and a brown colour (Fig. 28 B). Three thin beds with an estimated thickness of approximately 2 cm are also observed. These are recognized by their extremely fine grain size (claystone), black colour and shiny texture (Fig. 28 B). Small fragments with similar characteristics are also observed throughout the unit. The remaining part of the unit can be recognized by a grain size equivalent to a claystone and siltstone, and a dark grey colour (Fig. 28 C). The unit appears to be relatively homogeneous.

Interpretation

The overall dark colour of the unit is interpreted as an indication of high organic content (Stow, 2006). A sharp upper contact, such as the one described for this unit, is a typical feature of a palaeosol (Retallack, 1988; 2001). The three 8 – 10 cm thick beds are interpreted to stand out compared to the rest of the unit due a slight increase in grain size, but could also be an indication of leaching (Kraus, 1999). The brown colour could also suggest a high organic content. Based on these descriptions, the three 8-10 cm thick beds are interpreted as very-fine sandstones with a high organic content. The other three 2 cm thick beds, are based on their grain size, black colour and shiny texture, interpreted as thin coal seams. One of these beds is presented in Fig. 28 B. Their placement within Palaeosol 1 is indicated in Fig. 27. The small fragments observed within the unit with similar characteristics are defined as fragments of coalified organic material. Their occurrence has been noted in Fig. 27 as well. Based on the grain size and colour of the remaining portion of the unit, it has been defined as coaly shale.

The macro-scale characteristics of unit PS 1.1, such as being very fine-grained, well-sorted, rich in organic matter and the occasionally observed shiny texture, are consistent with the observed characteristics of floodplain deposits (Table 2; FA 3). Based on the high organic content of the unit in combination with the observed mineral fraction, unit PS 1.1 of Palaeosol 1 fits well with horizon A of Retallack, (2001; Appendix C). According to the author, horizon A is characterised by an accumulation of organic matter in conjunction with a mineral fraction. Horizon A can often be observed as the uppermost horizon of a palaeosol, as it has been interpreted for Palaeosol 1.

4.3.1.1.2 Unit PS 1.2 – Horizon C

The deposits in which unit PS 1.2 is composed of are interpreted as crevasse splay deposits (Table 2; FA 4).

Description

Unit PS 1.2 is the lowermost unit of Palaeosol 1, and has an approximate thickness of 115 cm. Its boundaries have been placed at 181 m and 182.15 m below present day surface, respectively (Fig. 27 & 28). Unit PS 1.2 is predominantly composed of pale, quartz-rich sandstone (Fig. 28 E & 28 F). The grain size is equivalent to fine to medium-grained sandstone. Due to the high percentage of quartz, sections within the horizon can appear relatively massive (Fig. 28 E). In areas where the sandstone is influenced by thin laminae of a darker and more fine-grained mineral, cross-lamination is observed (Fig. 28 F).

The contact between unit PS 1.1 and unit PS 1.2 is a diffuse contact, with a thickness of approximately 20 cm. This transition zone reflects characteristics of both horizons. The quartz-rich sandstone beds of unit PS 1.2 are herein separated by laminae of the coaly shale of unit PS 1.1. The laminae was also noted as appearing discontinuous and disturbed (Fig. 28 D). The units within the transition zone appear to be dipping. This can be observed as relatively steeply dipping beds in the uppermost section of the transition and much more gently dipping, sub-horizontal beds at its base (Fig. 28 C).

Elongated lineations and fragments of a third amorphous mineral are also observed within the unit (Fig. 28 D & 28 E). In the logged section, these can be recognized by a black colour, a grain size equivalent to claystone and a shiny texture. The elongated lineations are uneven in shape and size, and appear to radiate downwards within the core (Fig. 28 D).

Interpretation

A gradual transition, such as the one observed between units PS 1.1 and PS 1.2 is common between two horizons within a palaeosol (Retallack, 1988; 2001). A possible explanation for the light colour that is observed within the quartz-rich sandstone is that the horizon has been a zone of leaching within the palaeosol. Leaching is the removal of soluble minerals through dissolution (Buol et al., 2011). A removing agent, typically rainwater or ground-water percolates through the sediments. This dissolves non-resistant minerals, leaving the sediments relatively enriched by resistant minerals, such as quartz (Lehmann & Schroth, 2003; Sheldon & Tabor, 2009; Buol et al., 2011). The lack of structures described when the quartz content was very high can indicate that the unit is too well-cemented for structures to become apparent.

The elongated lineations (Fig. 28 D & 28 E) are interpreted as root structures. Where the roots are described as black and shiny in texture, they are interpreted to contain coalified organic material. This interpretation is also valid for the fragments with similar characteristics that are observed throughout the unit. As mentioned previously, root traces are burrows created in the sediments as the roots grew. They are regarded as the best indicator of palaeosols in the rock record because regardless of how developed the soil profile is, plants once grew in these sediments, thus defining it as a soil (Retallack, 1988; Buol et al., 2011). Burrowing of roots is also interpreted as the reason why the laminae in the transition zone between the two units appears to be discontinuous and disturbed. As the roots penetrate the sediments, their original position is shifted, thus causing a disturbance in the layering (Fig. 28 E). In Fig. 28 F, the cross-cutting laminae observed within the unit is displayed. Based on the set size and asymmetric appearance of the cross-cutting units, they are interpreted as current ripple cross-laminations.

Based on the grain size, large quantities of quartz and the observed current ripple cross-lamination, the deposits of unit PS 1.2 are consistent with the expected characteristics of crevasse splay deposits (Table 2; FA 4). The characteristics of the deposits are also consistent with the characteristics of horizon C, of Retallack, (2001; Appendix C). This horizon is characterised by a low degree of alteration due to soil forming activities and the presence of relict structures. In unit PS 1.2, such relict structures are the previously described current

ripple cross-laminations. If it was not for the root structures and the potential leaching observed within the unit, this horizon can often be mistaken for parent material.

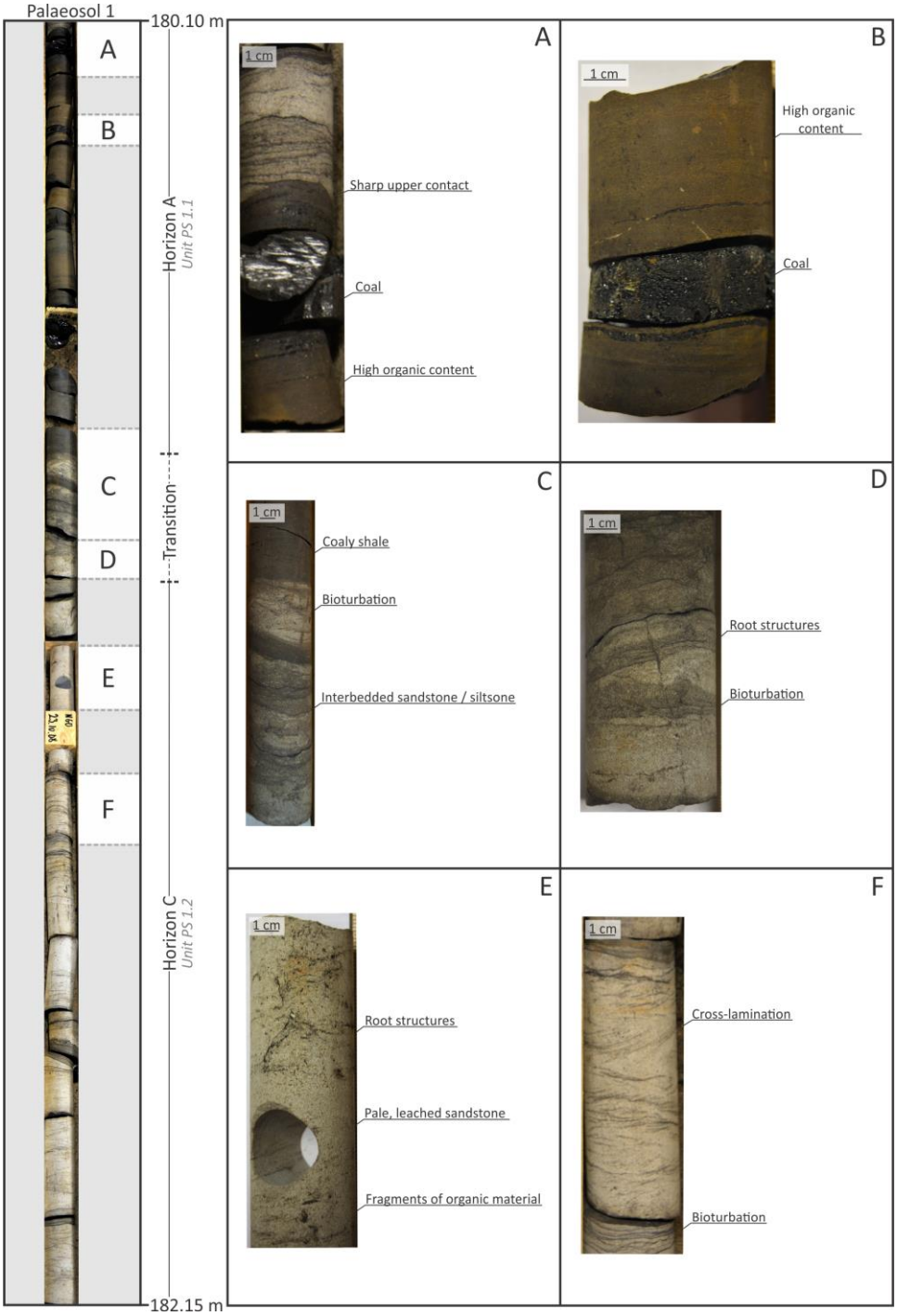

Figure 28: Representative core images of Palaeosol 1. Their placement within the palaeosol is indicated with the letters A to F on the left-hand side of the figure. ***Image A*** *displays the very sharp upper contact described in unit PS 1.1, as well as a thin coal seam. In* ***image B****, a thin coal seam can be observed between the two brown organic-rich sandstone beds, as described within unit PS 1.1.* ***Image C*** *and* ***D*** *represent the transition between unit PS 1.1 and PS 1.2. In this section, characteristics of both units can be observed. Disturbances in the laminae due to root structures is best seen in* ***image D****.* ***Image E*** *and* ***F*** *both display the characteristics of unit PS 1.2. They are both light in colour, suggesting leaching and a high quartz content. Root structures and fragments of coalified organic material is seen in* ***image E.*** *Current ripple cross-lamination is illustrated in* ***image F****. Horizons A and C are interpreted according to nomenclature of Retallack, (2001; Appendix C).*

4.3.1.2 Micro-scale observations

Four thin sections were produced from the deposits Palaeosol 1 is composed of. Their stratigraphic position within the perimeters of Palaeosol 1 is indicated in Fig. 27. In the following section, representative images of the thin sections will be presented. The mineralogical content of the thin sections is described and interpreted in order to compare the results with the observations made during macro-scale observations.

4.3.1.2.1 Thin section 17

Thin section 17 was collected from units PS 1.1, which is the more organic rich unit of Palaeosol 1, indicated in Fig. 29. The characteristics observed through petrographic analysis are presented in images A to C within the same figure. Based on the macro-scale observations of the palaeosol, the unit was interpreted as horizon A. This horizon is generally recognized by high organic content in conjunction with a mineral fraction (Retallack, 2001; Appendix C). The deposits that unit PS 1.1 is composed of were also interpreted as floodplain deposits (Table 2; FA 3).

Description

The thin section is largely dominated by a very fine-grained, dark coloured matrix. The other dominating feature of the sample is a mineral consisting of very small grains with an anhedral crystal shape (Fig. 29). Based on the appearance of the mineral, it fits well with the characteristics of monocrystalline quartz, presented in chapter *4.1.1.*

Several elongated lineations in varying shapes and sizes are also observed in thin section 17 (Fig. 29 A & 29 B). Occasionally, the lineations are observed branching out into several smaller lineations (Fig. 29 B). The majority of the lineations contain a red to golden coloured amorphous mineral, which remains unchanged in both plane and cross-polarized light, whereas other lineations appear to be transparent. Small fragments with similar characteristics are also observed throughout the thin section (Fig. 29 C). This amorphous mineral fits well with the characteristics of organic material, presented in chapter *4.1.8*.

Interpretation

The large fraction of matrix observed within the thin section is a possible theory as to why hand samples were described as brittle and dark in colour. Based on the elongated shape and observed branching of the organic material observed within the thin section, these are interpreted as root structures. Although root structures were not observed during macro-scale observations, their presence within thin section 17 strengthens the theory that this unit has been influenced by soil forming processes, and is therefore a part of a palaeosol. The transparent lineations are interpreted as being void of material. This could be because they are root structures where the organic material was removed, or because they are cracks created during soil formation. Cracks are often associated with the processes that occur during soil formation (Kraus, 1999; Retallack, 2001; Buol et al., 2011).

During macro-scale observations, the deposits of unit PS 1.1 were interpreted as floodplain deposits. Through micro-scale observations, an overall fine grain size, large quantities of muddy matrix and organic content is observed. This is consistent with the expected characteristics of floodplain deposits, as they were presented in Table 2; FA 3.

Based on the observations presented above, the material observed within thin section 17 is consistent with the expected characteristics of deposits collected from horizon A of a palaeosol. Both the organic material and the mineral fraction described by Retallack, (2001) are present in the thin section. The presence of root structures is also a strong indication of soil forming activities (Buol et al., 2011; Fig. 29 B).

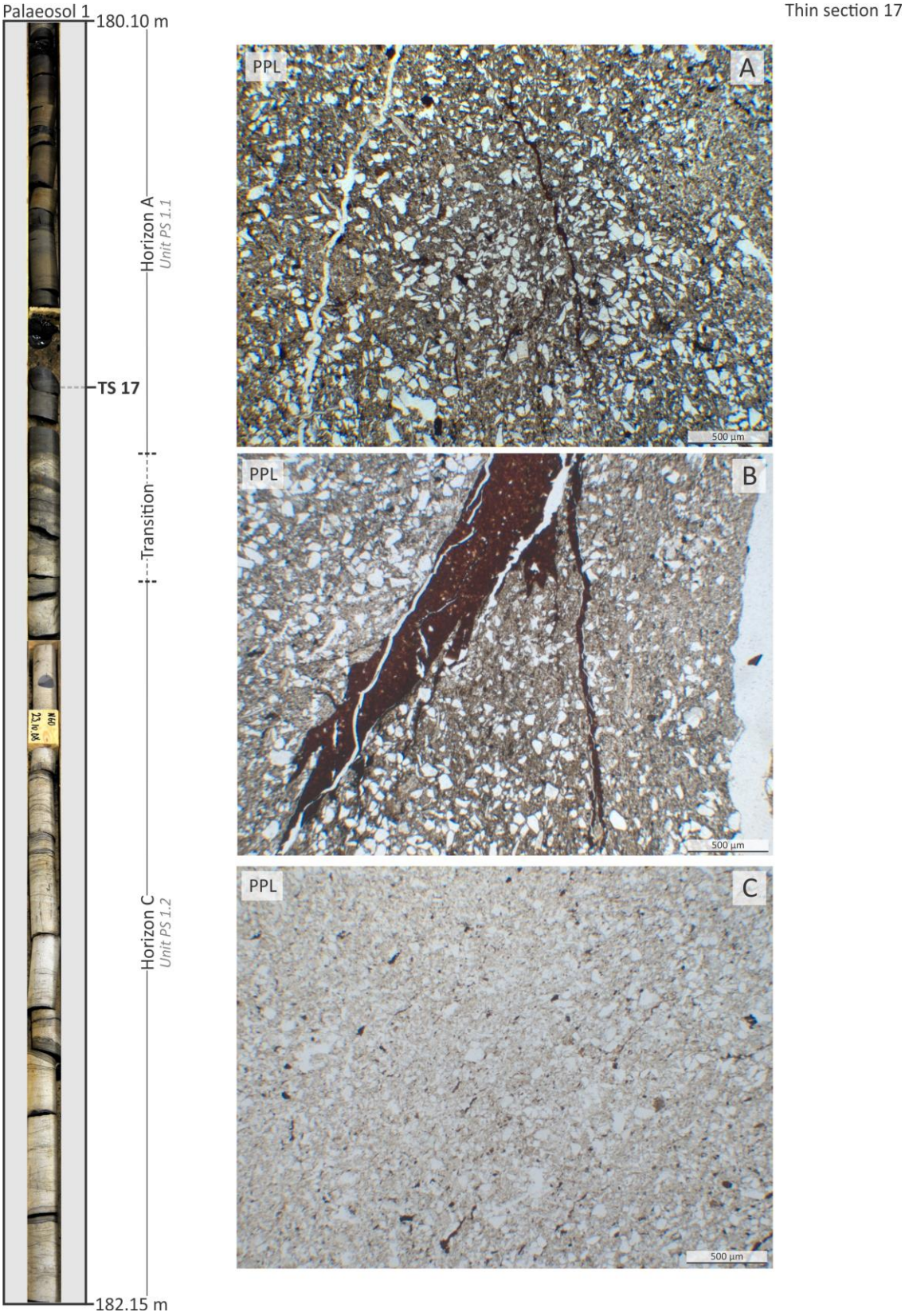

Figure 29: Representative photomicrographs of the mineralogical composition of thin section 17. Its location within Palaeosol 1 is indicated in the core image on the left-hand side of the figure. ***Images A to C*** *all display the large quantities of fine-grained matrix present within the sample. The small quartz grains can also be observed in all images. Root traces and/or cracks can be seen in* ***image A*** *and* ***B****. Fragments of organic material are best represented in* ***image A*** *and* ***C****. All photomicrographs in the figure are taken in plane polarized light (PPL).*

4.3.1.2.2 Thin section 18

Thin section 18 was collected stratigraphically below thin section 17. The thin section was collected from what is interpreted as the gradational transition zone between the overlying horizon A (unit PS 1.1) and the underlying horizon C (unit PS 1.2). Three photomicrographs representing the observed characteristics of thin section 18 are presented in Fig. 30.

Description

Thin section 18 predominantly consists of one mineral. The grain size is somewhat varying, but is overall equivalent to fine-grained sandstone. The crystal shape is typically anhedral, and the mineral is typically transparent. The characteristics of the mineral are consistent with the characteristics of monocrystalline quartz, presented in chapter *4.1.1*. The quartz is enclosed by a darker coloured matrix, with a grain size that is too small to distinguish through optical microscopy (Fig. 30 A). The matrix content within the sample is significant.

Black to redish coloured lineations are also observed throughout the sample (30 B and 30 C). These lineations commonly move around the grains of the dominant mineral, rather than cut through them (Fig. 30 C). The characteristics of this amorphous mineral are consistent with those of organic material, presented in chapter *4.1.8*.

Interpretation

Based on the elongated shape of the organic material in conjunction with its observed branch-like shape, these have been interpreted as roots structures (Figs. 30 B & 30 C). This suggests that the transition zone has been influenced by soil forming processes as well.

In macro-scale observations (Chap. *4.3.1.1*), horizon A was described as organic rich and fine-grained. Within horizon C on the other hand, the grain size was larger, and the organic content was significantly lower. In thin section 18, the quartz grains are significantly larger than those observed within thin section 17, but the overall matrix content is less than what was observed in thin section 17. The organic content is interpreted as being relatively high. Therefore, the characteristics of both horizon A (unit PS 1.1) and horizon C (unit PS 1.2) are present within thin section 18. This supports the theory that the thin section was collected from the transition zone between the two horizons. A relatively wide, diffuse transition zone between horizons within a palaeosol is relatively common (Retallack, 1988).

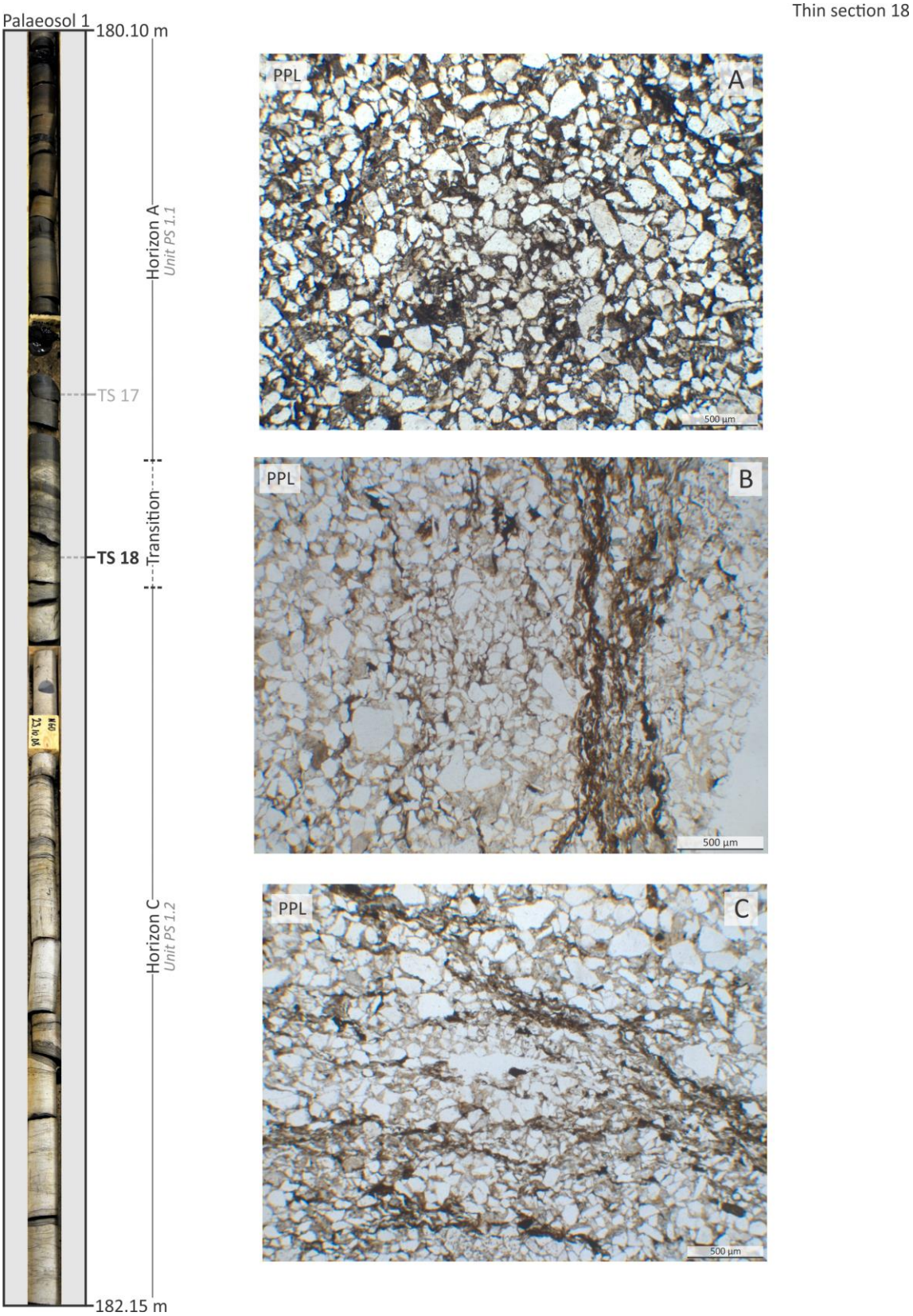

*Figure 30: Representative photomicrographs of the mineralogical composition of thin section 18. The location of thin section 18 within Palaeosol 1 is indicated in the core image on the left-hand side of the figure. This area is interpreted as the transition between horizons A and C. Therefore, areas of the thin section had a high matrix content (**image A**), while other areas were more quartz dominated (**image B** and **C**). Root structures and clasts of organic material were also observed within the sample. These are best seen in **image B** and **C**. All photomicrographs are taken in plane polarized light (PPL).*

4.3.1.2.3 Thin section 19

The origin of thin section 19 is indicated in Fig. 31, along three photomicrographs that represent the general characteristics of the thin section. During macro-scale description of the palaeosol, unit PS 1.2 was interpreted as horizon C of Retallack, (2001; Appendix C). The deposits of the unit were also interpreted as crevasse splay deposits (Table 2; FA 4).

Description

Thin section 19 is observed as predominantly consisting of a single mineral. This mineral is present in all images of Fig. 31, but is the main feature in Fig. 31 A. An anhedral crystal shape is observed, accompanied by a weak relief. The other characteristics of the mineral are consistent with those described for monocrystalline quartz, presented in chapter *4.1.1*. Very tight packing of the quartz grains is observed, as there are only very small amounts of matrix present between the grains, if present at all (Fig. 31 A).

Although far less abundant, the other dominating feature of the thin section are elongated lineations, containing a dark, amorphous mineral (Figs. 31 B & 31 C), similar to those observed in thin section 18. The lineations branch out and appear to trace around the quartz grains, rather than cut through them. The characteristics of amorphous mineral within the elongated lineations are consistent with those described for organic material, presented in chapter *4.1.8*.

Interpretation

Based on the observed branching of the elongated lineations, these are interpreted as root structures. This interpretation is strengthened by the observation of root structures during macro-scale observations as well. Root structures are the premier diagnostic feature of soil forming processes (Retallack, 2001; Buol et al., 2011), confirming that the thin section was sampled from palaeosol.

During macro-scale observations, unit PS 1.2 was described as a pale and relatively structureless sandstone. The tight packing of the quartz grains within thin section 19 offers a possible explanation to the lack of observed structures. Such tight packing can lead to cementation of the quartz grains, which can be observed as quartz overgrowth. Cementation of deposits can make primary structures difficult to observe. The large quantities of pale quartz observed in both macro and micro-scale observations could also be an indication of

leaching. Leaching occurs when soluble or non-resistant minerals are removed from the sedimentary package through dissolution (Lehmann & Schroth, 2003; Buol et al., 2011).The removing agent is typically either rain or ground-water. The deposits then become relatively enriched by more resistant minerals, such as quartz. Well-drained palaeosols are typically more heavily influenced by leaching, as the drainage promotes the movement of water through the palaeosol (Bown & Kraus, 1987; Cecil & Dulong, 2003).

Also during macro-scale observations, the deposits of units PS 1.2 were interpreted as crevasse splay deposits (Table 2; FA 4). Through micro-scale observations, large quantities of quartz, low matrix content and the presence of root structures and coalified plant debris is observed. Such observations are consistent with the expected characteristics of crevasse splay deposits, as they were presented in Table 2; FA 4.

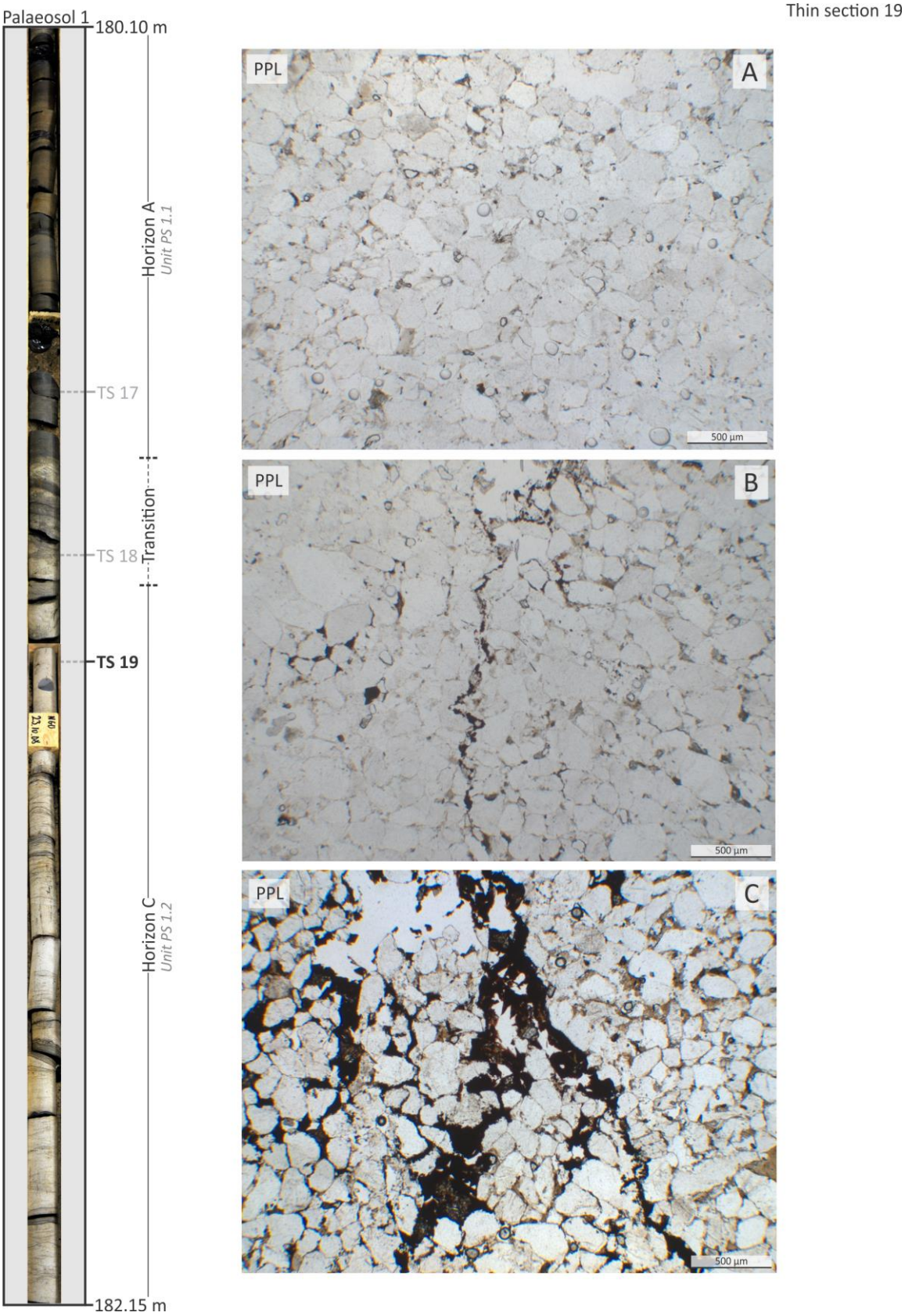

Figure 31: Representative photomicrographs of the mineralogical composition of thin section 19. The location of the sample within Palaeosol 1 is indicated in the core image on the left-hand side of the figure. ***Image A*** *displays the tight packing of the quartz grains within the thin section. In* ***image B*** *and* ***C****, elongated lineations of varying shapes and sizes are presented. These are interpreted as root structures. All photomicrographs are taken in plane polarized light (PPL).*

4.3.1.2.4 Thin section 20

Where thin section 20 was collected from within Palaeosol 1 is indicated in Fig. 32. Similarly to thin section 19, thin section 20 was also collected from unit PS 1.2, which was interpreted as horizon C during macro-scale observations of the palaeosol (Chap. *4.3.1.1.2)*. The deposits were interpreted as crevasse splay deposits (Table 2; FA 4). Two photomicrographs representing the characteristics of thin section 20 can be seen in Fig. 32, and will be discussed further below.

Description

Thin section 20 is dominated by a mineral whose general characteristics observed through optical microscopy are consistent with those described for monocrystalline quartz (Chap. *4.1.1*; Fig. 32). The grain size of the quartz is varying within the thin section, but is typically observed as very fine to medium-grained sandstone. The matrix content varies throughout thin section 20, but the thin section is overall observed as being relatively enriched in matrix compared to thin section 19 (Fig. 32 B).

Elongated lineations with similar characteristics as described within thin section 18 and 19 are observed. These are irregular in shape and size, black to golden in colour and are observed tracing the quartz grains within the thin section rather than cutting through them (Fig 32 A). The amorphous mineral within the lineations is consistent with the expected characteristics of organic material, presented in chapter *4.1.8*.

Interpretation

The larger quantities of matrix (Fig. 32 A) that are observed within thin section 20 compared to thin section 19 is a possible factor in the presence of current ripple cross-lamination within unit PS 1.2. As this section of unit PS 1.2 is not as tightly packed as it was observed to be in thin section 19, such structures are easier to observe. Based on the characteristics of the elongated lineations and the amorphous mineral they contain, they are interpreted as root structures containing coalified organic material.

As thin section 20 is interpreted to have been collected from the same pale and quartz-rich sandstone unit as thin section 19, the same potential effects of leaching are observed within the thin section. The relative abundance of quartz grains can indicate that other less-

resistant minerals potentially have been removed through dissolution (Sheldon & Tabor, 2009; Buol et al., 2011).

There are many shared characteristics with regards to mineralogical composition when comparing thin sections 19 and 20. Therefore, it is interpreted that the deposits that the thin sections are composed of were formed under similar conditions. This increases the probability of both thin sections originating within horizon C (Retallack, 2001; Appendix C). Both thin sections were dominated by abundant quartz, a lack of other minerals and a low organic content, which is consistent with the characteristics of horizon C. Similarly, as a result of the shared characteristics of thin sections 19 and 20, thin section 20 is also interpreted to have been collected from crevasse splay deposits (Table 2; FA 4).

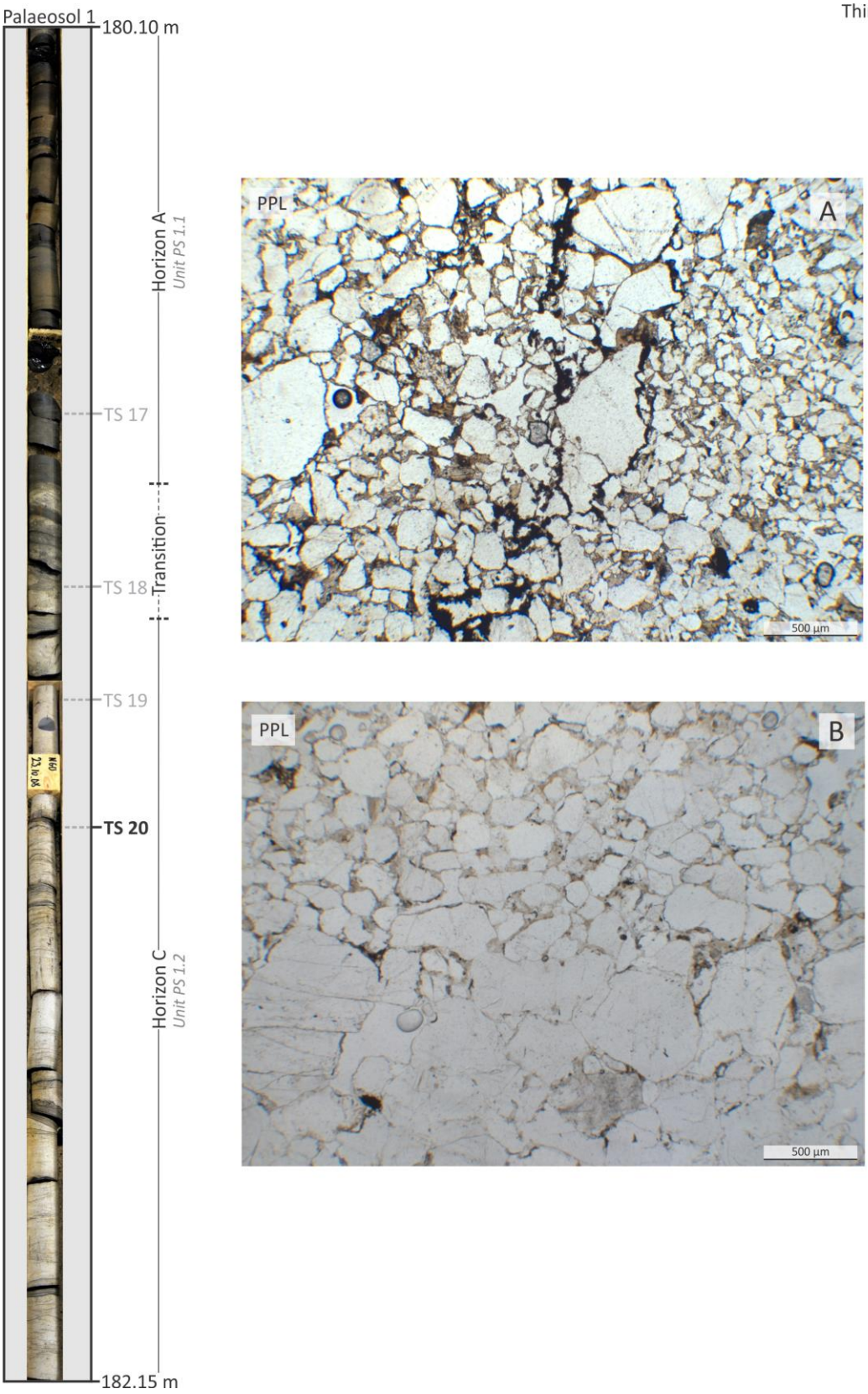

*Figure 32: Representative photomicrographs of the mineralogical composition of thin section 20. The origin of the sample within Palaeosol 1 is indicated in the core image on the left-hand side of the figure. Both **image A** and **B** display that the thin section was dominated by quartz, with some matrix separating the quartz grains. **Image B** illustrates the variation in grain size seen within the thin section. Coalified organic material and root structures is best seen in **image A**. Both photomicrographs are taken in plane polarized light (PPL).*

4.3.1.3 Classification of Palaeosol 1

Based on the characteristics of Palaeosol 1, observed through both micro and macro-scale observations, the palaeosol is interpreted to be composed of horizons A (unit PS 1.1) and C (unit PS 1.2). Horizon A is interpreted as being composed of floodplain deposits, whereas horizon C is interpreted as being composed of crevasse splay deposits (Table 2; FA 3 & FA 4). The boundaries of the horizons are indicated in Figs. 27. Current ripple cross-lamination was described within horizon C (Fig. 28 F). Such relict structures within a horizon generally suggest a low degree of alteration due to soil forming processes (Kraus, 1999; Retallack, 2001). Based on the weak development of the observed soil horizons, Palaeosol 1 fits well with the characteristics of an entisol (Wilding et al., 1984 A; Bown & Kraus, 1987; Kraus, 1999; Cecil & Dulong, 2003).

Entisols are immature palaeosols where the degree of alteration due to soil forming processes is minor (Wilding et al., 1984 A; Cecil & Dulong, 2003). In some cases, the only evidence of soil forming activities is the presence of root structures (Retallack, 1988; 2001,). The sediments that the palaeosol is composed of can be otherwise unaltered. As a result, original features, in this case sedimentary structures, of the parent material can still be present within the palaeosol. This was observed within Palaeosol 1 as current ripple cross-lamination.

There are several different reasons as to why a palaeosol can lack alteration due to soil forming processes. Examples here are that the conditions under which the soil was formed were unfavourable, or that the parent material is very resistant to weathering (Kraus, 1999). As seen in Table 2, the deposits that Palaeosol 1 has developed within are interpreted as a combination of floodplain deposits and crevasse splay deposits. Where relatively rapid and continuous deposition occurs, palaeosols will become buried relatively quickly by these sediments, thus disabling further reworking by the soil forming processes (Nemec, 1992; Kraus, 1999; Kraus & Aslan, 1999). For a more in-depth discussion on the topic, please see chapter *5.3.1*. As established through both macro and micro-scale observations, quartz is an abundant mineral in Palaeosol 1. This is a potential result of leaching.

As discussed in chapter *2.7*, the development of an entisol is not dependent on specific climatic conditions (Fig. 8). This suggests that Palaeosol 1 is not a useful proxy with regards to palaeo-climate. For further discussion on the topic, please see chapter *5.2* & *5.3.*

4.3.2 Palaeosol 2 (PS 2)

4.3.2.1 Macro-scale observations

Palaeosol 2 is located stratigraphically below Palaeosol 1 in the logged section of DH-1, separated by a relatively thin unit of parent material. The palaeosol is approximately 155 cm in thickness, and its boundaries have been set at 182.65 m and 184.1 m below present day surface. A detailed (1:10 cm) log of the palaeosol is presented in Fig. 33. Palaeosol 2 is interpreted as being composed solely of crevasse splay deposits (Table 2; FA 4). In the following section, Palaeosol 2 will be described based on macro-scale observations noted from the logging process of core DH-1.

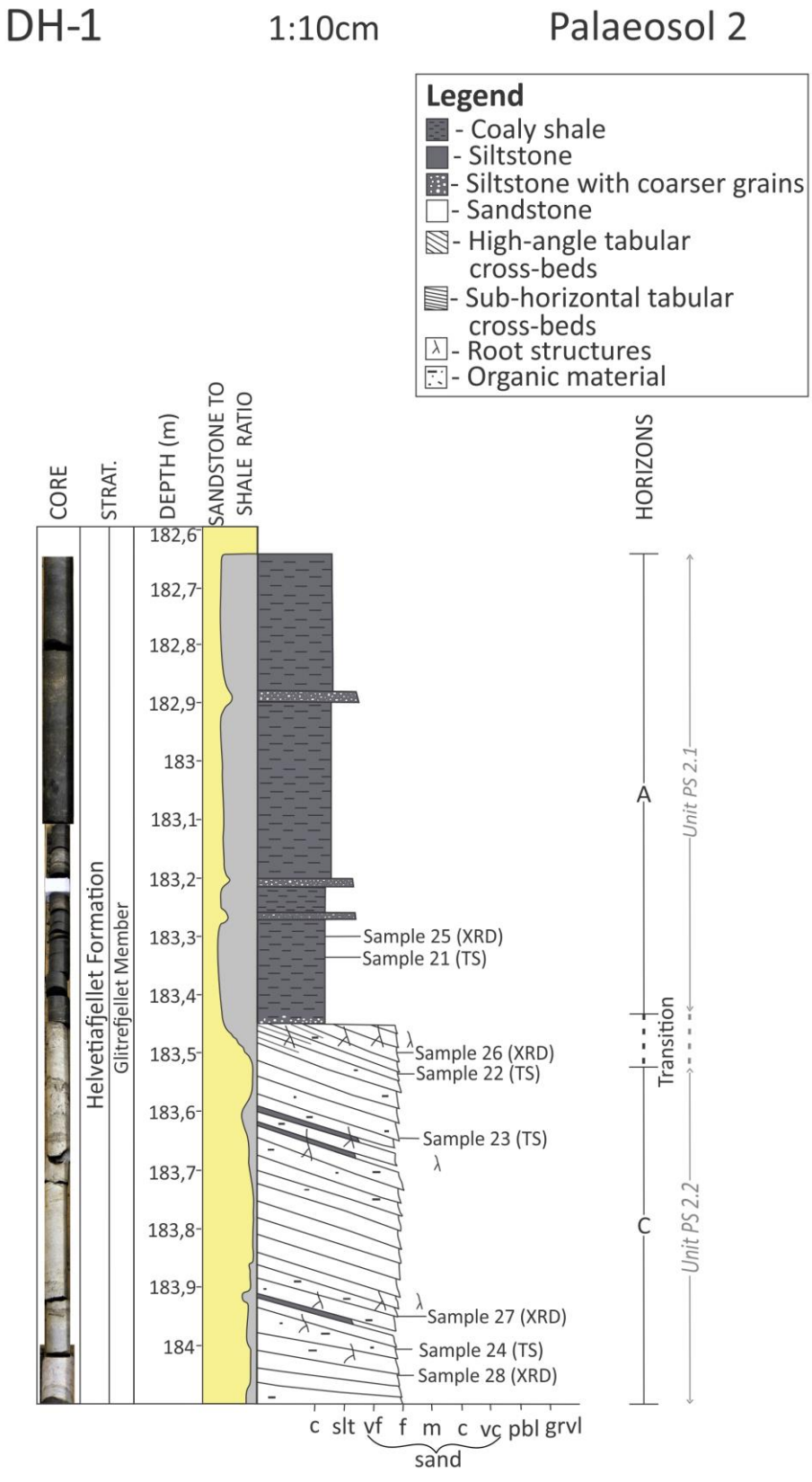

Figure 33: A 1:10 cm detailed log illustrating the characteristics of Palaeosol 2. The palaeosol was observed in core DH-1, from 182.65 to 184.1 meters depth. To the very left of the figure, the palaeosol as it was observed within core DH-1 is presented. Sandstone to shale ratio is included to illustrate the general composition of the deposits. The samples indicated in the figure were removed for both thin section (TS) and XRD-analysis (XRD). The horizons on the right-hand side of the figure are interpretations based on the scheme presented by Retallack, (2001; Appendix C).

4.3.2.1.1 Unit PS 2.1 – Horizon A

Description

Unit PS 2.1 consists of the upper 85 cm of Palaeosol 2. The unit is dominated primarily by dark grey coloured deposits, with an overall grain size that is equivalent to siltstone (Figs. 34 A & 34 B). The unit was observed to be relatively brittle. The between the top of Palaeosol 2 and the overlying parent material is not as abrupt as the one observed in Palaeosol 1. The unit appears to be relatively massive, with some exceptions. The upper 60 cm of unit PS 2.1 contains a higher percentage of coarser-grained material, compared to the lowermost 25 cm of the unit. This can be seen as white minerals with grains equivalent to fine-grained sandstone (Fig. 34 A). At depths of approximately 182.8 m, 183.05 m and 183.2 m, the coarser grains are more concentrated. This can be observed as lighter coloured beds with an approximate thickness of 4 cm (Fig. 34 A) that are enclosed by the dominating dark grey mineral. Some disturbances are also observed in the otherwise relatively massive unit. These can be recognized as dark coloured lineations, and small circular marks (Fig. 34 A). These are most prominent in the sections of the unit where the concentration of coarser grains is greater.

Interpretation

The dark colour described for the dominating mineral in the unit is regarded as an indicator of high organic content (Vodyanitskii & Savichev, 2017). Therefore, based on the grain size, the dark colour and brittle texture of the deposits, the dominating lithology of the unit is interpreted as coaly shale.

As stated above, the light coloured, coarser-grained minerals were concentrated into thin beds within the unit (Fig. 34 A). This can have occurred as a result of compaction post-burial, due to the weight of the overlying sediments (Fisher et al., 1999). The disturbance within the unit, observed as lineations and circular marks are interpreted as bioturbation by roots. As it has been stated previously, root traces are the premier indicator of soil formation in the rock record (Retallack, 2001; Buol et al., 2011).

Based on the high organic content of the unit in conjunction with the observed fraction of lithic grains, this unit fits well with the characteristics of horizon A of Retallack, (2001; Appendix C). The grain size, homogeneous appearance and high degree of sorting observed

within the deposits is also consistent with the characteristics of crevasse splay deposits (Table 2; FA 4).

4.3.2.1.2 Unit PS 2.2 – Horizon C

Description

The lowermost unit (PS 2.2) of Palaeosol 2 is approximately 60 cm in thickness. Its boundaries have been placed at 183.45 m and 184.1 m. The transition zone between the two main units of the palaeosol is diffuse and approximately 10 cm thick (Fig 34 B). A transitional contact between two units within a palaeosol relatively common (Retallack, 1988). Unit PS 2.2 can be recognized as very pale and quartz-rich, with an overall grain size equivalent to fine-grained sandstone. Approximately 1 cm thick, subparallel and gently dipping beds can be recognized within the unit due to a slight colour-change (Fig. 34 D).

Black coloured clasts and fragments can be seen throughout the unit (Fig. 34 C). These can be recognized by a shiny texture. Elongated lineations also disturb the bedding within the unit. The lineations are uneven in size and shape, and are occasionally observed to be branching out (Figs. 34 B, 34 C & 34 D).

Interpretation

The pale colour of the sandstone observed within the unit is a possible indication of leaching. As it was described for Palaeosol 1, leaching is the removal of minerals or nutrients, most commonly by dissolution (Lehmann & Schroth, 2003; Sheldon & Tabor, 2009). Both ground-water and rain can function as the removing agent (Buol et al., 2011). As a result, the unit becomes enriched by resilient minerals, such as quartz. Based on the morphology of the dipping beds observed within the unit, these are defined as tabular cross-beds. The tabular cross-beds are interpreted to be observable within the unit due to either a slight change in mineralogical composition, or a slight difference in grain size. Grains of similar size can concentrate into beds when the unit undergoes compaction, which is a possible consequence of burial (Fisher et al., 1999). Based on the shape and observed branching of the elongated lineations, these are interpreted as root traces. The black colour and shiny texture observed within some of the root traces is interpreted as coalified organic material. This interpretation is also valid for clasts and fragments with similar characteristics.

Based on the descriptions above, this unit fits well with the characteristics of horizon C of Retallack, (2001; Appendix C). The horizon is generally recognized by the presence of relict structures. Within unit PS 2.2, these structures are observed as tabular cross-beds. The presence of such structures within a palaeosol is typically indicative of only minor alterations due to soil forming processes. If not for the observed root traces within the unit, this horizon can easily be mistaken for parent material.

The grain size and high quartz content observed within the deposits of unit PS 2.2, in combination with the observation of organic material is consistent with the characteristics of crevasse splay deposits (Table 2; FA 4). Therefore, unit PS 2.2 is interpreted as being composed of crevasse splay deposits.

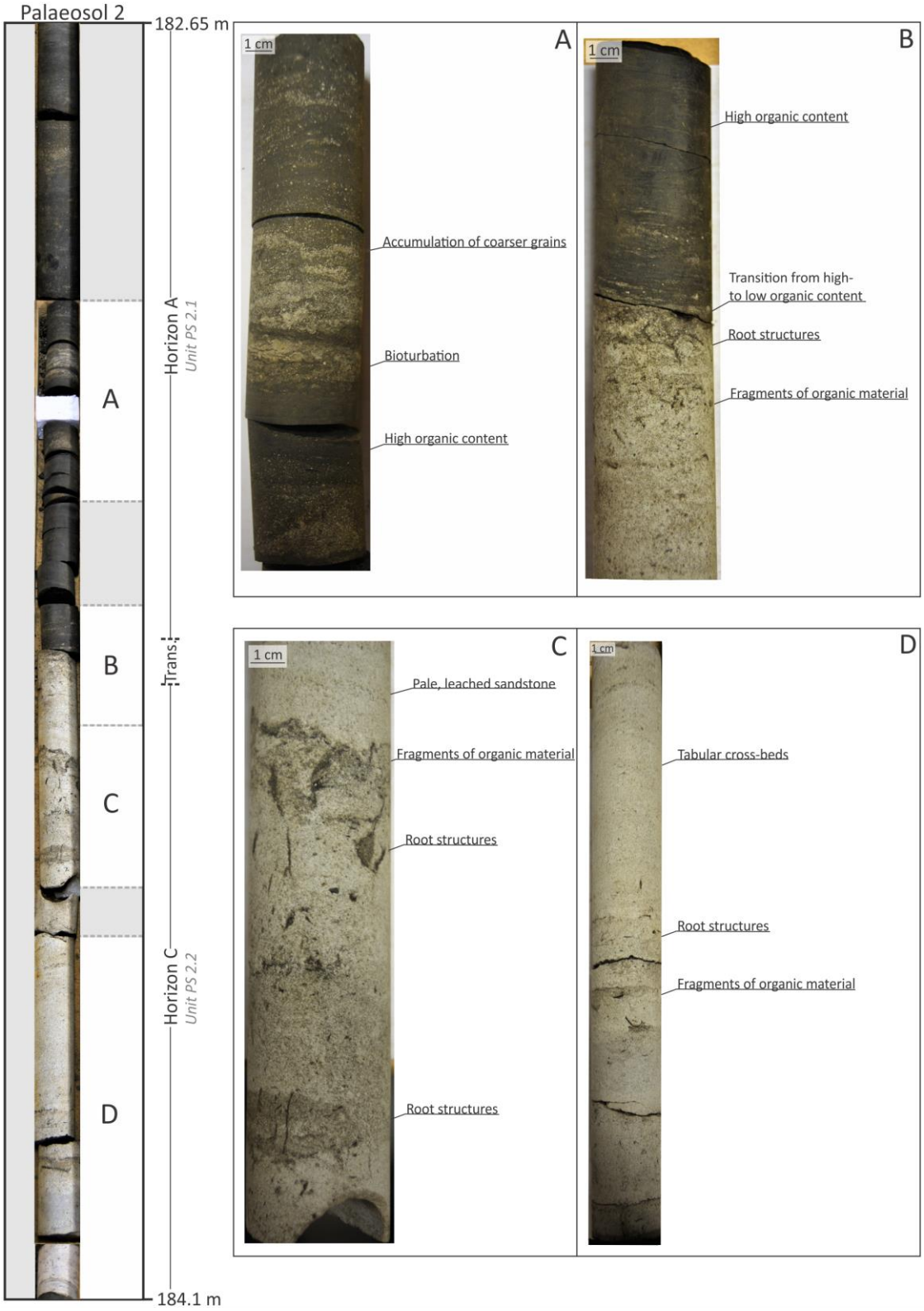

*Figure 34: Representative images of the observations made during the logging of Palaeosol 2. The different segments of the core are marked with the letters A to D, and their occurrence within the palaeosol is indicated on the left-hand side of the figure. Both unit PS 2.1 and PS 2.2 are also indicated in the figure. In **image A**, the more coarse-grained beds of unit PS 2.1 can be seen, alongside the otherwise dark coaly shale. In **image B**, the transitional contact between unit PS 2.1 and unit PS 2.2 can be seen. **Image C** displays the pale quartz penetrated by root traces and fragments of coalified organic material. In **image D**, the tabular cross-beds observed within the palaeosol can be observed. The units have been interpreted as horizons A and C according to the nomenclature of Retallack, (2001; Appendix C).*

4.3.2.2 Micro-scale observations

Three thin sections were produced from samples collected from Palaeosol 2. Their occurrence within Palaeosol 2 is indicated in Fig. 33. In the following section, representative images of all three thin sections will be presented and discussed.

As the fourth thin section (thin section 21) was not produced successfully, there is no mineralogical representation of unit PS 2.1 of Palaeosol 2 available. Therefore, all three thin sections from Palaeosol 2 represent the lowermost unit PS 2.2. This unit was interpreted as horizon C of Retallack, (2001; Appendix C) during macro-scale observation. The palaeosol is interpreted to have developed within crevasse splay deposits (Table 2; FA 4).

4.3.2.2.1 Thin section 22

The location of thin section 22 within Palaeosol 2 is indicated in Fig. 35. Three representative photomicrographs of the thin section are presented in the same figure, and will be discussed further below.

Description

One mineral dominates thin section 22 (Fig. 35 A). The crystal shape of the mineral is anhedral, and the grains are observed as being transparent in plane polarized light. The general characteristics of the mineral are consistent with those described for monocrystalline quartz in chapter *4.1.1*. The quartz grains are typically very tightly packed, thus allowing for only minimal pore space. Where some available pore space is present, it is generally void of material (Fig. 35 A). Therefore, there is very little matrix present within the thin section.

Elongated lineations are observed within the thin section (Fig. 35 B). They vary in both shape and size, and can often be observed with a black or a golden orange colour in both plane and cross-polarized light. Such characteristics are consistent with those previously described for organic material in chapter *4.1.8*.

The last mineral observed in thin section 22 occurs only in very small quantities (Fig. 35 C). When viewed in cross-polarized light, the mineral appears pearlescent. A rhombohedral cleavage is also observed. This is consistent with the characteristics of carbonate, described in chapter *4.1.7*.

Interpretation

Based on the shape and colour of the elongated lineations described in the thin section, they are interpreted as fossil root structures. Such features are the most definitive indication of soil forming activities (Retallack, 2001; Buol et al., 2011). In macro-scale observations, unit PS 2.2 was described as a pale, quartz-rich sandstone. This is reflected by the mineralogical composition of thin section 22 (Fig. 35), where quartz is far more abundant than the other observed minerals.

The relative abundance and pale colour of the observed quartz is a possible result of leaching. As previously discussed, leaching is the removal of soluble minerals, thus leaving the sediments relatively enriched in more resistant minerals (Lehmann & Schroth, 2003; Sheldon & Tabor, 2009).The removing agent is typically rainwater percolating through the sediments, or ground-water influence caused by fluctuations in the ground-water table. Leaching is often observed in palaeosols. Typically, well-drained palaeosols experience more extensive leaching (Bown & Kraus, 1987; Kraus, 1999; Buol et al., 2011).

The carbonate observed within thin section 22 occurs in very small quantities. If leaching occurred due to influence of the ground-water table, this carbonate could be interpreted as precipitated caliche (Wright & Tucker, 1991). However, as Palaeosol 2 is interpreted of have been developed within crevasse splay deposits, extensive influence of the ground-water table is unlikely. Caliche can also form close to the sediment surface under dry climatic conditions (Wright & Tucker, 1991). But as seen through XRD-analysis (Chap. *4.3.2.3*), Palaeosol 2 contains kaolinite, thus indicating a humid climate. The carbonate is therefore unlikely to be caliche. It is more likely to be a calcite, as previous studies have defined it as the most commonly occurring carbonate cement within the Helvetiafjellet Formation (Edwards, 1979; Prestholm & Walderhaug, 2000).

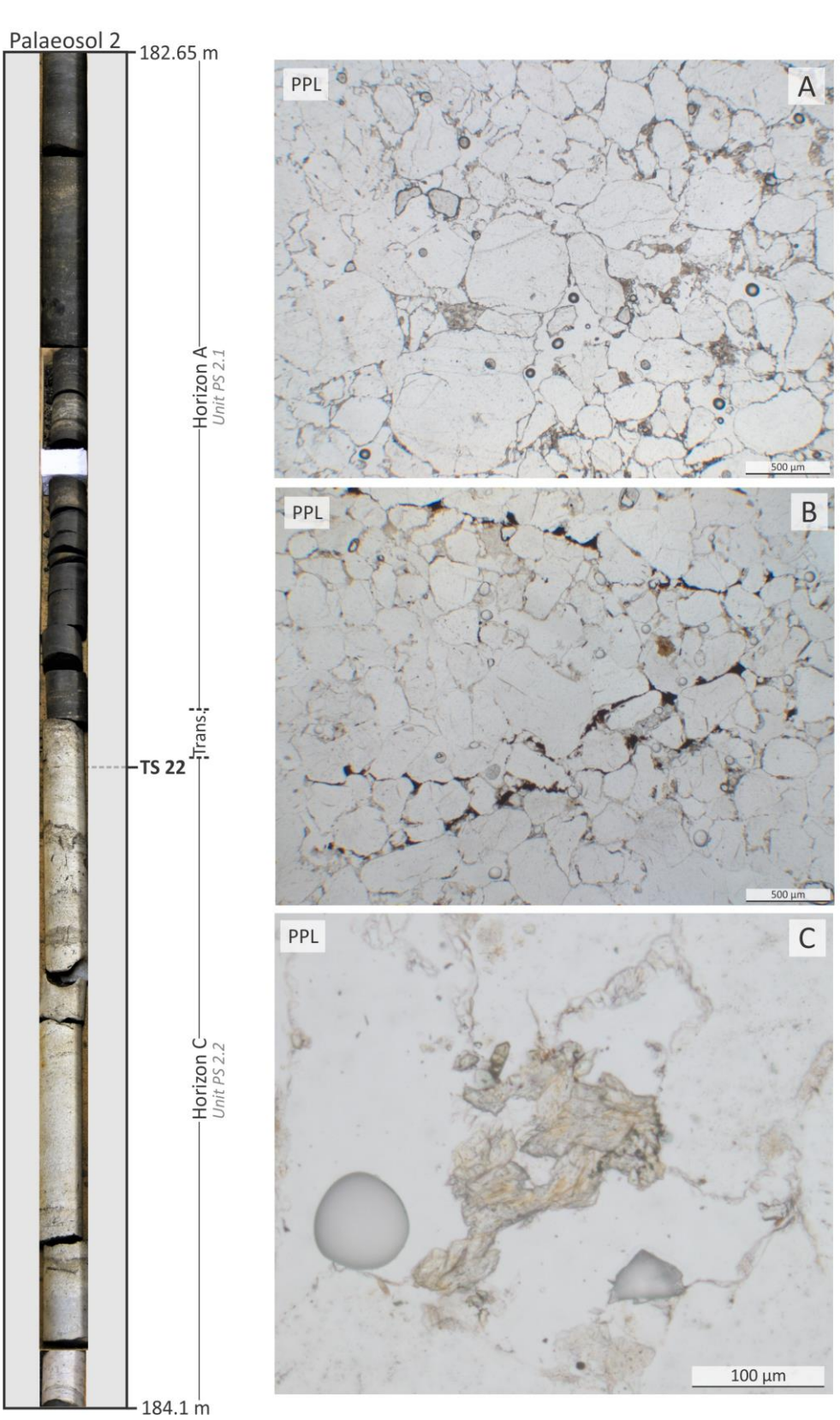

Figure 35: Representative photomicrographs of the mineralogical composition of thin section 22. Where the sample for thin section 22 was collected from within Palaeosol 2 is indicated in the figure. ***Image A*** *illustrates the variation in grain size and the abundance of quartz observed in the thin section.* ***Image B*** *displays an example of the root structures also observed in the thin section.* ***Image C*** *displays an example of the carbonate observed within the thin section. All photomicrographs are taken in plane polarized light.*

4.3.2.2.2 Thin section 23

Where thin section 23 was collected from within Palaeosol 2 is highlighted in Fig. 36. Four photomicrographs that represent the main features of the thin section are also presented in the same figure, and will be discussed further below.

Description

The dominating mineral of thin section 23 is best seen in Fig. 36 A. It consists of relatively small, anhedral grains, and is consistent with the characteristics of monocrystalline quartz, as presented in chapter *4.1.1.* The quartz grains are packed relatively tight, but some matrix is still present within the thin section (Fig. 36 A). The second observed feature of thin section 23 occurs in much smaller quantities. The amorphous mineral can be seen as redish brown fragments throughout the thin section (Fig. 36 B). The clasts are consistent with the characteristics of organic material, presented in chapter *4.1.8.*The last mineral observed within thin section 23 is presented in Fig. 36 C. The mineral has the rhombohedral cleavage and the pearlescent colour in cross-polarized light that is characteristic of a carbonate mineral (Chap. *4.1.7*).

Interpretation

Tabular cross-bedding was observed within unit PS 2.2 during macro-scale observations. Such relict structures are interpreted to be observable due to the presence of muddy matrix around the dominating quartz grains. If quartz-rich sandstones become too well-cemented, such structures can be difficult to observe.

Both thin section 22 and 23 were collected from the same pale, quartz-rich sandstone unit (unit PS 2.2). It is therefore suggested that thin section 23 also displays the effects of leaching, as it was interpreted for thin section 22. Similarly, a carbonate mineral was observed within both thin sections. As the thin sections were collected from the same horizon, it is unlikely that the climatic or stratigraphic conditions differ enough throughout the unit to allow for caliche precipitation within thin section 23. Therefore, the carbonate observed within thin section 23 is interpreted as calcite, as it is the most commonly occurring carbonate cement in the Helvetiafjellet Formation (Edwards, 1979; Prestholm & Walderhaug, 2000).

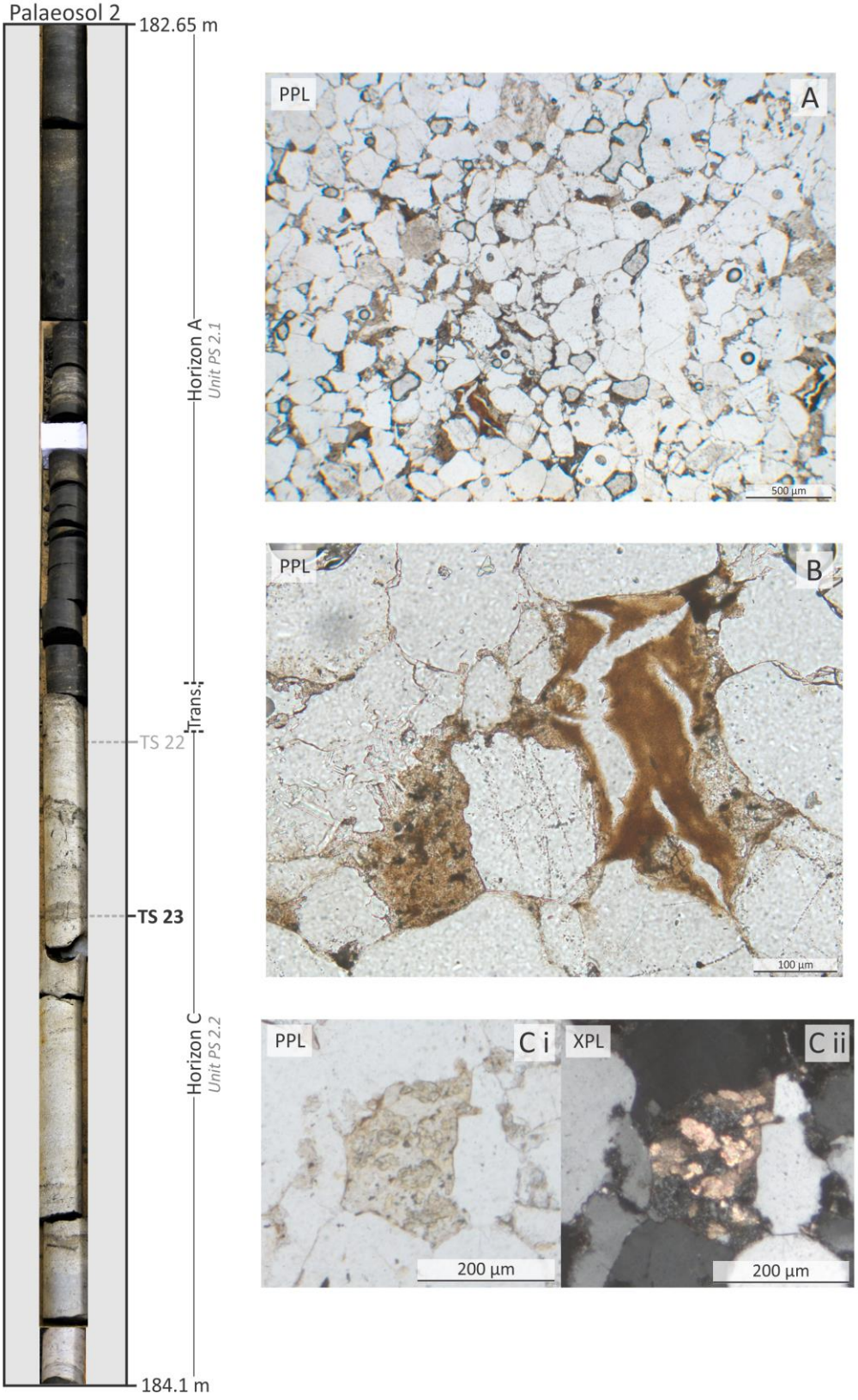

Figure 36: Representative photomicrographs of the mineralogical composition of thin section 23. Where sample 23 was collected from within the palaeosol is indicated in the figure. ***Image A*** *shows the general composition of the thin section with predominantly quartz, coalified clasts of organic material and some matrix. In* ***image B****, the fragments of coalified organic material can be observed. In* ***image C i*** *and* ***C ii****, an example of the carbonate observed within the thin section is presented, in both plane (PPL) and cross-polarized light (XPL).*

4.3.2.2.3 Thin section 24

Where thin section 24 was collected from within Palaeosol 2 is highlighted in Fig 37. Three photomicrographs are selected to represent the mineralogical composition of thin section 24. These are also presented Fig. 37, and will be discussed further below.

Description

Thin section 24 is predominantly composed of a single mineral (Fig. 37 A). Its mineralogical characteristics are consistent with those described for monocrystalline quartz, presented in chapter *4.1.1*. The quartz grains are packed extremely close together, resulting in little to no matrix being present (Fig. 37 A & 37 C). The available pore space is also considered to be insignificant.

One amorphous mineral can be observed within thin section 24 (Figs. 37 B & 37 C). It is observed as both elongated lineations (Fig 37 C) and irregularly shaped clasts (Fig 37 B), and can be recognized by a redish black colour. The observed colour and other general characteristics are consistent with the expected characteristics of organic material, as presented in chapter *4.1.8*.

Interpretation

Based on the varying shape of the organic material present in the thin section, the clasts are interpreted as clasts of coalified organic material, while the elongated lineations are interpreted as fossil root structures. The presence of root structures indicates that the thin section was collected from the horizon of a palaeosol (Retallack, 2001).

Thin sections 22, 23 and 24 were all collected from unit PS 2.2. Therefore, the abundance of quartz observed within thin section 24 is interpreted as a result of leaching, as it was for both thin section 22 and 23. Leaching was explained more in-depth previously (Chaps. *4.3.1.2.2* & *4.3.2.2.2*).

As mentioned in the introductory segment for micro-scale observations of Palaeosol 2 (Chap. *4.3.2.2*), all three samples were collected from horizon C within the palaeosol. The high quartz content and the relatively low content of organic material observed through thin section analysis is consistent with the characteristics of horizon C of Retallack, (2001; Appendix C). All three thin sections share enough characteristics that it can be argued that

they were collected from the same unit. It is therefore interpreted that thin sections 22 – 24 were all collected from horizon C.

The deposits of Palaeosol 2 were interpreted as crevasse splay deposits (Table 2; FA 4; Fig. 23) during macro-scale observations. The observed characteristics of all thin sections, such as high quartz content, domination of fine to medium-grained sandstone and observed organic content are consistent with the expected characteristics of crevasse splay deposits (Table 2; FA 4). It is therefore interpreted that all thin sections collected from Palaeosol 2 represent crevasse splay deposits.

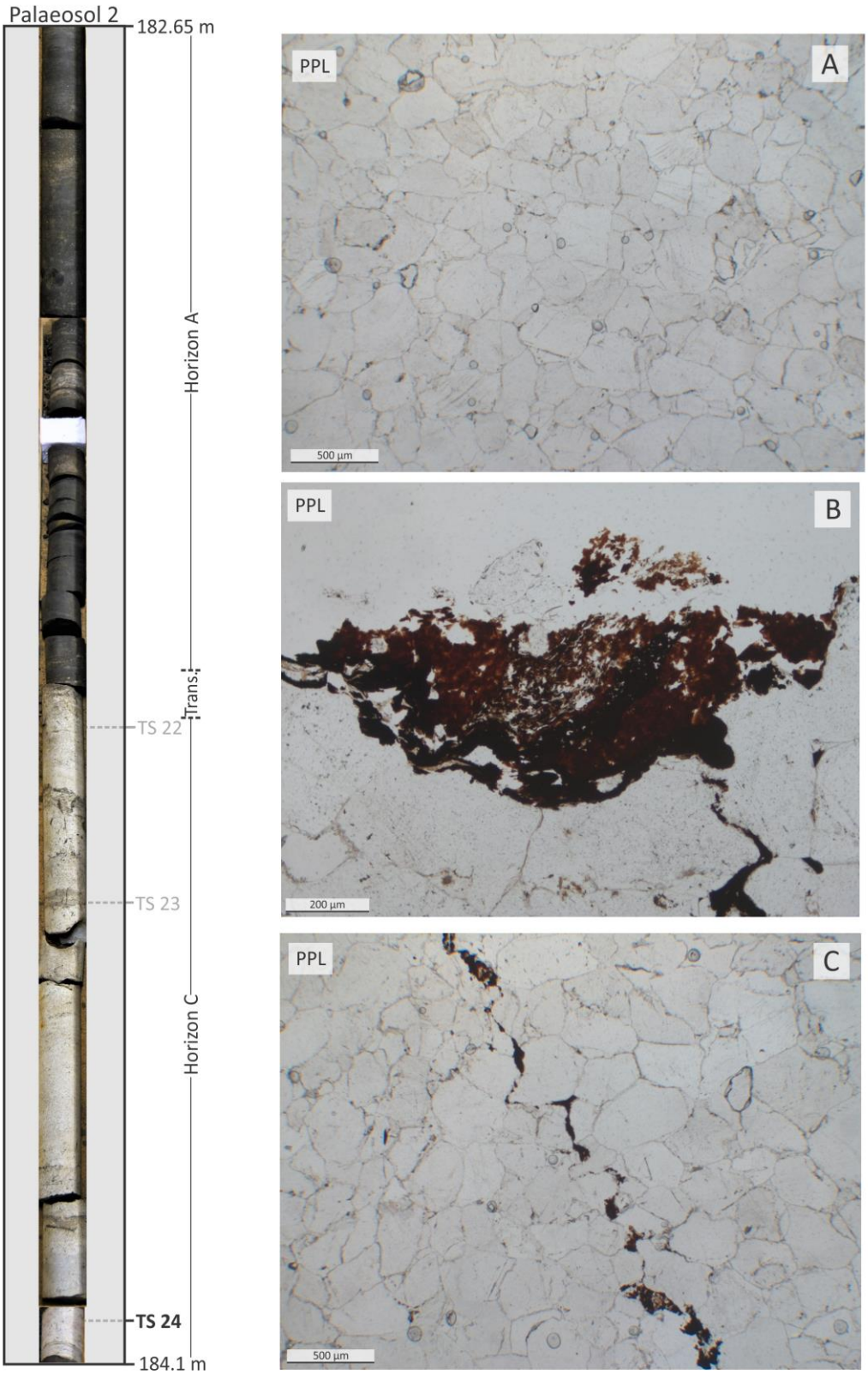

Figure 37: Representative photomicrographs of the mineralogical composition of thin section 24. Where the sample for thin section 24 was extracted from within the palaeosol is indicated within the figure. ***Image A*** *illustrates the abundance of quartz and the very tight packing that was observed.* ***Image B*** *and* ***C*** *present the different variations of organic matter observed within the thin section.* ***Image B*** *is an example of a fragment of coalified organic material, while* ***image C*** *shows a fossilised root structure. All photomicrographs are taken in plane polarized light (PPL).*

4.3.2.3 XRD-analysis

The XRD-analysis was performed by EARTHLAB at the University of Bergen, and the results are presented in Fig. 38. Where samples 25 to 28 were collected from within the Palaeosol 2 is also indicated in the figure. Prior to analysis, the samples underwent thorough preparation. All results were also corrected for baseline drift. These are small variations caused by fluctuations in temperature during the analysis.

As an x-ray comes into contact with a crystal surface, specific patterns are created based in the crystalline structure of the sample. Therefore, different minerals can be distinguished within a sample, based on the reflection patterns they produce (Cullity, 1978). For this thesis, the analysis was primarily preformed with the intention to identify clay minerals within the palaeosol. The term clay mineral generally refers to very fine-grained (<0.002 mm) sheet silicate minerals (Nesse, 2012). Due to this fine grain size, XRD-analysis is often required to identify clay minerals in a sample. In all graphs in Fig. 38, a black line can be seen. This represents the results of X-ray powder diffraction prior to heating. A ethylene glycol solvent is then added, which enables the swelling of certain clays, such as smectite (Nesse, 2012). The samples are then heated up to 500°C and the analysis is repeated. The results can be observed as a blue line in samples 25, 27 and 28, and as a red line in sample 26 (Fig. 38).

Based on the reflections presented in the graphs in Fig. 38, there are three main groups of minerals that stand out. Illite (**A**) is observed as a peak at around 8.8°, both before and after heating. Illite forms as a result of dewatering of smectite. This is a diagenetic process which occurs at temperatures ranging from 55°C to 200°C, which suggests low-grade diagenesis (Boggs, 2009).

Kaolinite (**B**) is interpreted as representing the second peak in the graphs (Fig. 38). Its reflection can be observed at approximately 12.5° prior to heating, but is suppressed after the heating process. Within palaeosols, kaolinite is typically indicative of humid climate, dominated by rainfall and fluctuating temperatures. Such conditions will typically lead to the leaching of sediments. Therefore, the presence of kaolinite is indicative of leaching conditions (Singer, 1980; Pal et al., 1989; Cecil & Dulong, 2003; Deepthy & Balakrishnan, 2005).

Sample 25 was extracted from unit PS 2.1. No thin section was successfully produced from deposits from this unit. Therefore, no mineralogical characteristics are available from micro-scale observations. The observation of minerals that are typical characteristics of some palaeosols, such as kaolinite within sample 25 thus indicates that unit PS 2.1 is indeed a part of a palaeosol. Furthermore, sample 25 indicates the presence of large quantities of quartz, and a relatively low content of other minerals. This is consistent with both macro and micro-scale observations previously made of Palaeosol 2. Therefore, it is reasonable to assume that sample 25, and therefore unit PS 2.1, is a part of Palaeosol 2.

The third, and final mineral is interpreted as quartz (**C**), and can be seen as peaks in the interval 18.5-27.5°. As mentioned previously, quartz is the most abundant mineral in most sandstones (Boggs, 2009), which is reflected in the graphs (Fig. 38). A high quartz content within cores DH-1 and DH-1A is consistent with previous observations made through both macro and micro-scale observations.

Based on the observed reflection patterns, all three mineral groups are present in all samples, with the exception of sample 28 (Fig. 38). During the XRD-analysis, no clay reflection peaks were observed within this sample. The lack of clay minerals within the lowermost section of Palaeosol 2 raises the question if this is a part of the palaeosol, or if the sample represents parent material. If this lowermost sample was collected from Palaeosol 2, the lack of kaolinite would suggest suggests less influence of leaching in this section of the palaeosol (Cecil & Dulong, 2003).

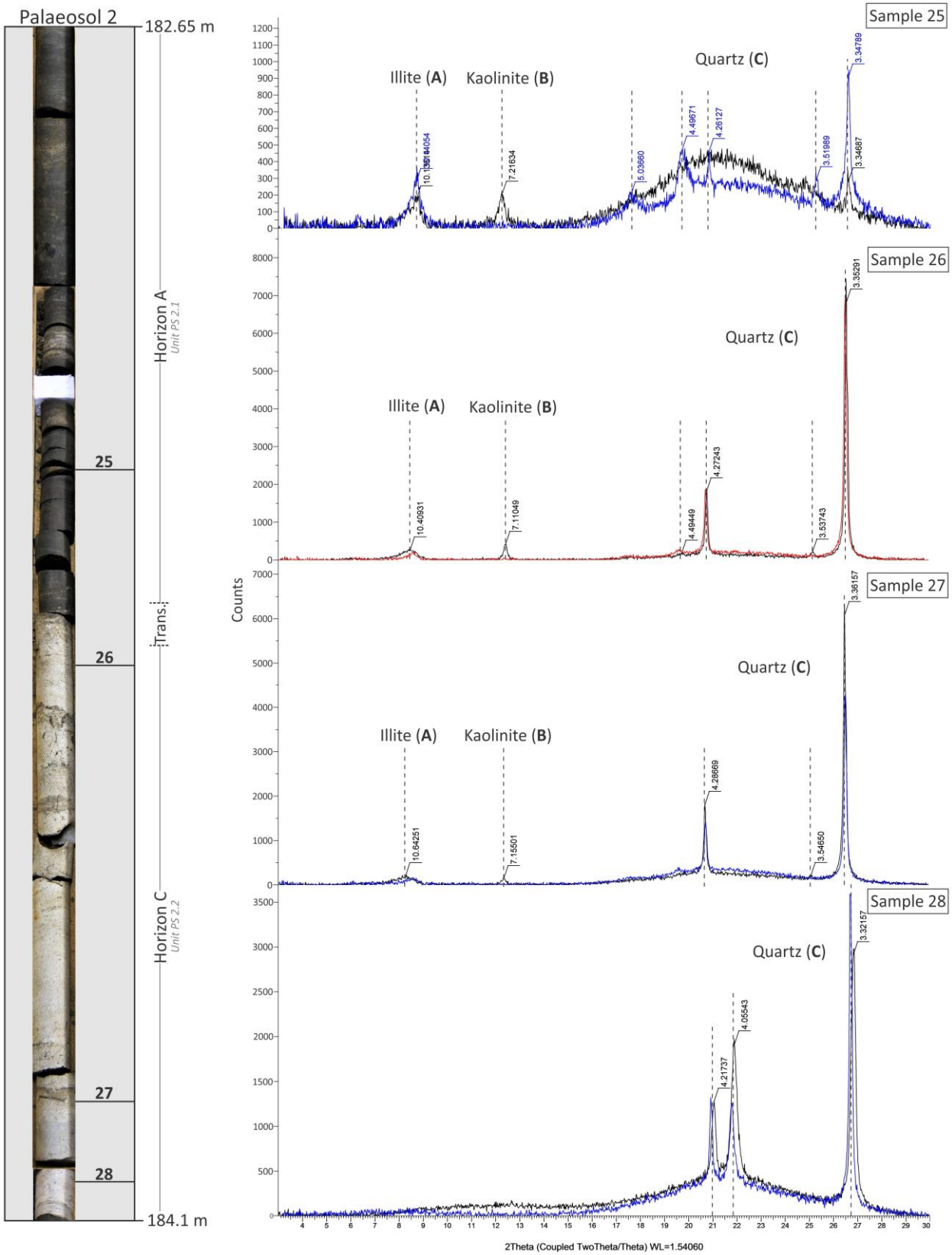

*Figure 38: XRD-analysis of samples 25 to 28. The occurrence of the samples within Palaeosol 2 is indicated in the image on the left-hand side. In each graph, the different reflection peaks represent different mineral groups. These are **A**: illite, **B**: kaolinite and **C**: quartz. All mineral groups were present in all four samples, with the exception of sample 28. Within samples 28, only quartz is registered. In all graphs, a black line can be seen. This represents analysis prior to heating. The blue and red (sample 26) line also seen in the graphs, represent analysis post-heating. All results are corrected for baseline drift.*

4.3.2.4 Classification of Palaeosol 2

The characteristics of Palaeosol 2 were identified through both macro and micro-scale observations, as well as the XRD-analysis (Chaps. *4.3.2.1—4.3.2.3*). Based on these observations, the palaeosol is interpreted to be composed of the horizons A and C of Retallack, (2001; Appendix C). Horizon A was described as having a relatively high organic content, alongside a mineral fraction (Fig. 33). The underlying horizon C was described as being pale in colour and rich in quartz (Fig. 33). The potential effects of leaching were also highlighted. In the lower half of horizon C, tabular cross-beds were observed (Fig. 34 D). When such relict structures are present within a palaeosol, it generally suggest that the alteration due to soil forming processes was minor. Palaeosols where the alteration due to soil forming processes is modest are commonly referred to as entisols (Wilding et al., 1984 A; Bown & Kraus, 1987; Kraus, 1999; Cecil & Dulong, 2003). In some entisols, the only indicator of soil forming activities observable is the presence of root structures or fossil roots (Retallack, 2001). This observation alone is enough to define the deposits as a palaeosol (Retallack, 1988). The sediments within the palaeosol can remain otherwise unaltered, thus preserving the primary structures of the sediments (Retallack, 2001; Buol et al., 2011). A lack of alteration can be caused by unfavourable conditions during the development of the soil profile. As presented in Table 2, Palaeosol 2 is interpreted to have developed in crevasse splay deposits. In crevasse splay deposits, sediment influx can be relatively high and as a result, the palaeosol can be buried relatively quickly, thus terminating the soil forming processes (Wilding et al., 1984 A; Kraus, 1999; Kraus & Aslan, 1999). Another contributing factor to the underdevelopment of palaeosols is the mineralogical composition of the palaeosol. As seen through micro-scale observations, quartz is an abundant mineral in Palaeosol 2 (e.g. Fig. 37). Parent material that is very resistant to weathering, such as quartz, can cause the alterations made due to soil forming processes to be minimal (Wilding et al., 1984 A). The mineralogical composition of the palaeosol, in conjunction with the interpreted depositional environment that Palaeosol 2 was formed in fits well with the conditions required for an entisol to form. Therefore, Palaeosol 2 is hereby defined as an entisol. As seen in chapter *2.7*, entisols can form regardless of the dominating climatic conditions (Fig. 8). This indicates that Palaeosol 2 is not a useful proxy with regards to palaeo-climate. For further discussion on the topic, please see chapter *5.2*.

5 Discussion

5.1 Mineral assemblages and their origin

Previous studies of the mineralogical composition of the sandstone beds of the Helvetiafjellet Formation have revealed two main groups of sandstones (Worsley, 1986; Maher et al., 2004). These are quartz arenites with minor basement components and sublithic to lithic arenites with a considerable plagioclase component (Edwards, 1979; Maher et al., 2004). The plagioclase-rich sandstones also contain larger quantities of basement-derived sediments than the quartz arenites (Worsley, 1986; Maher et al., 2004).

The observed variation in sandstone characteristics has previously been linked to influx of plagioclase-rich source material as a result of the emplacement of mafic HALIP extrusives in the eastern regions of Svalbard (Kong Karls Land and Frantz Josef Land) (Worsley, 1986; Maher et al., 2004). The formation of plagioclase-rich sands is more common with andesitic volcanism (Pettijohn et al., 1987). However, Maher et al., (2004) has indicated that the occurrence of plagioclase within the mafic HALIP deposits can potentially be explained by the weathering of basaltic glass that contains plagioclase phenocrysts. Such deposits have been observed on Franz Josef Land in previous studies (Dibner, 1998).

Not only are the HALIP deposits interpreted as the source of plagioclase-rich deposits, the emplacement of the HALIP is also suggested to have caused the uplift of the strata, which in turn enabled the erosion of the basement (Maher, 2001; Senger et al., 2014). Therefore, the increased quantities of plagioclase and basement components within the sublithic to lithic arenites is largely associated with HALIP activity (Maher et al., 2004). The sublithic to lithic arenites are typically observed in the upper part of the Helvetiafjellet Formation, within the Glitrefjellet Member, particularly in the NE and along the E coast of Spitsbergen (Maher et al., 2004).

The investigated sandstone beds of cores DH-1 and DH-1A have in this study been defined largely as quartz arenites. Where other accessory minerals, such as mica and various feldspars were present (Table 1), these were only observed in very small amounts. Although the mineralogical characteristics of cores DH-1 and DH-1A are relatively consistent with the characteristics of the interpreted facies associations (Chap. *4.2.1*; Table 2), the sublithic to lithic arenites with a strong plagioclase component described in other works (Worsley, 1986;

Maher et al., 2004) appear to be absent. Therefore, it becomes apparent that although the emplacement of the HALIP is known to have influenced the development of the Helvetiafjellet Formation, this is not reflected in the mineralogical composition of the deposits in cores DH-1 and DH-1A. As presented in Fig. 9, cores DH-1 and DH-1A were collected from the Adventdalen area in Svalbard. Therefore, a potential theory as to why the deposits of cores DH-1 and DH-1A do not contain minerals that reflect the HALIP activity, is their close proximity to the sedimentary source area. Previous studies have indicated that the source area for the Helvetiafjellet Formation was located in the W-NW (Parker, 1967; Nagy, 1970; Dörr et al., 2011), which is in close proximity to the Adventdalen area. This is largely supported by palaeo-current measurements (Gjelberg & Steel, 1995; Midtkandal et al., 2007). The analysis of U/Pb data collected from both the Wandel Sea Basin in North Greenland and the Helvetiafjellet Formation in Svalbard indicates a similar sedimentary source area for both successions (Røhr et al., 2008). Based on the shared characteristics of the two successions as well as palaeo-current measurements, the sedimentary source area for the Helvetiafjellet Formation could be composed of basement-derived sediments originating in, or in close proximity to NE Greenland (Røhr et al., 2008).

Sediments deposited near the sedimentary source area are heavily influenced by the source area, and are thus likely to reflect its mineralogical characteristics. It is therefore possible that the sedimentary input from the source area in the W-NW was too high for potential input from a volcanic source area in the E-NE to be reflected in the deposits of cores DH-1 and DH-1A. Potentially, increased influence from the volcanic source area can be observed within the deposits of the Helvetiafjellet Formation with relative distance to the clastic source area in the W-NW. If this is the case, sublithic to lithic arenites with a strong plagioclase component should be observed in the more distal areas of the Helvetiafjellet Formation. This is consistent with the change in sandstone characteristics throughout the Helvetiafjellet Formation observed by Edwards, (1979).

5.2 Palaeosols of the Helvetiafjellet Formation as climatic proxies

The climate in Svalbard during the Cretaceous period has been interpreted as relatively warm, with mean temperatures of 7—10 ^{O}C (Hurum et al., 2016; Hurum et al., 2016 A; Grundvåg & Olaussen, 2017). The observation of coal seams, seatearths, Ornithopod tracks and warm-water dinoflagellates are all indicative of a relatively warm and humid climate (Steel & Worsley, 1984; Århus, 1992; Grøsfjeld, 1992; Nemec, 1992; Harland et al., 2007; Hurum et al., 2016). However, arctic belemnites, glendonites and ice rafted debris has also been observed within the Lower Cretaceous strata (Dalland, 1977; Pickton, 1981; Harland & Kelly, 1997; Maher et al., 2004; Price & Nunn, 2010). Such observations are regarded as indicators of cooler, perhaps polar conditions.

Because soils are formed as a result of subaerial exposure, they are directly influenced by the dominating climatic conditions at the time of their formation. If these climatic conditions are recorded within a palaeosol that is preserved in the rock record, they may function as powerful climatic proxies (Mack & James, 1994; Kraus, 1999; Sheldon & Tabor, 2009).

Despite the apparent fluctuations in climatic conditions during the Barremian-Aptian, these are not reflected in the characteristics of Palaeosol 1 and 2. Both palaeosols investigated in this study were identified as enitsols (Chaps. *4.3.1.3* and *4.3.2.4*). Such palaeosols are not limited to specific climatic conditions (Cecil & Dulong, 2003; Cecil, et al., 2003; Fig. 8), and are thus regarded as poor indicators of the climatic conditions under which they were formed. There are several different factors that can influence which type of palaeosol is formed other than the climatic conditions. These are discussed below.

5.3 Processes influencing palaeosol development and maturity

Typically, underdeveloped and immature palaeosols are less likely to reflect the climatic conditions under which they were formed (Mack & James, 1994). How mature and well-developed a palaeosol becomes is largely dependent on the rate of sedimentation compared to the rate of pedogenesis, depositional environment, climate, the sea-level and its impact on the ground-water table and the mineralogical composition of the sediments in which the soil is forming ((Wilding et al., 1984 A; Kraus, 1999; Kraus & Aslan, 1999).

If the sediment deposition is rapid and unsteady, compound palaeosols are formed (Kraus, 1999; Kraus & Aslan, 1999; Fig. 39 A). These soil profiles are typically vertically stacked and weakly developed. If the rate of sedimentation is exceeded by the rate of pedogenesis, composite palaeosols will develop (Kraus, 1999; Kraus & Aslan, 1999; Fig. 39 B). The boundary between each individual palaeosol is typically less abrupt within composite palaeosols compared to the compound palaeosols. If the sedimentary input is relatively continuous, cumulative palaeosols typically form (Fig. 39 C). These are generally much thicker than the compound palaeosol as a result of prolonged deposition (Kraus, 1999; Kraus & Aslan, 1999). If the deposition occurs at a relatively slow rate, these palaeosols can typically become more mature and well-developed than the compound and composite palaeosols.

If deposition has been negligible or interrupted by erosion, this is typically recognized by truncation within sets of palaeosols. This can occur in compound, composite and cumulative palaeosol sets alike (Kraus, 1999; Kraus & Aslan, 1999).

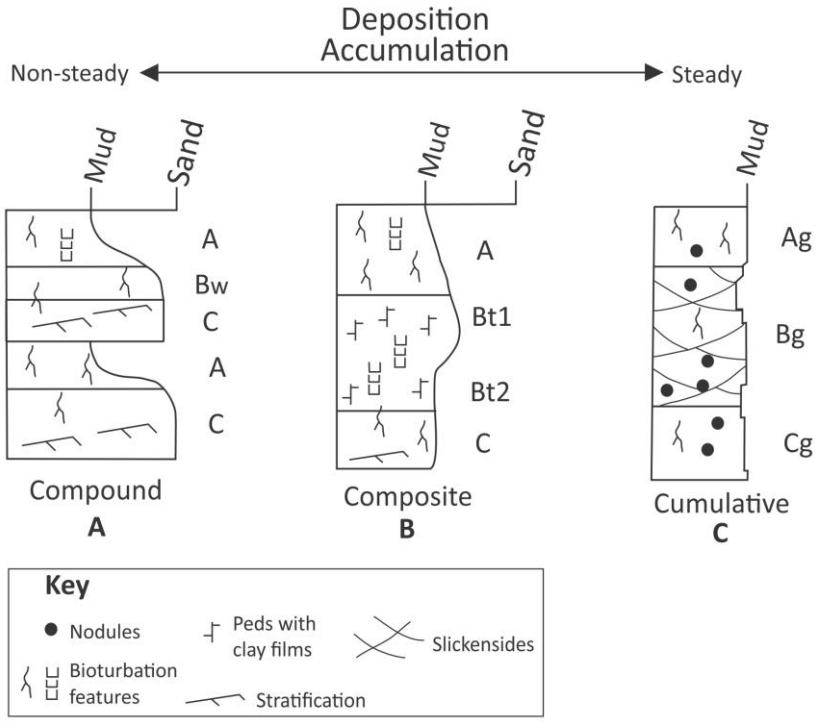

*Figure 39: Illustration of (**A**) compound, (**B**) composite and (**C**) cumulative palaeosols. Compound palaeosols represent non-steady sediment deposition and accumulation, whereas cumulative palaeosols represent steady deposition and accumulation. As a result, cumulative palaeosols are generally more mature than compound palaeosols. Composite palaeosols are typically also relatively immature, but have less abrupt boundaries between the vertically stacked palaeosols compared to compound palaeosols. This figure is not to scale, and is modified from Kraus, (1999).*

The characteristics of the palaeosols examined in this thesis are consistent with the general characteristics of compound palaeosols. Palaeosols 1 and 2 were vertically stacked and separated by a thin unit of relatively unaltered sandstone (Figs. 23, 27 & 33). Both palaeosols were largely composed of fine to medium-grained sandstone. Some ripple cross-lamination and tabular cross-bedding was preserved in both palaeosols (Figs. 28 F & 34 D). The recognition of primary structures suggests only slight alteration due to soil forming processes, thus indicating that the palaeosols are immature.

5.3.1 Depositional environment – proximity to fluvial channels

In previous studies of the Lower Eocene Willwood Formation of the Bighorn Basin, NW Wyoming, weakly developed palaeosols were observed in sediments deposited in close proximity to a channel (Bown & Kraus, 1987). As the distance to the channel increased, the observed palaeosols were described as being progressively better developed (Bown & Kraus, 1987). This is illustrated in Fig. 40, with compound palaeosols developing proximal to the channel and cumulative palaeosols located more distally.

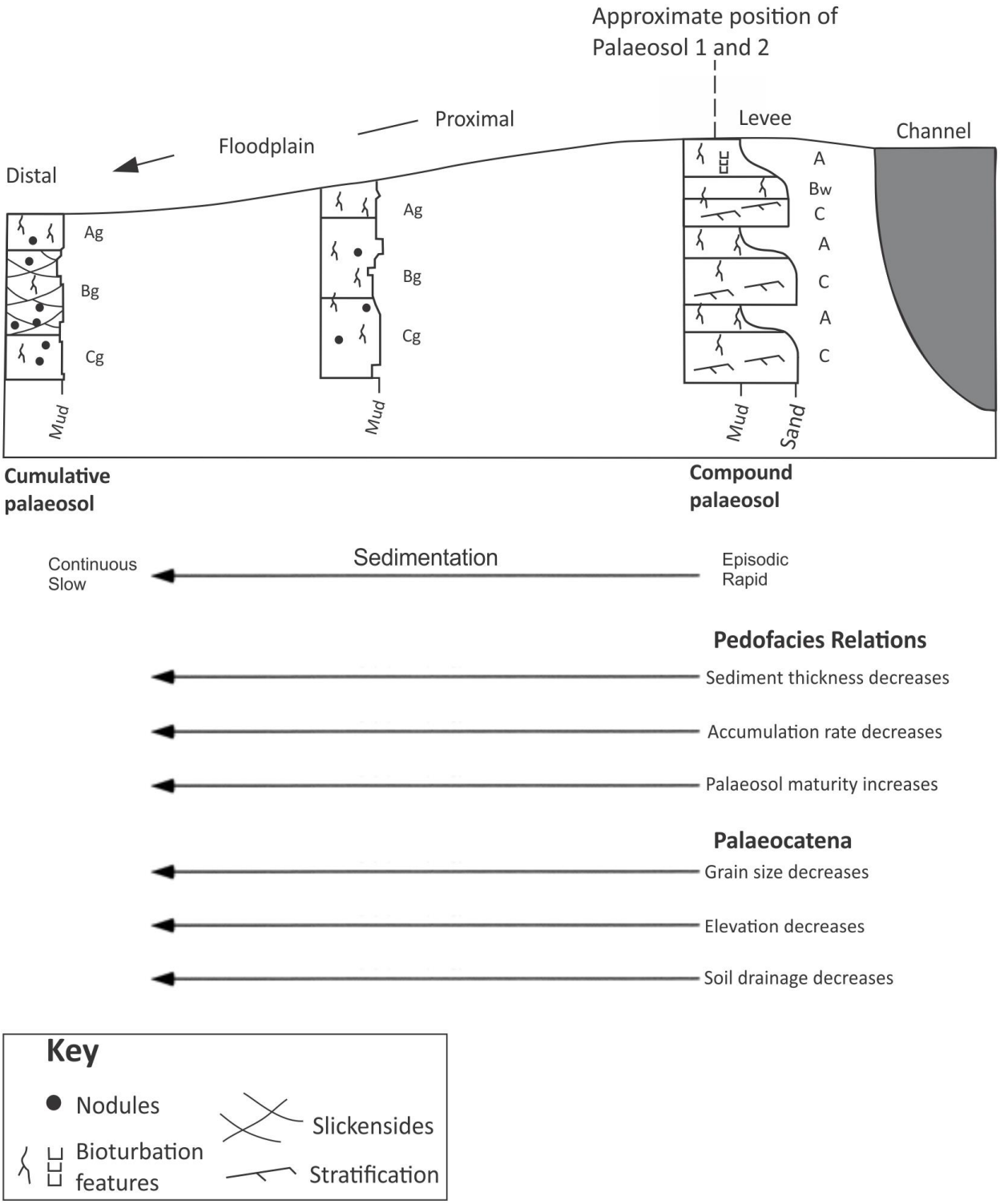

Figure 40: Illustration of the change in palaeosol composition relative to the proximity to an active channel. Palaeocantena refers to a sequence of soil profiles that are developing simultaneously on a slope. The change in grain size and topography influences the characteristics of the palaeosols. Proximal to the channel, the sedimentary influx is relatively high. Moving away from the channel, the sediment deposition decreases, but the accumulation is more continuous. This leads to immature, composite palaeosols observed in proximal areas and more mature, cumulative palaeosols developing in distal areas. Several compound palaeosols are formed in the same time-span as one cumulative palaeosols is formed. The approximate position of palaeosols 1 and 2 is indicated in the figure. This figure is not to scale and is modified from Kraus, (1999).

As Fig. 40 indicates, significant differences in palaeosol characteristics can occur over a relatively short geographical distance. Proximal to the channel, the sedimentary input is relatively high, thus causing the thickness of the deposits to be greatest close to the channel. This can cause levees to form. Because the largest grain size fraction is deposited first as the energy of the transporting medium decreases, the grain size will be largest proximally and decrease distally (Berner, et al., 2011).

Rapid deposition proximally to the channel causes this area to become elevated relative to the distal areas. This difference in elevation causes the distal palaeosols to become more prone to influence from the ground-water table. In the proximal areas, the larger grain size promotes more permeable deposits, while the elevation relative to the surroundings causes the water to move faster through the sediments. This generally allows more water to percolate through the sediments over a given period of time, thus leading to better drainage in the proximal areas (Bown & Kraus, 1987; Kraus, 1999).

In the proximal areas, the sedimentary input is frequent and rapid (Fig. 40). Therefore, the palaeosols found in this area are typically weakly developed, compound or composite palaeosols (Wilding et al., 1984; Kraus, 1999). The effective drainage system of compound palaeosols can lead to oxidized conditions, often seen as a brown A horizon and low quantities of organic material (Kraus, 1999). Palaeosols fitting these characteristics are often found on levees or in crevasse splay deposits (Wilding et al., 1984; Kraus, 1999; Buol et al., 2011).

Nemec, (1992) described similar conditions for the deposits of the Helvetiafjellet Formation. The dominating depositional environments interpreted for the Helvetiafjellet Formation are braidplain and delta plain environments (Steel & Worsley, 1984; Nemec, 1992; Gjelberg & Steel, 1995). Within such environments, the sedimentary influx can be relatively high. The formation was therefore described as a highly dynamic system where changes occurred quickly. Indicators of the occurrence of an overall transgression during the deposition of the Helvetiafjellet Formation have also been documented (Nemec, 1992; Gjelberg & Steel, 1995; Grundvåg & Olaussen, 2017). As a consequence of the dominating depositional environments and the overall relative sea-level rise, the channels that formed within the deposits of the Helvetiafjellet Formation were described as being highly avulsive.

Nemec, (1992) also described the occurrence of depositional “windows” within the Helvetiafjellet Formation. These are short windows of time, occurring only on a local scale, where deposition of clastic sediments was low, thus allowing plant growth and the accumulation of organic material to occur. Such windows could for instance form due to a shift in depositional area as a result of avulsion. Therefore, these depositional “windows” played a critical role in when accumulation of organic material could occur and thus when palaeosols could develop. Due to the short-lived nature of these breaks in deposition, the time in which plants were allowed to grow and organic material allowed to accumulate was limited. Such conditions are interpreted to favour the development of immature, compound soils.

Further away from an active channel, the conditions typically change. In the more distal areas, both the grain size and rate of sedimentary influx decreases (Fig. 40). The slower sedimentation rate offers more time for palaeosols to develop, which leads to more mature, cumulative palaeosols developing in the distal areas (Kraus, 1999). However, the combination of the lower elevation relative to the more proximal palaeosols and the overall finer grain size can lead to relatively poor drainage. Because of the lower topographic position of the palaeosols, these are generally more heavily influenced by the ground water table. This can lead to reducing conditions (Kraus, 1999), which favours the accumulation and preservation of organic material. This promotes the formation of coal.

When comparing Palaeosol 1 and 2 with the observations of the palaeosols within the Lower Eocene Willwood Formation, it becomes apparent that palaeosols 1 and 2 contain many of the characteristics that are expected with a palaeosol that formed in close proximity to an active channel. They are both quartz dominated, light in colour and contain small amounts of organic material, which could suggest oxidizing conditions. Palaeosol 1 also displays some brown sections in horizon A, which is another possible consequence of oxidization, as it was described by Kraus, (1999; Figs. 27 & 28 B). Primary structures were also observed, such as ripple cross-lamination and tabular cross-bedding. This suggests limited influence of soil forming processes. The immaturity of the palaeosols could potentially be due to rapid deposition and burial, which is consistent with the previous observations of the depositional environment, as presented by Nemec, (1992).

According to the facies associations interpreted for cores DH-1 and DH-1A (Table 2), Palaeosol 1 has mixed composition of FA 3 and FA 4, which are floodplain deposits and crevasse splay deposits, respectively. The variation in facies association within a single palaeosol is possible due to the lateral migration of an active channel across a floodplain. Palaeosol 2 on the other hand, has been interpreted to be composed of only crevasse splay deposits (FA 4). These are deposits that can occur in close proximity to an active channel, thus promoting rapid deposition and limited time for palaeosol development. If palaeosols developed within deposits of either of these facies associations, it is not unlikely that they would contain many of the characteristics observed in both Palaeosol 1 and 2.

Based on the abovementioned factors, it becomes apparent that palaeosols within a small geographical area can display a vast variety of characteristics with regards to palaeosol maturity. As a result, palaeosols developed within a small geographical area can indicate very different climatic conditions, as immature palaeosols typically do not develop strong palaeo-climatic indicators. It has also been highlighted how different depositional environments generally favour different palaeosols with regards to maturity. Based on the interpreted depositional environment of the Helvetiafjellet Formation as it was presented by Nemec, (1992), it is possible that the overall depositional conditions of the formation favours the formation of immature compound and composite palaeosols, rather than mature cumulative palaeosols.

However, it is not only the relative proximity to an active channel or overall depositional environment that is influential with regards to the maturity of a palaeosol and how well-developed the climatic characteristics within a palaeosol are. Mack & James, (1994) found that the climatic signature of a palaeosol can become masked by other factors, such as landscape position and time of development. In such scenarios, leaching, grain size and depositional rate can make the observation of palaeo-climatic indicators problematic, even if they originally were present within the palaeosol. As the observed effects of landscape position and time of development were discussed in the previous subchapter, other factors such as the effects of climate and relative sea-level, leaching, grain size and mineralogical composition will be discussed further in the following subchapters.

5.3.2 Climate and sea-level

Both overall the climatic conditions and the relative sea-level can influence the rate of soil development and the characteristics that form within a soil profile. The climatic conditions at the time of soil development does not only influence the characteristics of the soil horizons, it also has major influence on the rate of soil development (Retallack, 2001). Tropical to subtropical climates promote rapid plant growth and as a result, palaeosols that formed in warm climates are generally more developed (Retallack, 2001).

Based on the topography of an area, a rise in relative sea-level will generally lead to a rise of the ground-water table (Kraus, 1999). An increase in the position of the ground-water table can also be caused by heavy rainfall and therefore, the position of the ground-water table is to some extent also controlled by the dominating climatic conditions (Wu et al., 1996). In areas where the ground-water table is high, plant growth is promoted (Nemec, 1992). Within a soil profile, a high-standing ground-water table will typically lead to poor drainage, which can lead to reducing conditions (Kraus, 1999; Kraus & Aslan, 1999). This can typically be seen as gleying, which is the reduction and mobilization of primarily iron and manganese (Duchaufour, 1982; Kraus & Aslan, 1999). Gleying also produces grey horizons and mottles within the soil profile (Duchaufour, 1982; Kraus & Aslan, 1999).

Nemec, (1992) interpreted the climate during Early Cretaceous as relatively mild. This is consistent with other studies of the Helvetiafjellet Formation where mean temperatures of 7-10^{o}C has been suggested (Hurum et al., 2016; Hurum et al., 2016 A; Grundvåg & Olaussen, 2017). Due to the interpreted large-scale transgression during the Early Cretaceous period (Nemec, 1992; Gjelberg & Steel, 1995; Midtkandal et al., 2008), the ground-water table is interpreted to have been relatively high. Nemec, (1992) also interpreted the ground-water to be of very low salinity, thus facilitating plant growth. Based on these favourable conditions, mature palaeosols should be expected to develop within the deposits of the Helvetiafjellet Formation.

However, the observed effects of the interpreted temperate climate and relatively high ground-water table are limited within palaeosols 1 and 2. Both palaeosols were interpreted as entisols, which is a type of palaeosol not indicative of specific climatic conditions. Based on the relict structures present within horizon C of both palaeosols, the lack of climatic

characteristics could potentially be due to a limited amount of time where the soil forming processes were allowed to rework the parent material, and for soil characteristics to develop. No indications of reducing conditions have been observed within the palaeosols, which potentially indicates less influence from the ground-water table than originally implied by Nemec, (1992).

5.3.3 Mineralogical composition

5.3.3.1 The significance of quartz content

Through both macro and micro-scale observations, the lower horizons of palaeosols 1 and 2 were characterised as very quartz-rich (Figs. 27 & 33). This is often regarded as a result of the relative stability of quartz (Rimstidt, 1997; Martín-García et al., 2015). Quartz is often abundant in palaeosols, primarily due to the physical weathering of parent material, but also as a product of diagenetic processes (Wilding et al., 1984; Martín-García et al., 2015). Palaeosols can also become relatively enriched by quartz due to the removal of more soluble minerals through leaching (Wilding et al., 1984 A; Lehmann & Schroth, 2003; Buol et al., 2011). As quartz is very stable and not easily removed, the deposits become enriched with quartz. Within Palaeosol 1 and 2, the inferred proximity of the investigated succession to the clastic sedimentary source area in the W-NW is interpreted at the dominating factor for the observed high quartz content.

The mineralogical composition of a palaeosol can greatly affect the development of soil characteristics (Wilding et al., 1984 A). Parent material that is very resistant to alteration, such as quartz, can inhibit the development of strong soil characteristics. Quartz-rich deposits can also be relatively poor in nutrients and as a result, only a limited selection of plants will grow in such sediments (Ågren et al., 2012). This can result in the observation of immature, underdeveloped palaeosols within quartz-rich deposits. Therefore, it is possible that regardless of how accommodating the other conditions of soil growth and development are, mature palaeosols are not able to form due to the mineralogical composition of the parent material. Based on the abovementioned factors, the high quartz content observed in Palaeosol 1 and 2 is a possible contributor to their underdevelopment. It is therefore possible that the proximal area of the Helvetiafjellet Formation, represented through cores DH-1 and DH-1A, is too rich in quartz to allow mature and well-developed palaeosols to form.

However, the Glitrefjellet Member has in other locations been described as mudstone dominated (Parker, 1967; Birkenmajer, 1984). Therefore, the development of more mature palaeosols could occur in other, perhaps more distal areas of the Helvetiafjellet Formation where the overall conditions were more favourable.

5.3.3.2 The significance of kaolinite content

Nemec, (1992) states that due to the relative sea-level rise and the relatively low topography of alluvial plain environments, the ground-water table has been interpreted as relatively high during the Early Cretaceous in Svalbard, thus promoting reducing conditions within a soil profile. However, as seen through both macro and micro-scale observations of Palaeosol 1 and 2, such signs of reducing conditions are not present. Kaolinite was observed within Palaeosol 2 through XRD-analysis (Chap. *4.3.2.*3; Fig. 38). The formation of kaolinite is typically linked with significant leaching and oxidizing conditions (Cecil & Dulong, 2003), rather than reducing conditions. As subhumid to perhumid climates favour leaching, the presence of kaolinite is regarded as a palaeo-climatic indicator for humid climates, characterised by frequent rainfall and fluctuations in temperature (Murali et al., 1978; Singer, 1980; Pal et al., 1989; Cecil & Dulong, 2003).

The observation of oxidizing conditions rather than reducing conditions indicates less influence of the ground-water table than previously suggested by Nemec, (1992). This could be due to an overall lower ground-water table in Svalbard than first interpreted by Nemec, (1992), or that the topography of the levee in which palaeosols 1 and 2 are interpreted to have formed on was elevated high enough to not be influenced by the fluctuations of the ground-water table. As palaeosols 1 and 2 developed within the proximal area of the Helvetiafjellet Formation, is it also possible that the effects of the relative sea-level rise was less noticeable within these deposits.

Although kaolinite is regarded as a palaeo-climatic indicator of humid climates, one pitfall is presented by Singer, (1980). The author presents a scenario where the climate is humid, causing kaolinite to form. If the climate is to change to drier conditions, the kaolinite is stable enough to remain unaltered within the sediments. Therefore, the indicators of a previously humid climate is represented within the rock record despite a later change in climatic conditions. However, if the climatic conditions initially are predominantly dry, other

clay minerals, such as smectite will typically form (Singer, 1984). A shift in climatic conditions will thus cause it to become predominantly humid. The likelihood of a clay mineral deposited under dry climatic conditions becoming unstable when exposed to humid climatic conditions is significant. The unstable clay is then likely to alter into kaolinite, because it is stable in humid conditions. Singer, (1980) therefore concludes that the ancient sedimentary deposits indicative of humid climates are overrepresented within the rock record, and are perhaps not accurate.

However, based on the many other previously described climatic indicators suggesting a humid climate during the Early Cretaceous in Svalbard, such as coal seams, seatearths, dinosaur tracks and warm-water dinoflagellates (Steel & Worsley, 1984; Nemec, 1992; Århus, 1992; Grøsfjeld, 1992; Harland et al., 2007; Hurum et al., 2016; Grundvåg & Olaussen, 2017), it is likely that the observed kaolinite reflects actual humid conditions during the development of Palaeosol 2.

5.4 Regional correlation of palaeosols within the Helvetiafjellet Formation

Theoretically, palaeosols are relatively easy to recognize within the rock record. Most palaeosols form almost instantaneously (2000-30 000 years), and are generally morphologically distinctive and regionally extensive. This makes them excellent tools for correlation, both on a local and a regional scale (Kraus, 1999).

As it has been highlighted in this thesis, palaeosol characteristics typically vary with the proximity to an active channel (Fig. 40). Palaeosols located in close proximity to a channel experience rapid deposition, which disables the soil forming processes relatively quickly. In the more distal areas, the deposition is not as rapid, thus allowing the parent material to be reworked for an extended period of time. As discussed above, the influence of the ground-water table also affects soil characteristics. Therefore, palaeosol maturity has been interpreted to decrease with the proximity to the channel (Bown & Kraus, 1987). With this knowledge as a foundation, regional correlation based on palaeosol characteristics and maturity is possible. Due to rapid sedimentation in proximal areas, several immature, stacked palaeosols will form in the same time span as a single, more mature palaeosol in distal areas. This must be accounted for in order to achieve accurate correlation (Bown & Kraus, 1987).

For the deposits of the Helvetiafjellet Formation, the principle described above should be valid. If a sediment horizon is geographically extensive and possible to trace, the maturity of a palaeosol should indicate where the sediments were deposited in a regional context, and in such enable regional correlation. However, as described by Gjelberg & Steel, (1995), the deposits of the Helvetiafjellet Formation are very lenticular and thus difficult to correlate, even over short distances. If the deposits themselves are difficult to correlate, then the palaeosols that occur within the deposits can also prove to be problematic to correlate, at the very least in the field.

Coal seams have previously been observed in conjunction with the palaeosols of the Glitrefjellet Member (Nemec, 1992). Coal seams are also regarded as deposits that are eligible as tools for regional correlation. However, Nemec, (1992) described the coal seams of the Helvetiafjellet Formation as occurring primarily on a very local scale. Therefore, the coal seams and their associated palaeosols are generally difficult to trace within the formation, and are thus perhaps not suitable for correlation.

Although both the climatic and ground-water conditions appear to have been favourable with regards to the development of strong soil characteristics, the disadvantage created by the clastic environment is interpreted as being too strong and therefore preventing long-term development of palaeosols within the Helvetiafjellet Formation. If proven to be true, the occurrence of mature palaeosols within the Helvetiafjellet Formation is unlikely, thus making palaeosols relatively poor candidates as climatic proxies for the formation. This also relates to the potential regional correlation of palaeosols within the Helvetiafjellet Formation. If mature palaeosols are lacking within the formation, regional correlation can prove to be challenging, as the development of palaeosol characteristics according to their geographical placement in a regional context is unlikely to occur.

5.5 Depositional environments of iron ooids and their climatic implication

As stated in chapter *4.1.9*, iron ooids were observed within thin section 16 (Fig. 20) which was collected at the boundary between the Helvetiafjellet and the Carolinefjellet formations. The iron ooids were observed within the conglomerate that marks the very top of the Helvetiafjellet Formation. Within the Lower Cretaceous succession in Svalbard, iron ooids have previously only been observed within the lowermost sandstone beds of the Dalkjegla Member of the Carolinefjellet Formation (Mutrux et al., 2008). For the Helvetiafjellet Formation however, the existence of iron ooids has not previously been documented. This is an interesting finding, as iron ooids are known palaeo-climatic indicators of greenhouse conditions and warm climatic conditions (Mutrux et al., 2008).

For the precipitation of iron ooids to occur, the deposition of clastic sediments must be low, the depositional environment must be relatively calm and a source of iron must be present (Collin et al., 2005; Mutrux et al., 2008). There are several different situations that enable the precipitation of iron ooids, which are briefly touched upon by Mutrux et al., (2008) and Siehl & Thein, (1989). In this section, three possible scenarios for iron ooid formation within the Helvetiafjellet Formation are discussed.

5.5.1 Formation of iron ooids from colloidal riverine iron in a saltwater-freshwater mixing environment

A possible theory to explain the occurrence of iron ooids within the Helvetiafjellet Formation is similar to the theory proposed for the Carolinefjellet Formation by Mutrux et al., (2008). Gjelberg & Steel, (1995) describes the Helvetiafjellet Formation as being dominated by an overall transgression, with fluvial deposits (the Festningen Member) at its base transitioning into coastal and deltaic deposits (the Glitrefjellet Member) in its upper units. In addition, Nemec et al., (1988) reported the observation barrier deposits in the uppermost Glitrefjellet Member in the Kvalvågen area in eastern Spitsbergen.

The iron required for the formation of the ooids to occur can have been supplied as colloidal iron through channels occurring in the proximal area of the Glitrefjellet Member (Fig. 41). The restricted conditions required for ooid formation to occur can have been caused by the formation of barrier bars, which have been observed on the distal areas of the Glitrefjellet Member (Nemec et al., 1988; Gjelberg & Steel, 1995). Such barrier bars can limit seaward influence, thus creating lagoonal conditions in landward direction. Within the coastal

lagoons, iron-rich freshwater and saltwater was allowed to mix, thus promoting the formation of iron ooids (Mutrux et al., 2008; Fig. 41). The conglomerate observed in the uppermost unit of the Glitrefjellet Member is interpreted to have been created by the reworking of waves.

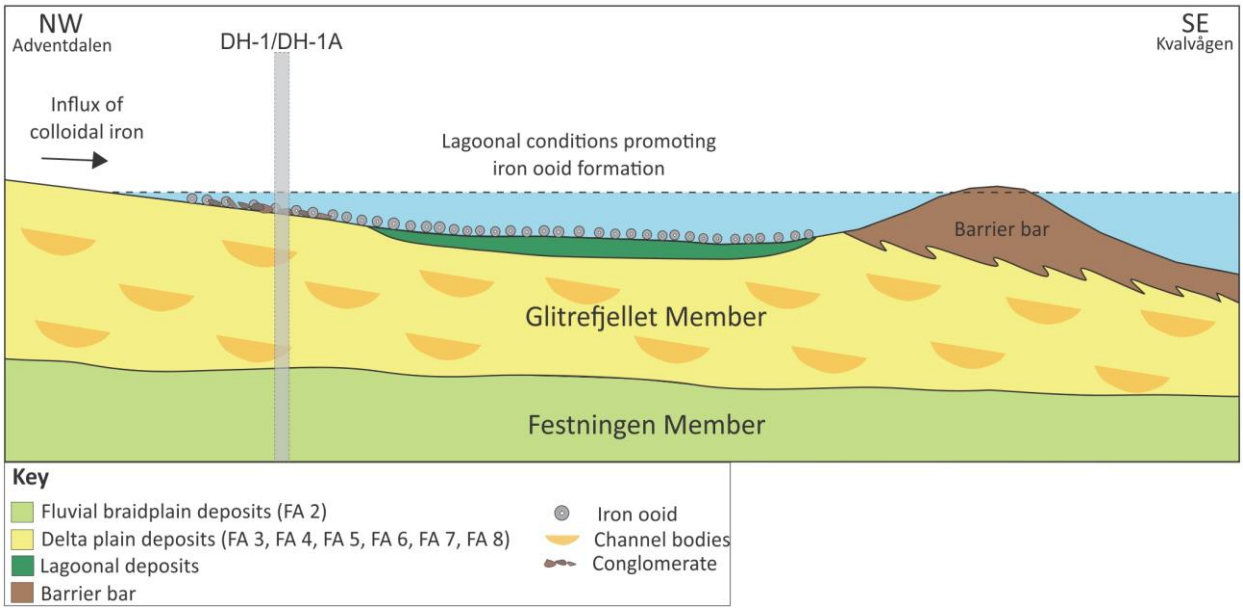

Figure 41: Colloidal iron is supplied through channels. Due to waves reworking the delta front, barrier bars are formed. This creates protected, lagoonal conditions in landwards direction. Such environments allow the mixing of fresh- and saltwater to occur, thus promoting the formation of iron ooids. The facies associations (FA) represented by deposits within the figure are indicated. The characteristics of the facies associations are presented in Table 2. This figures also illustrates the approximate position of cores DH-1 and DH-1A. This transect is not to scale, and is modified form Mutrux et al., (2008).

5.5.2 Formation of iron ooids in sediment starved shallow-marine conditions

Sediment starved conditions can occur in shallow-marine areas as a result of overall transgression (Taylor et al., 2002; Mutrux et al., 2008). As a relative rise of the sea-level occurs, large amounts of the sediments transported by channels are deposited in river mouths and valleys, rather than being transported and deposited further seaward (Taylor et al., 2002). This promotes the formation sediment starved conditions in the distal areas of the Glitrefjellet Member (Taylor et al., 2002). As less sediments are deposited on the distal delta, waves will begin to rework the delta front, eventually creating barrier bars (Fig. 42 A). Due to continuous sea-level rise, the barrier bars will being to migrate proximally (Fig. 42 B). Sediment starvation and the episodic storm reworking of the deposits causes the shallow-marine areas to become relatively enriched with iron (Taylor et al., 2002; Fig. 42 B). The low sedimentation rates and relative enrichment in iron promotes the formation of iron ooids (Taylor et al., 2002; Mutrux et al., 2008; Fig. 42 B).

At some point during the relative sea-level rise, the rate of the transgression will exceed the rate of the retreat of the barrier bar complex. As a result, water will flood the barrier bar and effectively inhibit any further migration (Cattaneo & Steel, 2003; Fig. 42 B). As the transgression progresses further, the more proximal areas, such as the coastal plain will also become flooded (Fig. 42 B). This relative rise in sea-level induces reworking of the barrier bars through wave erosion. Continuous erosion will remove the fine-grained fraction of the deposits, leaving only a coarse-grained conglomerate, also referred to as a transgressive lag (Posarnentier & Allen, 1999; Cattaneo & Steel, 2003; Fig. 42 B). A conglomerate was observed in cores DH-1 and DH-1A, in the uppermost unit of the Helvetiafjellet Formation (Fig. 23 & 24). Barrier bar deposits have been described in the distal units of the Glitrefjellet Member in previous works (Nemec et al., 1988; Gjelberg & Steel, 1995). Therefore, as cores DH-1 and DH-1A were drilled in the interpreted proximal area of the Helvetiafjellet Formation, it is possible that the conglomerate represents a transgressive lag, formed due to the flooding and subsequent wave reworking of the barrier bar complex and the coastal plain.

Iron ooids typically measure <2 mm (Simone, 1981), which is roughly equivalent to very coarse sandstone. Therefore, it is possible that iron ooids that formed during the transgression will not be removed due to wave erosion, and can therefore be observed within the transgressive lag (Fig. 42 B & 42 C). As a result of sudden increase in water depth, the formation of iron ooids is no longer possible. Rather, the deposition of a transgressive mud blanket occurs (Fig. 42 C). Within cores DH-1 and DH-1A, this abrupt deepening is represented by a black shale, herein referred to as the lower Aptian flooding surface (Grundvåg et al., 2017).

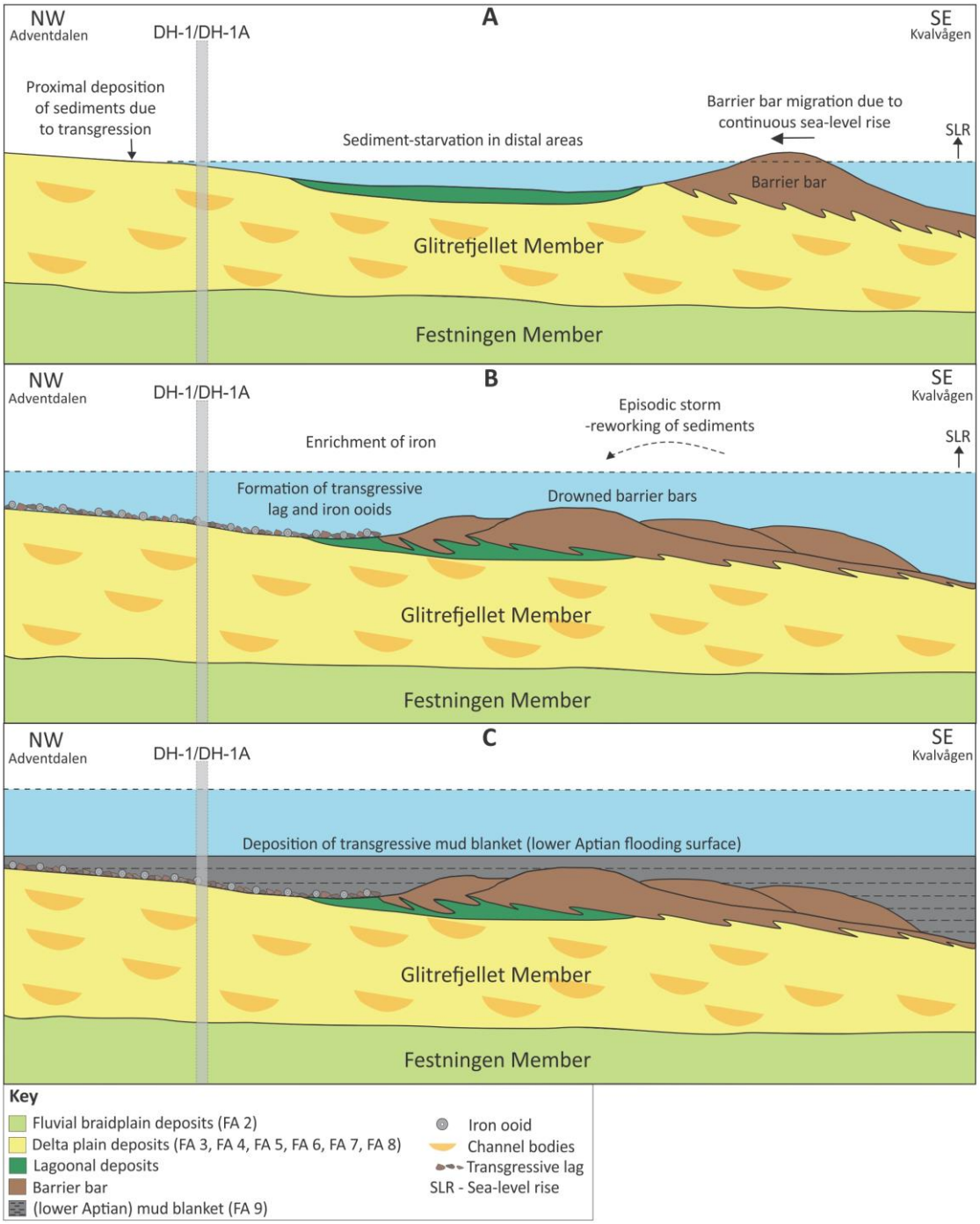

*Figure 42: **A**: The relative sea-level rise causes deposition to occur in proximal areas, thus creating sediment starved conditions distally. Due to the lack of sediment input, waves begin to rework the distal delta, thus creating barrier bars. Such barrier bars have previously been observed within the Helvetiafjellet Formation by Nemec, (1992). Continuous sea-level rise promotes the proximal migration of the barrier bars. **B**: Further sea-level rise causes drowning of the barrier bars, thus inhibiting further migration. More proximal areas are also flooded. The lack of sediment deposition and the episodic reworking of the sediments causes relative enrichment of iron in the shallow-marine area. This promotes the formation of iron ooids. The flooding of the barrier bars promotes influence of wave erosion. After prolonged erosion, the fine-grained fraction of the sediments are removed, thus leaving only a transgressive lag. As iron ooids typically are equivalent to very coarse sandstone, these are not likely to have been removed during wave erosion, and can therefore be observed within the transgressive lag. **C**: A sudden increase in water depth inhibits further erosion or iron ooid formation and instead promotes the deposition of a transgressive mud blanket. Within cores DH-1 and DH-1A, this is seen as a black shale, and marks the lower Aptian flooding surface. The approximate position of cores DH-1 and DH-1A is indicated within the transect. This transect is conceptual, and is therefore not to scale. Based on the illustrations of Mutrux et al., (2008).*

5.5.3 Formation of iron ooids in a terrestrial setting

A terrestrial origin for the iron ooids within the Helvetiafjellet Formation was also considered. In this model, iron ooids are formed as a result of pedogenic processes (Siehl & Thein, 1989) in terrestrial conditions. When such iron ooids are observed within shallow marine strata, it is interpreted as a result of erosion, transportation and subsequent deposition (Taylor, 1996).

The formation of iron ooids within a palaeosol is most commonly observed in tropical to subtropical environments, within iron-rich soil profiles (Siehl & Thein, 1989). Due to changes between dry and humid seasons, the ground-water table generally fluctuates (Siehl & Thein, 1989). When the ground-water table is high, reducing conditions dominate. This typically leads to the mobilization of primarily manganese and iron (Duchaufour, 1982; Kraus & Aslan, 1999). As the ground-water table lowers, oxidizing conditions will generally be favoured (Kraus, 1999). Water percolating through the soil profile promotes leaching and subsequent precipitation of iron hydroxide. Continued leaching and precipitation leads to the formation of ferruginous nodules, also referred to as iron ooids, within the soil profile (Siehl & Thein, 1989).

Continental deposits have been observed within the Helvetiafjellet Formation (Steel, 1977; Nemec, 1992; Mørk et al., 1999), thus potentially enabling the formation of terrestrial iron ooids. However, evidence of the iron-rich palaeosols and the tropical to subtropical climate required for the formation of iron ooids to occur is not observed within the Helvetiafjellet Formation. The deposits of the formation rather suggests a temperate climate (Århus, 1992; Grøsfjeld, 1992; Hurum et al., 2016; Hurum et al., 2016 A; Grundvåg & Olaussen, 2017). Therefore, a terrestrial origin for the iron ooids within the Helvetiafjellet Formation is rejected.

Both depositional models presented in chapters *5.5.1* and *5.5.2* can potentially be the cause of iron ooid precipitation within the Helvetiafjellet Formation. The fluvial channels could have supplied a lagoonal area of the Glitrefjellet Member with the iron required for the formation of iron ooids to occur. The known transgression during the Early Cretaceous could have caused shallow-marine and sediment starved conditions, which can have led to precipitation of iron ooids.

However, the iron ooids were observed within the conglomerate in the uppermost unit of the Helvetiafjellet Formation. This conglomerate has previously been interpreted as a transgressive lag which represents the remainders of a barrier bar complex, migrating from the distal areas of the Glitrefjellet Member (Grundvåg et al., 2017). These are conditions similar to what was described in Chap. *5.5.2.* Therefore, based on previous descriptions of barrier bars within the Glitrefjellet Member (Nemec et al., 1988; Gjelberg & Steel, 1995), the known transgression occuring during the Cretaceous period in Svalbard and the observations of a conglomerate capping the Helvetiafjellet Formation within cores DH-1 and DH-1A, precipitation of iron ooids in sediment starved shallow-marine conditions (Chap. *5.5.2*) is interpreted as the most likely cause for iron ooid formation within the Helvetiafjellet Formation.

5.6 Palaeoclimatic implications

Based on the observations made through both macro and micro-scale observations of the Helvetiafjellet Formation as a whole, as well as within palaeosols 1 and 2, it becomes apparent that even though the observed palaeosols themselves were not indicative of specific climatic conditions, other observed climatic indicators suggest a warm and humid climate during the Barremian to Aptian in Svalbard. These indicators are kaolinite observed within Palaeosol 2 through XRD-analysis, and the iron ooids observed in the uppermost part of the Helvatiafjellet Formation through thin section analysis.

The presence of kaolinite is indicative of highly leached conditions, which is favoured by subhumid to perhumid climates. The occurrence of iron ooids has previously been linked to greenhouse conditions and warm climates (Mutrux et al., 2008). The presence of iron ooids within the Helvetiafjellet Formation is therefore indicative of warm climatic conditions at the time of deposition.

Therefore, the palaeo-climatic indicators presented in this thesis support a relatively warm and humid climate in the Early Cretaceous in Svalbard. As iron ooids have never been observed within the Helvetiafjellet Formation previously, their discovery could add to the ongoing debate surrounding the climatic conditions during the Cretaceous period.

6 Conclusion

In this thesis, cores DH-1 and DH-1A extracted from the Adventdalen area have formed the foundation for petrographic analysis of the Helvetiafjellet Formation. Based on observations made through logging and thin section analysis, the mineralogical composition of the formation in relation to the interpreted facies associations has been assessed. The study has also incorporated both macro and micro-scale observations, as well as XRD-analysis in the description and classification of two palaeosols observed within the Helvetiafjellet Formation. Based on the work presented in this thesis, the following conclusions are drawn:

- The mineralogical changes that are observed within cores DH-1 and DH-1A are in agreeance with the interpreted facies associations, as they were presented by Thea Engen in Thesis 1. The regional shift in sandstone characteristics and influx of volcanic derived sediments observed in other areas of the Helvetiafjellet Formation is not observed within the cores. This has been interpreted as a consequence of their close proximity to the clastic sedimentary source area.
- The two palaeosols analysed for this project have been classified as enitsols, which are regarded as immature palaeosols. The immaturity of the palaeosols has largely been linked to rapid deposition, the high quartz content of the sediments hosting the palaeosols and their interpreted close proximity to an active channel.
- The quartz content observed within cores DH-1 and DH-1A was perhaps too high to allow for the development of mature palaeosols to occur. Resistant parent material can inhibit the development of strong soil characteristics. The high quartz content was interpreted as a consequence of the inferred proximity of the cores DH-1 and DH-1A to the clastic sedimentary source area.
- Due to the low maturity of the palaeosols, the palaeosols as a whole are not eligible as palaeo-climatic proxies. However, the occurrence of kaolinite within Palaeosol 2 suggests significant leaching, which is favoured by subhumid to perhumid climates.
- The observation of iron ooids within the Helvetiafjellet Formation points to a warm climate at the time of deposition. The iron ooids are regarded as new potential palaeo-climatic indicators for the formation. The formation of the iron ooids is associated with transgressive conditions, which established sediment starved shallow-marine conditions across the study area.

7 References

Allaby , M. (2013). *A Dictionary of Geology and Earth Sciences* (4th ed.). Oxford: Oxford University Press.

Berner, Z. A., Bleeck-Schmidt, S., Stüben, D., Neumann, T., Fuchs, M., & Lehmann, M. (2011). Floodplain deposits: A geochemical archive of flood history - A case study of the River Rhine, Germany. *Applied Geochemistry, 27*(3), 543-561.

Birkenmajer, K. (1984). Sedimentary features of the Helvetiafjellet Formation (Barremian) at Agarhdbukta, East Spitsbergen. *Studia Geologica Polonica, LXXX*, 59-90.

Boggs, S. J. (2009). *Petrology of Sedimentary Rocks* . Cambridge: Cambridge University Press.

Bown, T. M., & Kraus, M. J. (1987). Integration of channel and floodplain suites, I. Developmental sequence and lateral relations of alluvial paleosols. *Journal of Sedimentary Petrology, 57*(4), 587-601.

Braathen, A., Bælum, K., Christensen, H. H., Dahl, T., Eiken, O., Elvebakk, H., . . . Vagle, K. (2012). The Longyearbyen CO2 Lab of Svalbard, Norway - initial assessment of the geological conditions for CO2 sequestration. *Norwegian Journal of Geology, 92*(4), 353-376.

Brekke, H., & Olaussen, S. (2013). Høyt hav og lave horisonter. In I. B. Ramberg, I. Bryhni, A. Nøttvedt, & K. Rangnes, *Landet Blir Til - Norges Geologi* (2nd ed., pp. 425-447). Trondheim: Norsk Geologisk Forening.

Buchan, S. H., Challinor, A., Harland, W. B., & Parker, J. R. (1965). The Triassic Stratigraphy of Svalbard. *Norsk Polarinstitutt Skrifter nr. 135*, 5-93.

Buol, S. W., Southard, R. J., Graham, R. C., & McDaniel, P. A. (2011). *Soil Genesis and Classification* (6th ed.). West Sussex: John Wiley & Sons Ltd.

Cattaneo, A., & Steel, R. J. (2003). Transgressive deposits: a review of their variability. *Earth-Science Reviews, 62*, 187-228.

Cecil, C. B., & Dulong, F. T. (2003). Precipitation Models for Sediment Supply in Warm Climates. *Society of Sedimentary Geology (SEPM), 77*, 21-27.

Cecil, C. B., Dulong, F. T., Harris, R. A., Cobb, J. C., Gluskoter, H. G., & Nugroho, H. (2003). Observations on Climate and Sediment Discharge. *Society for Sedimentary Geology (SEPM), 77*, 29-50.

Coffin, M. F., & Eldholm, O. (1994). Large Igneous Provinces: Crustal Structure, Dimensions, and External Consequences. *Reviews of Geophysics, 32*(1), 1-36.

Cohen, K. M., Finney, S. C., Gibbard, P. L., & Fan, J.-X. (2013). The ICS International Chronostratigraphic Chart. 199-204. Retrieved from http://www.stratigraphy.org/ICSchart/ChronostratChart2017-02.pdf

Coleman, J. M. (1976). *Deltas: Processes of deposition and models for exploration.* Champaign: Continuing Education Publication Company.

Coleman, J. M., & Prior, D. B. (1981). Deltaic environments of deposition. In P. A. Scholle, & D. Spearing, *Sandstone depositional environments* (pp. 139-178). AAPG: Memoirs.

Collignon, M., & Hammer, Ø. (2002). Petrography and sedimentology of the Slottsmøya Member at Janusfjellet, central Spitsbergen. *Norwegian Journal of Geology, 92*, 89-101.

Collin, P. Y., Loreau, J. P., & Courville, P. (2005). Depositional environments and iron ooid formation in condensed sections (Callovian-Oxfordian, south-eastern Paris basin, France. *Sedimentology, 52*, 969-985.

Collinson, J., Mountney, N., & Thompson, D. (2006). *Sedimentary Structures .* Edinburgh: Dunedin Academic Press Ltd. .

Corfu, F., Polteau, S., Planke , S., Faleide, J. I., Svensen, H., Zayoncheck, A., & Stolbov, N. (2013). U-Pb geochronology of Cretaceous magmatism on Svalbard and Franz Josef Land, Barents Large Igneous Province. *Geological Magazine, 150*(6), 1127-1135.

Cullity, B. D. (1978). *Elements of X-ray Diffraction* (2nd ed.). Reading: Addison-Wesley Publishing Company Inc.

Dalland, A. (1977). Erratic clasts in the Lower Tertiary deposits of Svalbard - evidence of transport by winter ice. *Norsk Polarinstitutt, Årbok 1976*, 151-165.

Dallmann, W. (1999). *Lithostratigraphic Lexicon of Svalbard: review and recommendations for nomenclature use: Upper Palaeozoic to Quartenary bedrock .* Tromsø: Norsk Polarinstitutt .

Dallmann, W. K. (2015). Physical geography. In W. K. Dallmann, *Geoscience Atlas of Svalbard* (pp. 20-23). Tromsø: Norsk Polarinsitutt.

Deepthy, R., & Balakrishnan, S. (2005). Climatic control on clay mineral formation: Evidence from weathering profiles developed on either side of the Western Ghats. *Journal of Earth System Science, 114*(5), 545-556.

Dibner , V. D. (1998). *Geology of Franz Josef Land .* Oslo : Norsk Polarinstitutt .

Druckenmiller, P. S., Hurum, J. H., Knutsen, E. M., & Nakrem, H. A. (2012). Two new ophthalmosaurids (Reptilia: Ichthyosauria) for the Agardhfjellet Formation (Upper Jurassic: Volgian/Tithonian), Svalbard, Norway. *Norwegian Journal of Geology, 92*, 311-339.

Duchaufour, P. (1982). *Pedology.* London: Allen & Unwin.

Dypvik, H., Eikeland, T. A., Backer-Owe, K., Andersen, A., Johanen, H., Elverhøi, A., . . . Bjærke, T. (1991). The Janusfjellet Subgroup (Bathonian to Hauterivian) on central Spitsbergen: a revised lithostratigraphy. *Polar Research, 9*(1), 21-44.

Dypvik, H., Håkansson, E., & Heinberg, C. (2002). Jurassic and Cretaceous palaegeography and stratigraphic comparisons in the North Greenland-Svalbard region. *Polar Reseach, 21*(1), 91-108.

Dörr, N., Lisker, F., Clift, P., Carter, A., Gee, D., Tebenkov, A., & Spiegel, C. (2011). Late Mesozoic-Cenozoic exhumation history of northern Svalbard and its regional significance: Constraints from apatite fission track analysis. *Elsevier*, 81-92.

Edwards, M. B. (1976). Depositional environments in Lower Cretaceous regressive sediments, Kikutodden, Sørkapp Land, Svalbard. In D. Worsley, & M. B. Edwards, *Depositional environments in regressive sediments* (pp. 35-50).

Edwards, M. B. (1979). Sandstone in Lower Cretaceous Helvetiafjellet Formation, Svalbard: Bearing on Reservoir Potential of Barents Shelf. *The American Association of Petroleum Geologists Bulletin, 63*(12), 2193-2203.

Elvevold, S., Dallmann, W., & Blomeier, D. (2007). *Geology of Svalbard.* Tromsø: Norwegian Polar Institute.

Ezaki, Y., Kawamura, T., & Nakamura, K. (1994). Kapp Starostin Formation in Spitsbergen: A Sedimentary and Faunal Record of Late Permian Palaeoenvironments in an Arctic Region. *Pangea: Global Environments and Resources Memoir 17*, 647 - 655.

Faleide, J. I., Gudlaudsson, S. T., & Jacquart, G. (1984). Evolution of the western Barents Sea. *Marine and Petroleum Geology, 1*(2).

Fisher, Q. J., Casey, M., Clennell, M. B., & Knipe, R. J. (1999). Mechanical compaction of deeply buried sandstones of the North Sea. *Marine and Petroleum Geology, 16*(7), 605-618.

Gall, Q. (1992). Precambrian paleosols in Canada. *Canadian Journal of Earth Sciences, 29*(12), 2530-2536.

Gay, A. L., & Grandstaff, D. E. (1980). Chemistry and Mineralogy of Precambrian Paleosols at Elliot Lake, Ontario, Canada. *Precambrian Research, 12*(1-4), 349-373.

Gjelberg, J., & Steel, R. (1995). Helvetiafjellet Formation (Barremian-Aptian), Spitsbergen: characteristics of a transgressive succession. In R. S. al., *Sequence stratigraphy on the northwest European Margin* (Vol. 5, pp. 571-593). Amsterdam: Elsevier.

Gjelberg, J., & Steel, R. (2012). Depositional model for the Lower Cretaceous Helvetiafjellet Formation on Svalbard - diachronous vs. layer-cake models. *Norwegian Journal of Geology, 92*, 41-54.

Grantz, A., Hart, P. E., & Childers, V. A. (2011). Geology and tectonic development of the Amerasia and Canada Basins, Arctic Ocean. In A. M. Spencer, D. Gautier, A. Stoupakova, A. Embry, & K. Sørensen, *Arctic Petroleum Geology* (pp. 771-799). London: Geological Society, London Memoirs.

Grogran, P., Østvedt-Ghazi, A., Larssen, G., Fotland, B., Nyberg, K., Dahlgren, S., & Eidvin, T. (1999). Structural elements and petroleum geology of the Norwegian sector of the northern Barents Sea. *Petroleum Geology of Northwest Europe; Proceedings of the 5th Conference, 5*, 247-259. doi:10.1144/0050247

Grundvåg, S.-A. (2015). Cretaceous. In W. K. Dallmann, *Geoscience Atlas of Svalbard* (pp. 122-125). Tromsø: Norsk Polarinstritutt.

Grundvåg, S.-A., & Olaussen, S. (2017). Sedimentology of the Lower Cretaceous at Kikutodden and Keilhaufjellet, southern Spitsbergen: implications for an onshore-offshore link. *Polar Research, 36*(1), 1-20.

Grundvåg, S.-A., Marin, D., Kairanov, B., Sliwinska, K., Nøhr-Hansen, H., Jelbye, M., . . . Olaussen, S. (2017). The Lower Cretaceous succession of the northwestern Barents Shelf: Onshore and offshore correlations. *Marine and Petroleum Geology, 86*, 834-857.

Grøsfjeld, K. (1992). Palynological age constraints on the base of the Helvetiafjellet Formation (Barremian) on Spitsbergen. *Polar Research, 11*(1), 11-19.

Harland, M., Francis, J. E., Brentnall, S. J., & Beerling, D. J. (2007). Cretaceous (Albian-Aptian) conifer wood from Northern Hemisphere high latitudes: Forest composition and palaeoclimate. *Review of Palaeobotany and Palynology, 143*(3-4), 167-196.

Harland, R. (1994). Dinoflagellate Cysts and Climate Change through the Neogene. In M. C. Boulter, & H. C. Fisher, *Cenozoic Plants and Climates of the Arctic* (pp. 93-105). Berlin: Springer.

Harland, W. B. (1969). Contribution of Spitsbergen to Understanding of Tectonic Evolution of North Atlantic Region. In M. Kay, *North Atlantic: Geology and Continental Drift* (pp. 817-851). Mem. Am. Assoc. Petrol. Geol. .

Harland, W. B., & Kelly, S. R. (1997). Jurassic - Cretaceous history. *Geological Society of London, Memoirs*, 363-387.

Harland, W. B., Pickton, C. A., & Wright, N. J. (1976). Some coal-bearing strata in Svalbard . *Norsk Polarinstitutt Skrifter* , 7-28.

Heintz, N. (1962). Dinosaur-footprints and polar wandering. 35-43.

Hurum, J. H., Druckenmiller, P. S., Hammer, Ø., Nakrem, H. A., & Olaussen, S. (2016). The theropod that wasn't there: an ornithopod tracksite from the Helvetiafjellet Formation (Lower Cretaceous) of Boltodden, Svalbard. *The Geological Society of London*.

Hurum, J. H., Roberts, A. J., Dyke, G. J., Grundvåg, S.-A., Nakrem, H. A., Midtkandal, I., . . . Olaussen, S. (2016 A). Bird or maniraptoran dinosaur? A femur from the Albian strata of Spitsbergen. *Palaeontologia Poloncia*, 137-147.

Jones, J. A., & Hartley, A. J. (1993). Reservoir characteristics of a braid-plain depositional system: the Upper Carboniferous Pennant Sandstone of South Wales. In C. P. North, & D. J. Prosser, *Characterization of Fluvial and Aeolian Reservoirs* (pp. 143-156). London : Geological Society Special Publication.

Koevoets, M. J., Abay, T. B., Hammer, Ø., & Olaussen, S. (2016). High-resolution organic carbon-isotope stratigraphy of the Middle Jurassic-Lower Cretaceous Agardhfjellet Formation of central Spitsbergen, Svalbard. *Palaeogeography, Palaeoclimatology, Palaeoecology, 449*, 266-274.

Koevoets, M. J., Hammer, Ø., Olaussen, S., Senger, K., & Smelror, M. (2018). Intergrating subsurface and outcrop data of the Middle Jurassic to Lower Cretaceous Agardhfjellet Formation in central Spitsbergen. *Norwegian Journal of Geology*(98), 1-34.

Kottek, M., Grieser, J., Beck, C., Rudolf, B., & Rubel, F. (2006). World Map of the Köppen-Geiger climate classification. *Meteorologische Zeitschrif, 15*, 259-263.

Kraus, M. J. (1999). Paleosols in clastic sedimentary rocks: their geologic applications. *Earth-Science Reviews, 47*(1-2), 41-70.

Kraus, M. J., & Aslan, A. (1999). Palaeosol sequences in floodplain environments: a hierarchial approach. *Palaeoweathering, Palaeosurfaces and Related Continental Deposits, 27*, 303-321.

Lane, L. S. (1997). Canada Basin, Arctic Ocean: Evidence Against a Rotational Origin. *Tectonics, 16*(3), 363-387.

Lehmann, J., & Schroth, G. (2003). Nutrient Leaching. In G. Schroth, & F. L. Sinclair, *Trees, Crops and Soil Fertility* (p. 151). Wallingford: Centre for Agriculture and Bioscience International .

Mack, G. H., & James, W. C. (1994). Paleoclimate and the Global Distribution of Paleosols. *The Journal of Geology, 102*(3), 360-366.

Mack, G. H., James, W. C., & Monger, H. C. (1993). Classification of Paleosols. *Geological Society of America Bulletin, 105*(2), 129-136.

Maher, H. (2001). Manifestations of the Cretaceous High Artic Large Igneous Province in Svalbard. *The Journal of Geology, 109*(1), 91-104.

Maher, H. D., Hays, T., Shuster, R., & Mutrux, J. (2004). Petrography of Lower Cretaceous sandstones on Spitsbergen. *Polar Research, 23*(2), 147-165.

Martín-García, J. M., Márquez, R., Delgado, G., Sánchez-Marañón, M., & Delgado, R. (2015). Relationships between quartz weathering and soil type (Entisol, Inceptisol and Alfisol) in Sierra Nevada (southeast Spain). *European Journal of Soil Science*, 179-193.

Midtkandal , I., & Nystuen, J. (2009). Depositional Architecture of a Low-gradient Ramp Shelf in an Epicontiental Sea: the Lower Cretaceous on Svalbard. *Basin Research, 21*, 655-675.

Midtkandal, I., Nystuen, J. P., & Nagy, J. (2007). Paralic sedimentation on an epicontinental ramp shelf during a full cycle of relative sea-level fluctuation; the Helvetiafjellet Formation in Nordenskiöld Land, Spitsbergen. *Norwegian Journal of Geology, 87*, 343-359.

Midtkandal, I., Nystuen, J., Nagy, J., & Mørk, A. (2008). Lower Cretaceous lithostratigraphy across a regional subaerial unconformity in Spitsbergen: the Rurikfjellet and Helvetiafjellet formations. *Norwegian Journal of Geology, 88*, 287-304.

Midtkandal, I., Svensen, H., Planke, S., Corfu, F., Polteau, S., Torsvik, T., . . . Olaussen, S. (2016). The Aptian (Early Cretaceous) oceanic anoxic event (OAE1a) in Svalbard, Barents Sea, and the absolute age of the Barremian-Aptian boundary. *Elsevier: Palaeography, Palaeoclimatology, Palaeoecology, 463*, 126-135.

Milliken, K. L. (2003). *Treatise on Geochemistry* . Oxford: Elsevier Ltd.

Miranda-Tervino, J. C., & Coles, C. A. (2003). Kaolinite properties, structure and influence of metal retention on pH. *Applied Clay Science, 23*(1-4), 133-139.

Mjøs, R., Walderhaug, O., & Prestholm, E. (1993). Crevasse Splay Sandstone Geometries in the Middle Jurassic Ravenscar Group of Yorkshire, UK. In M. Marzo, & C. Puigdefábregas, *Alluvial Sedimentation* (pp. 167-184). Oxford: Blackwell Publishing Ltd.

Mohanty, S. P., & Nanda, S. (2015). Geochemistry of a paleosol horizon at the base of the Sausar Group, central India: Implications on atmospheric conditiona at the Archean-Paleoproterozoic boundary. *Geoscience Frontiers, 7*(5).

Murali, V., Krishna Murti, G. S., & Sarma, V. A. (1978). Clay Mineral Distribution in Two Topsequences of Tropical Soils of India. *Geoderma, 20*(3-4), 257-269.

Mutrux, J., Maher, H., Shuster, R., & Hays, T. (2008). Iron ooid beds of the Carolinefjellet Formation, Spitsbergen, Norway. *Polar Research, 27*(1), 28-43.

Müller, R. D., & Spielhagen, R. F. (1990). Evolution of the Central Tertiary Basin of Spritsbergen: towards a synthesis of sediment and plave tectonic history. *Palaeogeography, Palaeoclimatology, Palaeoecology, 80*(2), 153-172.

Mørk, A., Dallmann, W., Dypvik, H., Johannessen, E., Larssen, G., Nagy, J., . . . Worsley, D. (1999). Mesozoic lithostratigraphy. In W. Dallmann, *Stratigraphic Lexicon of Svalbard* (pp. 127-208). Tromsø: Norwegian Polar Institute, Polar Environmental Centre.

Mørk, A., Knarud, R., & Worsley, D. (1982). Depositional and Diagenetic Environments of the Triassic and Lower Jurassic Succession of Svalbard. *Canadian Society of Petroleum Geologists*, 371-398.

Nagy, J. (1970). Ammonite faunas and stratigraphy of Lower Cretaceous (albian) rocks in southern Spitsbergen . *Norsk Polarinstitutt Skrifter Nr. 152*, 5-60.

Nakrem, H. A., Orchard, M. J., Weitschat, W., Hounslow, M. W., Beatty, T. W., & Mørk, A. (2008). Triassic conodonts from Svalbard and their Boreal correlations. *Polar Research, 27*(3), 523-539.

Nemec, W. (1992). Depositional controls on plant growth and peat accumulation in a braidplain delta environment: Helvetiafjellet Formation (Barremian - Aptian), Svalbard. *Geological Society of America Special Paper 267*, 209-224.

Nemec, W., Steel, R. J., Gjelberg, J., Collinson, J. D., Prestholm, E., & Øxnevad, I. E. (1988). Anatomy of Collapsed and Re-established Delta Front in Lower Cretaceous of Eastern Spitsbergen: Gravitational Sliding and Sedimentation Processes. *The American Association of Petroleum Geologists Bulletin, 72*(4), 454-476.

Nesse, W. D. (2012). *Introduction to mineralogy .* Oxford : Oxford University Press.

Nøttvedt, A., Cecchi, M., Gjelberg, J. G., Kristensen, S. E., Lønøy, A., Rasmussen, A., . . . Van Veen, P. M. (1992). Svalbard-Barents Sea correlation: A short review. In T. O. Vorren, E. Bergsager, Ø. A. Dahl-Stamnes, E. Holter, B. Bohansen, E. Lie, & T. B. Lund, *Arctic Geology and Petroleum Potential* (pp. 363-375). Amsterdam: Elsevier.

Olaussen, S. (2015). Jurassic. In W. K. Dallmann, *Geoscience Atlas of Svalbard* (pp. 118-121). Tromsø: Norsk Polarinstitutt.

Onderdonk, N., & Midtkandal, I. (2010). Mechanisms of Collapse of the Cretaceous Helvetiafjellet Formation at Kvalvågen, Eastern Spitsbergen. *Marine and Petroleum Geology, 27*(10), 2118-2140.

Pal, D. K., Deshpande, S. B., Venugopal, K. R., & Kalbande, A. R. (1989). Formation of Di- and Trioctahedral Smectite as Evidence for Paleoclimatic Changes in Southern and Central Peninsular India. *Geoderma, 45*, 175-184.

Parker, J. (1967). The Jurassic and Cretaceous sequence in Spitsbergen. *Geological Magazine , 104*(5), 487-505.

Pettijohn, F. J., Potter, P. E., & Siever, R. (1987). *Sand and sandstone* (2nd ed.). New York: Springer Verlag.

Pickton, C. A. (1981). Palaeogene and Cretaceous dropstones in Spitsbergen. In M. J. Hambrev, & W. B. Harland, *Earths pre-Pleistocene glacial record* (pp. 567-569). Cambridge: Cambridge University Press.

Polteau, S., Hendriks, B. W., Planke, S., Ganerød, M., Corfu, F., Faleide, J. I., . . . Myklebust, R. (2016). The Early Cretaceous Barents Sea Sill Complex: Distribution, 40Ar/39Ar geochronology, and implications for carbon gas formation. *Palaeogeography, Palaeoclimatology, Palaeoecology, 441*, 83-95.

Posarnentier, H. W., & Allen, G. P. (1999). *Siliciclastic Sequence Stratigraphy - Concepts and Applications .* SEPM Society for Sedimentary Geology .

Prestholm, E., & Walderhaug, O. (2000). Synsedimentary Faulting in a Mesozoic Deltaic Sequence, Svalbard, Arctic Norway - Fault Geometries, Faulting Mechanisms, and Sealing Properties. *The American Association of Petroleum Geologists Bulletin, 84*(4), 505-522.

Price, G. D., & Nunn, E. V. (2010). Valanginian isotope variation in glendonites and belemnites from Arctic Svalbard: Transient glacial temperatures during the Cretaceous greenhouse. *Geological Society of America, 38*(3), 251-254.

Ramberg , I. B., Bryhni, I., Nøttvedt, A., & Rangnes, K. (2013). *Landet blir til - Norges geologi.* Trondheim: Norsk Geologisk Forening .

Reineck, H.-E., & Singh, I. B. (1980). *Depositional Sedimentary Environments .* New York: Springer-Verlag Berlin Heidelberg.

Retallack, G. J. (1988). Field recognition of paleosols. *Geological Society of America Special Paper 216*, 1-20.

Retallack, G. J. (2001). *Soils of the Past: An introduction to paleopedology.* Oxford: Blackwell Science Ltd.

Rimstidt, J. D. (1997). Quartz solubility at low temperatures. *Geochimica et Cosmochimica Acta, 61*(13), 2553-2558.

Røhr, T. S., Andersen, T., & Dypvik, H. (2008). Provenance of Lower Cretaceous sediments in the Wandel Sea Basin, North Greenland. *Journal of the Geological Society, 165*, 755-767.

Selleck, B. W., Carr, P. F., & Jones, B. G. (2007). A review and synthesis of glendonites (pseudomorphs after ikaite) with new data: assessing applicability as recorders of ancient coldwater conditions. *Journal of Sedimentary Reseach, 77*(11), 980-991.

Senger, K., Tveranger, J., Ogata, K., Braathen, A., & Planke, S. (2014). Late Mesozoic magmatism in Svalbard: A review. *Earth-Science Reviews, 139*, 123-144.

Sheldon, N. D., & Tabor, N. J. (2009). Quantitative paleoenvironmental and paleoclimatic reconstruction using paleosols. *Earth-Scienve Reviews (95)*, 1-52.

Siehl , A., & Thein, J. (1989). Minette-type ironstones. In T. P. Young, & W. E. Taylor, *Phanerozoic Ironstones* (pp. 175-193). Geological Society Special Publication .

Simone , L. (1981). Ooids: A Review. *Earth-Science Reviews, 16*, 319-355.

Singer, A. (1980). The Paleoclimatic Interpretation of Clay Minerals in Soils and Weathering Profiles. *Earth-Science Reviews, 15*(4), 303-326.

Singer, A. (1984). The Paleoclimatic Interpretation of Clay Minerals in Sediments - a Review. *Earth-Science Reviews, 21*, 251-293.

Smelror, M. (1994). Jurassic Stratigraphy of the western Barents Sea Region: A Review. *GEOBIOS, 17*, 441-451.

Smelror, M., & Dypvik, H. (2006). The Sweet Aftermath: Environmental Changes and Biotic Restoration Following the Marine Mjølnir Impact (Volgian-Ryazanian Boundary, Barents Shelf). In C. Cockell, I. Gilmour, & C. Koeberl, *Biological Processes Associated with Impact Event. Impact Studies* (pp. 143-178). Berlin: Heidelberg.

Smelror, M., & Larssen, G. B. (2016). Are there Upper Cretaceous sedimentary rocks preserved on Sørkapp Land, Svalbard? *Norwegian Journal of Geology, 96*(2), 1-12.

Soil Survey Staff. (1999). *Keys to Soil Taxonomy: A basic system for soil classification for making and interpreting soil surveys.* Washington: United Stated Department of Agrculture .

Steel, R. (1977). Observations on some Cretaceous and Tertiary sandstone bodies in Nordenskiöld Land, Svalbard. *Norsk Polarinstitutt*, 43-66.

Steel, R. J., Crabaugh, J., Schellpeper, M., Mellere, D., Plink-Bjorklund, P., Deibert, J., & Loeseth, T. (2000). Deltas vs. Rivers on the Shelf Edge: Their Relative Contributions to the Growth of Shelf-Margins and Basin-Floor Fans (Barremian and Eocene, Spitsbergen). *Deep-Water Reservoirs of the World*, 981-1009.

Steel, R. J., Gjelberg, J., Helland-Hansen, W., Kleinspehn, K., Nøttvedt, A., & Rye-Larsen, M. (1985). The Tertiary strike-slip basins and orogenic belt of Spitsbergen. *The Society of Economic Paleontologists and Mineralogists* , 339-359.

Steel, R., & Worsley, D. (1984). Svalbard`s post-Caledonian strata - an atlas of sedimentational patterns and palaeographic evolution. *Petroleum Geology of the North European Margin*, 109-135.

Steel, R., Gjelberg, J., & Haarr, G. (1978). Helvetiafjellet Formation (Barremian) at Festningen, Spitsbergen - a field guide. *Norsk Polarinstitutt Årbok 1977*, 111-128.

Stow, D. A. (2006). *Sedimentary Rocks in the Field - A Color Guide* . Burlington : Academic Press.

Suess, E., Blazer, W., Hesse, K.-F., Müller, P. J., Ungerer, C. A., & Wefer, G. (1982). Calcium Carbonate Hexahydrate from Organic-Rich Sediments of the Antarctic Shelf: Precursors of Glendonites. *Science, 216*, 1128-1131.

Taylor, K. G. (1996). Early Cretaceous iron ooids in the Paris Basin: pedogenic versus marine origin and their palaeoclimatic significance. *Cretaceous Research, 17*, 109-118.

Taylor, K. G., Simo, J. T., Yocum, D., & Leckie, D. A. (2002). Stratigraphic significance of ooidal ironstones from the Cretaceous western interior seaway: the Peace River Formation, Alberta, Canada, and the Castlegate Sandstone, Utah, U.S.A. *Journal of Sedimentary Research, 72*(2), 316-327.

Torsvik, T. H., Van der Voo, R., Preeden, U., Niocaill, C. M., Steinberger, B., Dubrovine, P. V., . . . Cocks, L. M. (2012). Phanerozoic polar wander, palaeogeography and dynamics. *Earth-Science Reviews*, 325-368.

Tucker, M. E. (2011). *Sedimentary Rocks in the Field* . Oxford: Wiley-Blackwell.

Vickers, M. L., Price, G. D., Jerrett, R. M., & Watkinson, M. (2017). Stratigraphic and geochemical expression of Barremian–Aptian global climate change in Arctic Svalbard. *Geosphere, v.12, no. 5*, 1-12.

Vodyanitskii, Y. N., & Savichev, A. T. (2017). The influence of organic matter on soil color usinf the regression equation of optical parameters in the system CIE-L*a*b*. *Annals of Agrarian Science, 15*(3), 380-385.

Waugh, B. (1970). Formation of quartz overgrowths in the Penrith sandstone (Lower Permian) of northwest England as revealed by scanning electron microscopy. *Sedimentology, 14*(3-4), 309-320.

Wilding, L. P., Smeck, N. E., & Hall, G. F. (1984 A). *Pedogenesis and Soil Taxonomy II. The Soil Orders.* Amsterdam: Elsevier.

Wilding, L. P., Smeck, N. E., & Hall, G. F. (1984). *Pedogenesis and Soil Taxonomy I. Concepts and Interactions.* Amsterdam: Elsevier.

Worden, R. H., & Burley, S. D. (2003). Sandstone diagenesis: the evolution of sand to sandstone. In S. D. Burley, & R. H. Worden, *Sandstone Diagenesis: Recent and Ancient* (pp. 3-43). Malden: Blackwell Publishing Ltd.

Worsley, D. (1986). *The geological history of Svalbard - evolution of an archipelago.* Stavanger: Den norske stats oljeselskap .

Worsley, D. (2008). The post-Caledonian development of Svalbard and the western Barents Sea. *Polar Research, 27*, 298-317.

Wright, V. P. (1992). Paleosol Recognition: a Guide to Early Diagenesis in Terrestrial Settings. *Development in Sedimentology (47)*, 591-619.

Wright, V. P., & Tucker, M. E. (1991). Calcretes: An Introduction. In V. P. Wright, & M. E. Tucker, *Calcretes* (pp. 1-22). The International Association of Sedimentologists .

Wu, J., Zhang, R., & Yang, J. (1996). Analysis of rainfall - recharge relationships. *Journal of Hydrology, 177*, 143-160.

Young, T. P., & Taylor, W. E. (1989). Iron-rich ooids, their mineralogy and microfabrics: clues to their origin and evolution. *Geological Society Special Publication 46*, 141-164.

Ågren, G. I., Wetterstedt , J. M., & Billberger, M. F. (2012). Nutrient limitation on terrestrial plant growth . modeling the interaction between nitrogen and phosphorus. *New Phytologist, 194*, 953-960.

Århus, N. (1992). Some dinoflagellate cysts from the Lower Cretaceous of Spitsbergen. *Grana, 31*(4), 305-314.

Appendix A

DH-1

1:50cm

Legend

- Coal
- Black shale
- Coaly shale
- Siltstone
- Sandstone
- Conglomerate
- Wavy beds
- Steeply dipping beds
- Sub-horizontal beds
- Root structures
- Bioturbation
- Lenticular structures
- Undifferentiated ripple cross-lamination
- Soft sediment deformation

C.: Carolinefjellet Formation
DA.: Dalkjegla Member
RF.: Rurikfjellet Formation
KM.: Kikutodden Member

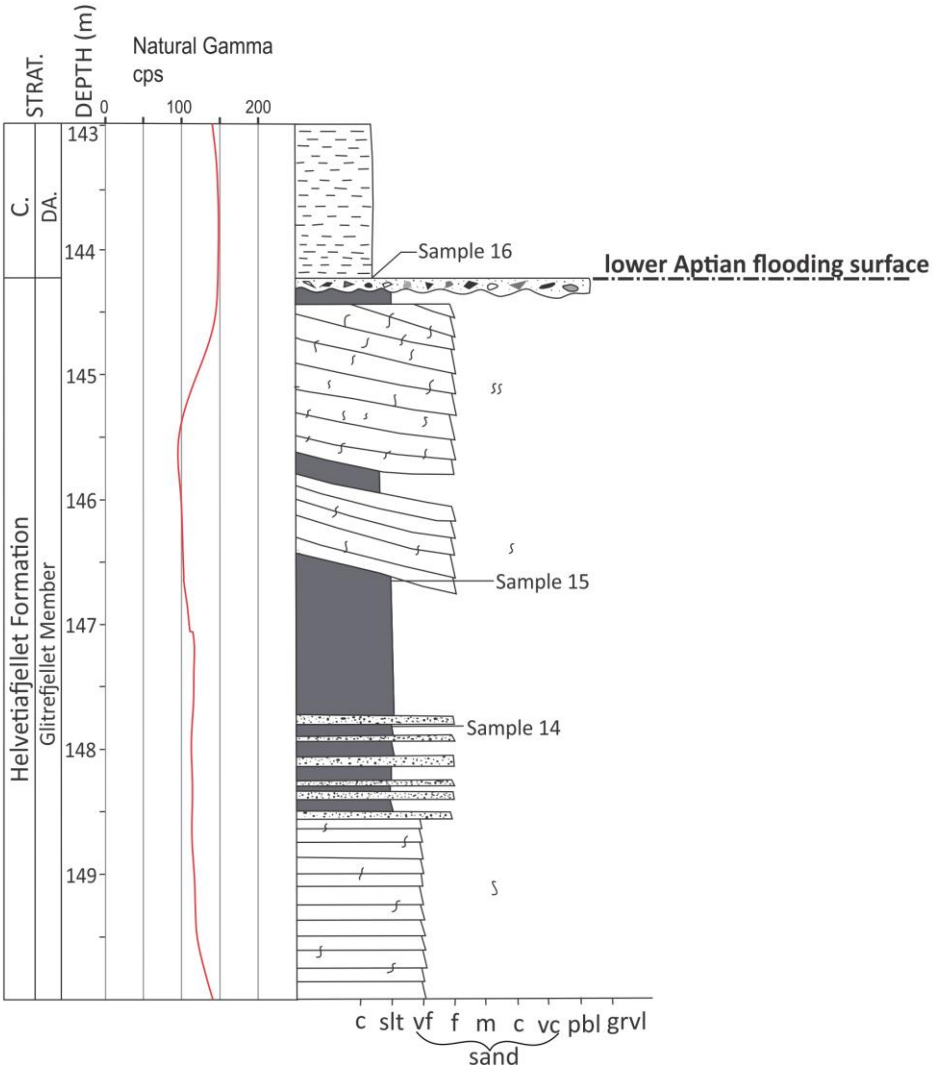

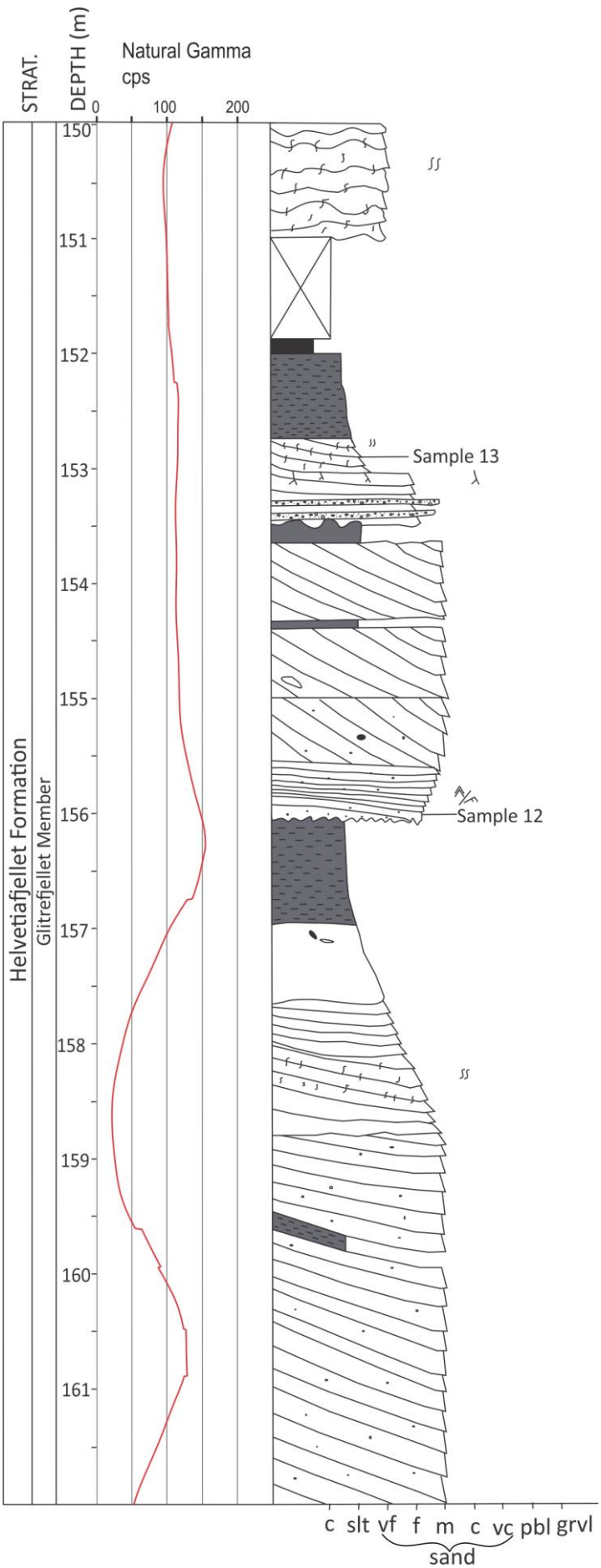
STRAT.
DEPTH (m)
Natural Gamma
cps
0
100
200
150
151
152
153
154
155
156
157
158
159
160
161
Helvetiafjellet Formation
Glitrefjellet Member
Sample 13
Sample 12
c slt vf f m c vc pbl grvl
sand

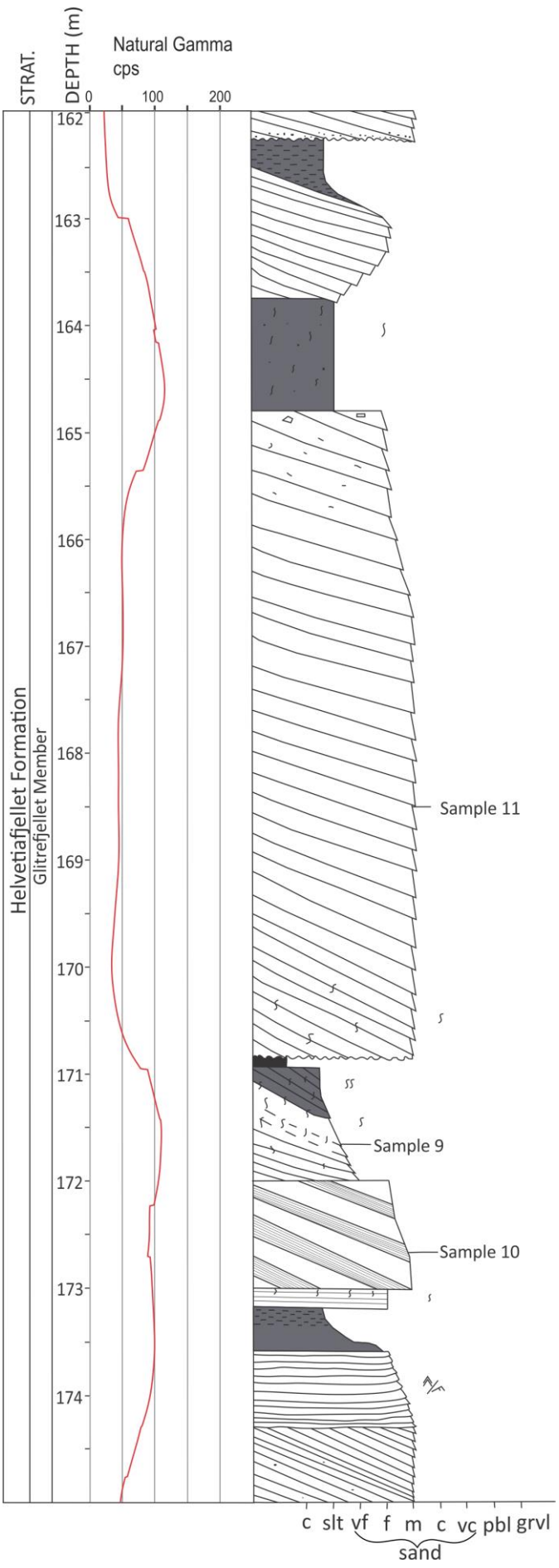
STRAT.
DEPTH (m)
Natural Gamma
cps
0
100
200
162
163
164
165
166
167
168
169
170
171
172
173
174
Helvetiafjellet Formation
Glitrefjellet Member
Sample 11
Sample 9
Sample 10
c slt vf f m c vc pbl grvl
sand

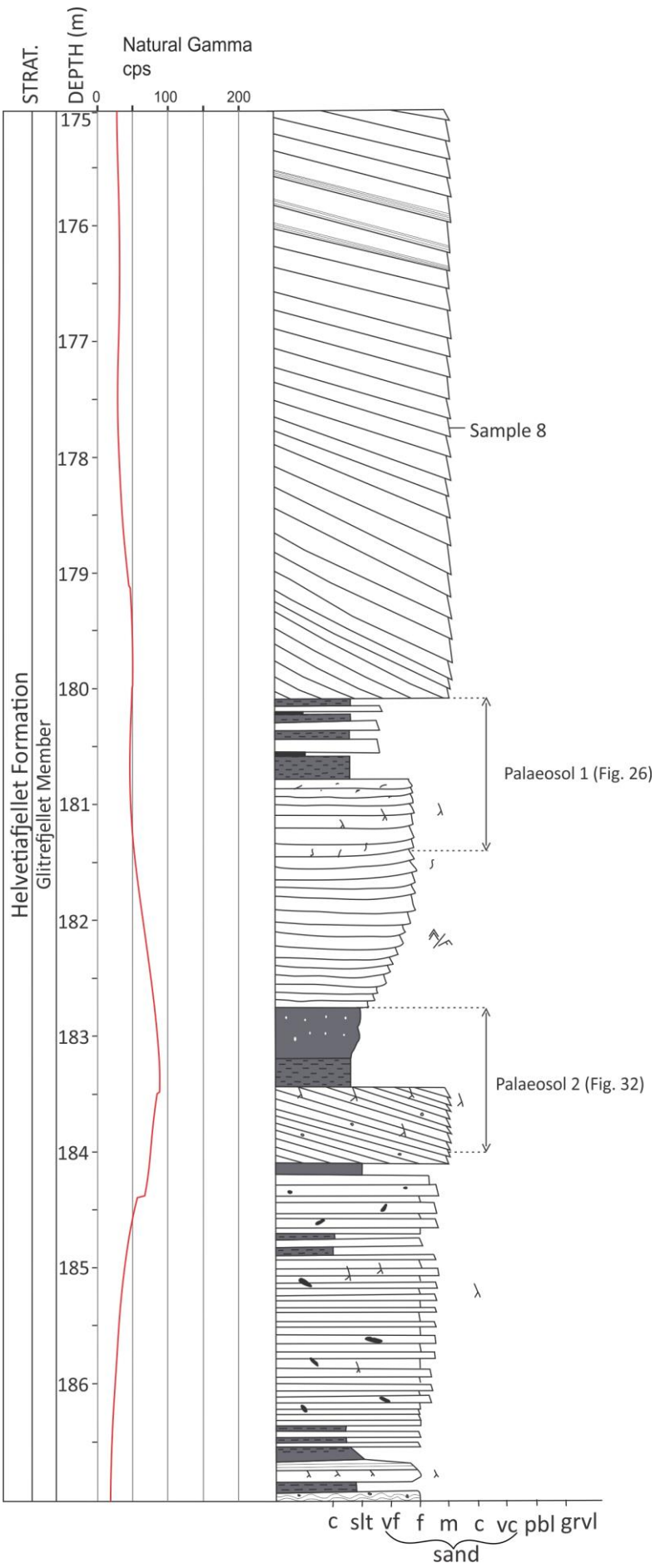
STRAT.
DEPTH (m)
Natural Gamma
cps
0
100
200
175
176
177
178
179
180
181
182
183
184
185
186
Helvetiafjellet Formation
Glitrefjellet Member
Sample 8
Palaeosol 1 (Fig. 26)
Palaeosol 2 (Fig. 32)
c slt vf f m c vc pbl grvl
sand

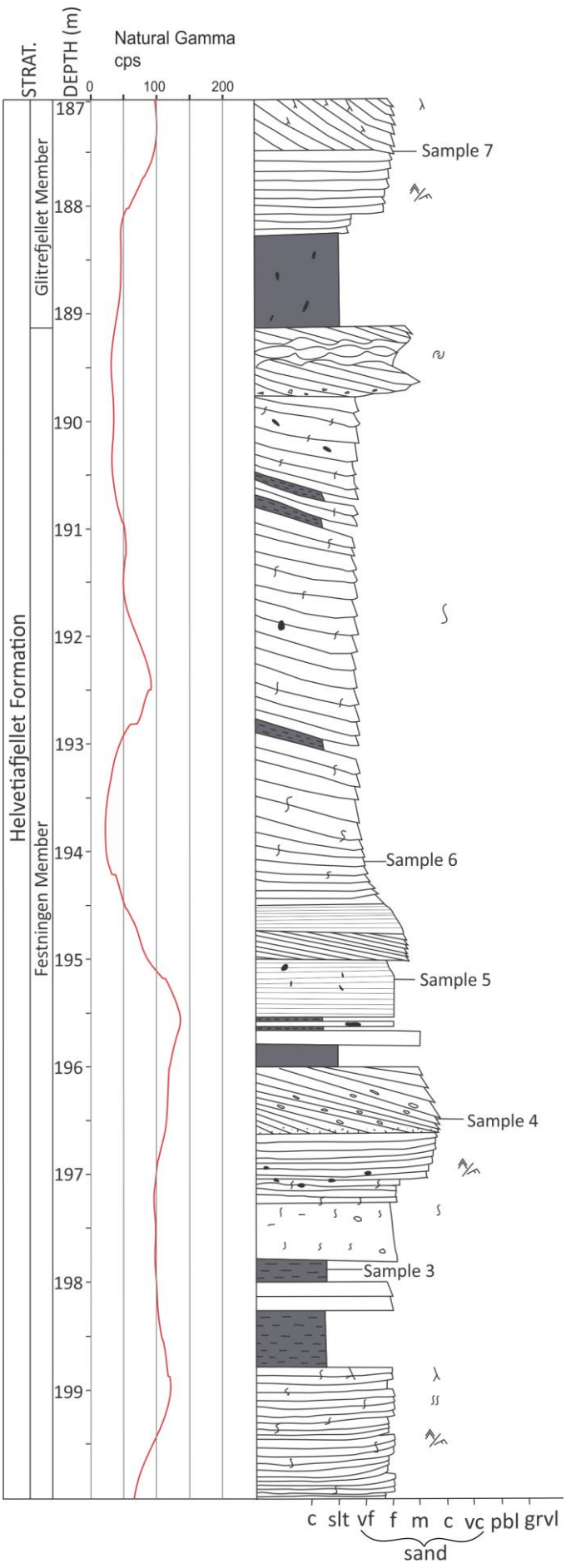
STRAT.
DEPTH (m)
Natural Gamma
cps
0
100
200
Helvetiafjellet Formation
Glitrefjellet Member
Festningen Member
187
188
189
190
191
192
193
194
195
196
197
198
199
Sample 7
Sample 6
Sample 5
Sample 4
Sample 3
c slt vf f m c vc pbl grvl
sand

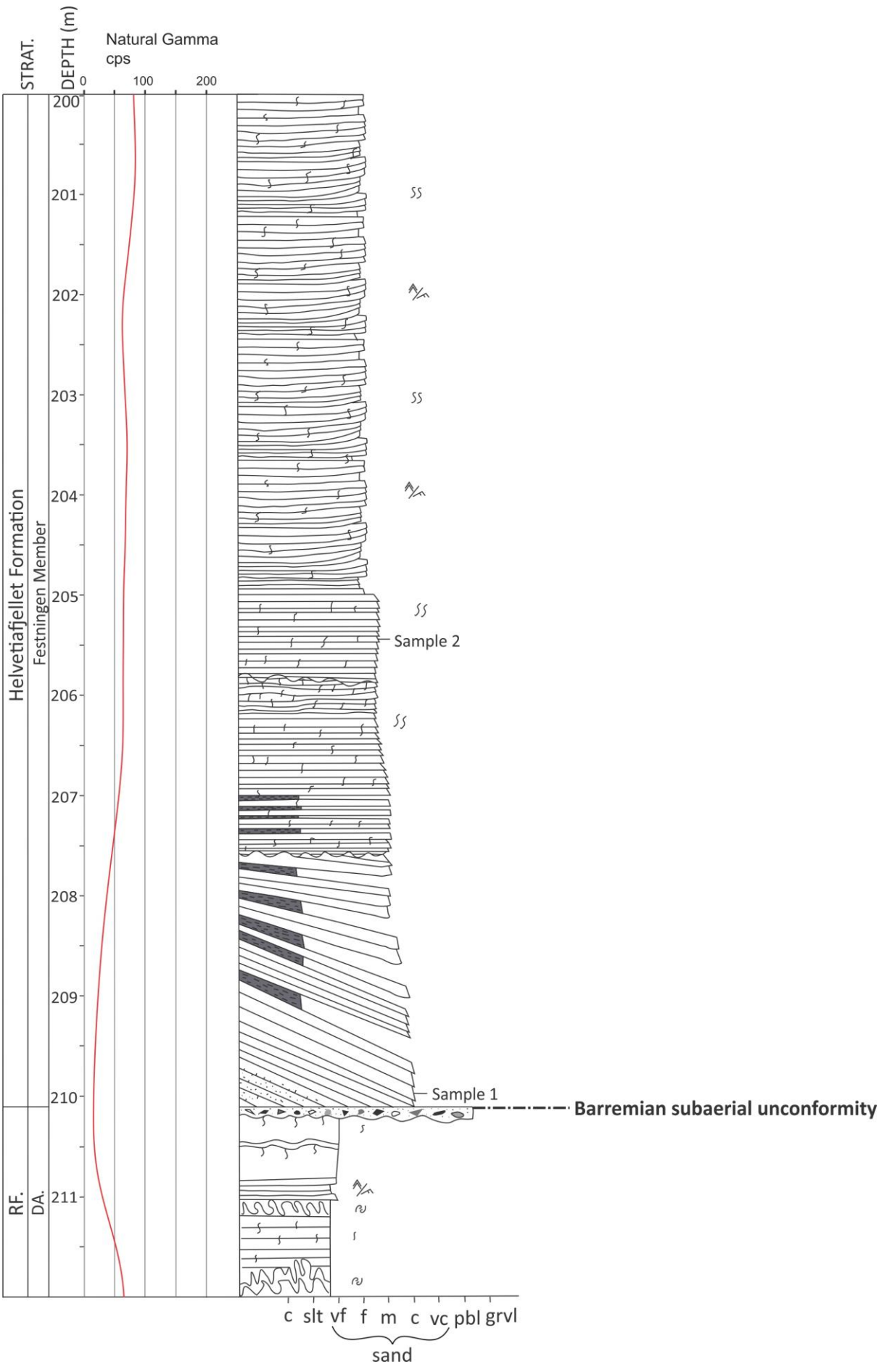
STRAT.
DEPTH (m)
Natural Gamma
cps
0
100
200
200
201
202
203
204
205
206
207
208
209
210
211
Helvetiafjellet Formation
Festningen Member
RF.
DA.
Sample 2
Sample 1
Barremian subaerial unconformity
c slt vf f m c vc pbl grvl
sand

DH-1A

1:50cm

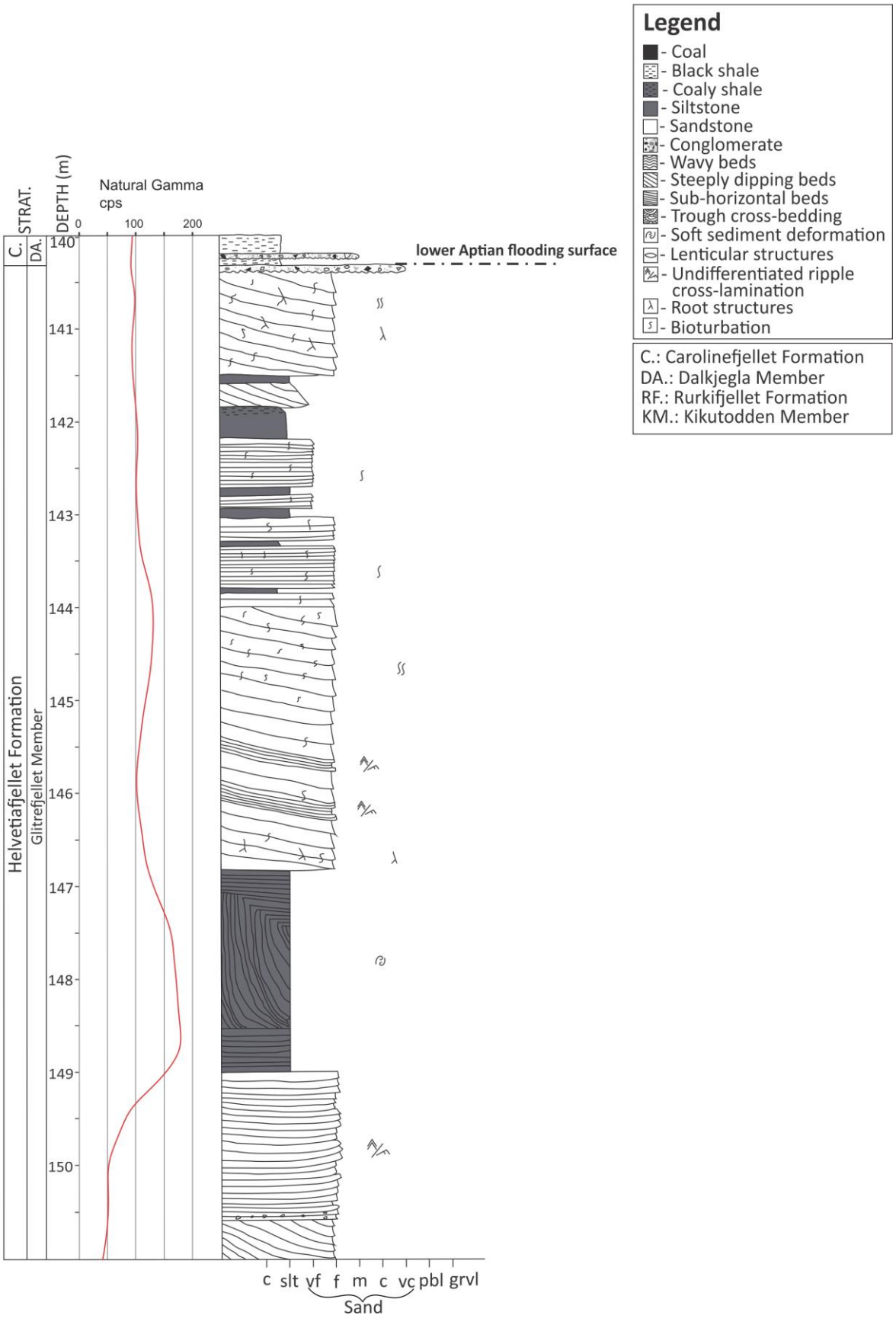
Legend
- Coal
- Black shale
- Coaly shale
- Siltstone
- Sandstone
- Conglomerate
- Wavy beds
- Steeply dipping beds
- Sub-horizontal beds
- Trough cross-bedding
- Soft sediment deformation
- Lenticular structures
- Undifferentiated ripple cross-lamination
- Root structures
- Bioturbation
C.: Carolinefjellet Formation
DA.: Dalkjegla Member
RF.: Rurkifjellet Formation
KM.: Kikutodden Member
C.
STRAT.
DA.
DEPTH (m)
Natural Gamma
cps
0
100
200
140
141
142
143
144
145
146
147
148
149
150
lower Aptian flooding surface
Helvetiafjellet Formation
Glitrefjellet Member
c slt vf f m c vc pbl grvl
Sand

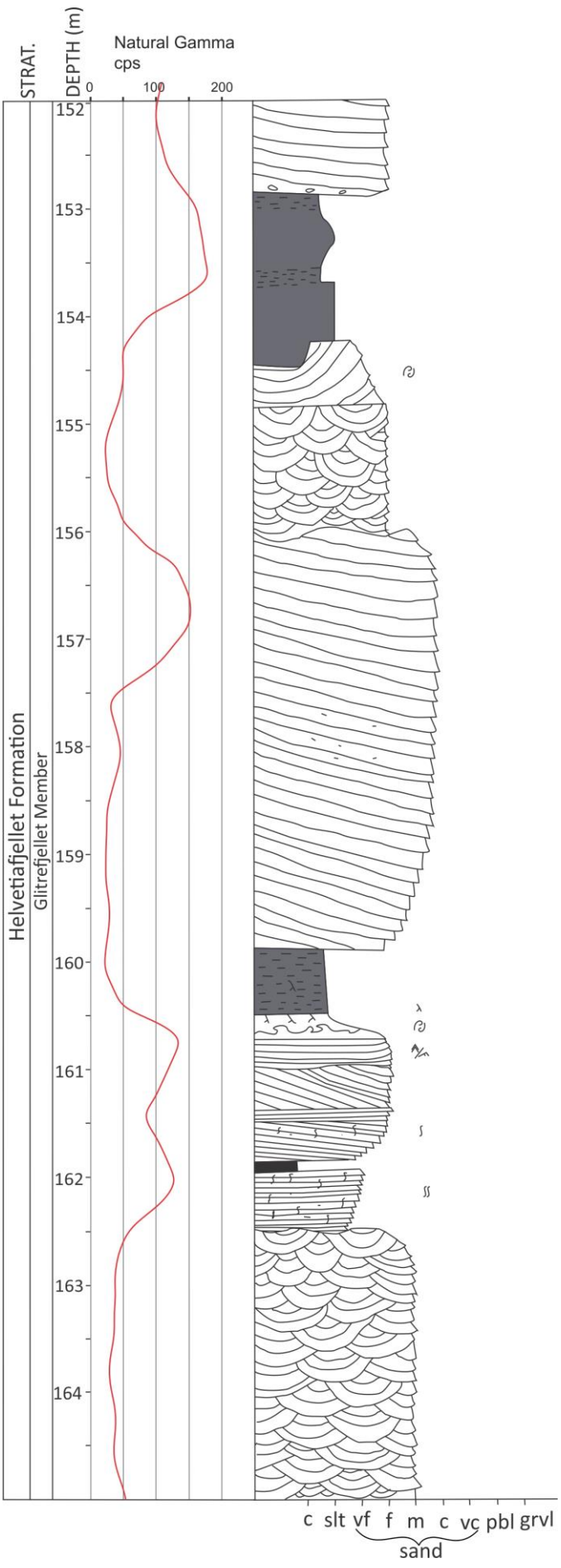
STRAT.
DEPTH (m)
Natural Gamma
cps
0
100
200
152
153
154
155
156
157
158
159
160
161
162
163
164
Helvetiafjellet Formation
Glitrefjellet Member
c slt vf f m c vc pbl grvl
sand

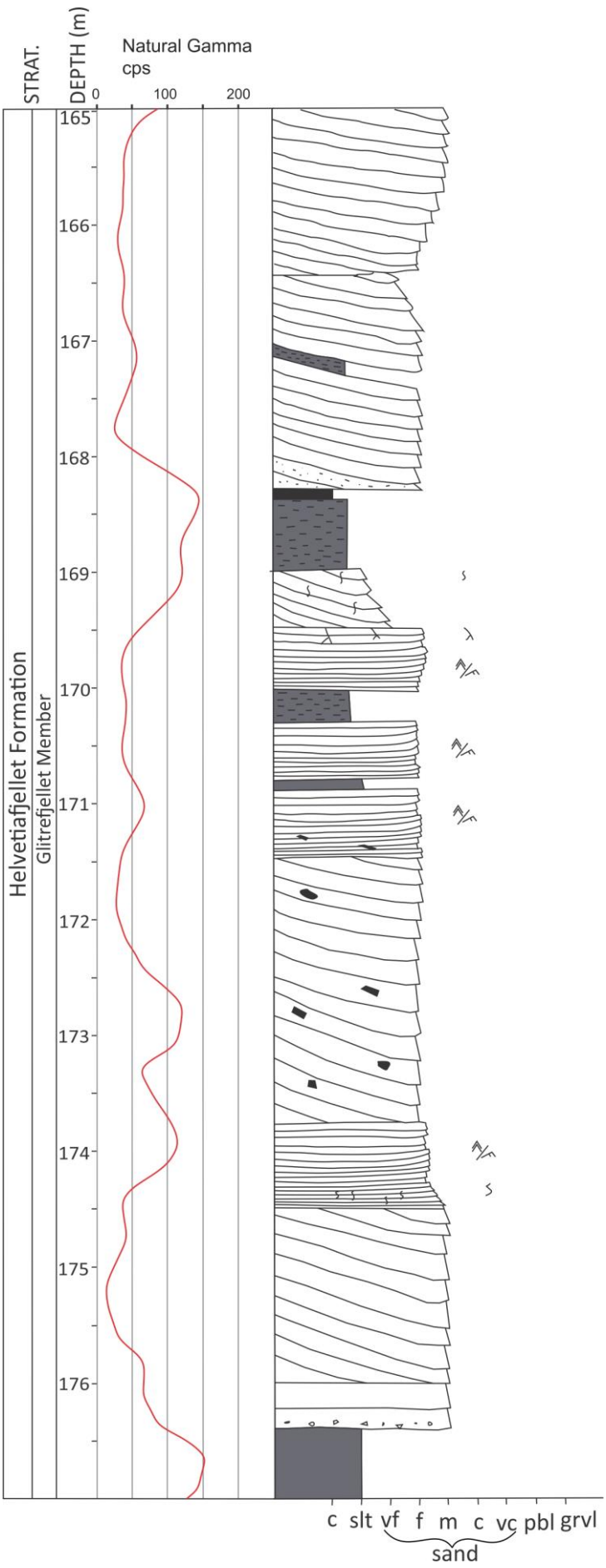
STRAT.
DEPTH (m)
Natural Gamma
cps
0
100
200
165
166
167
168
169
170
171
172
173
174
175
176
Helvetiafjellet Formation
Glitrefjellet Member
c slt vf f m c vc pbl grvl
sand

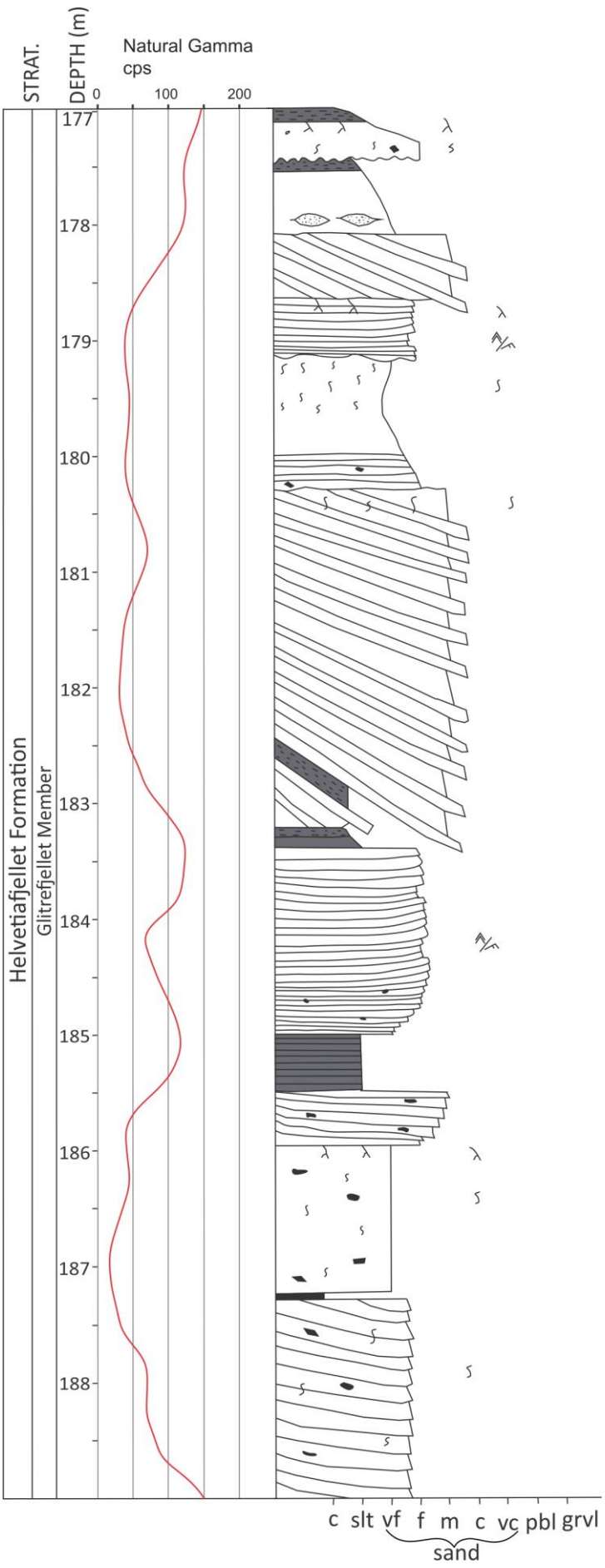
STRAT.
DEPTH (m)
Natural Gamma
cps
0
100
200
177
178
179
180
181
182
183
184
185
186
187
188
Helvetiafjellet Formation
Glitrefjellet Member
c
slt
vf
f
m
c
vc
pbl
grvl
sand

X

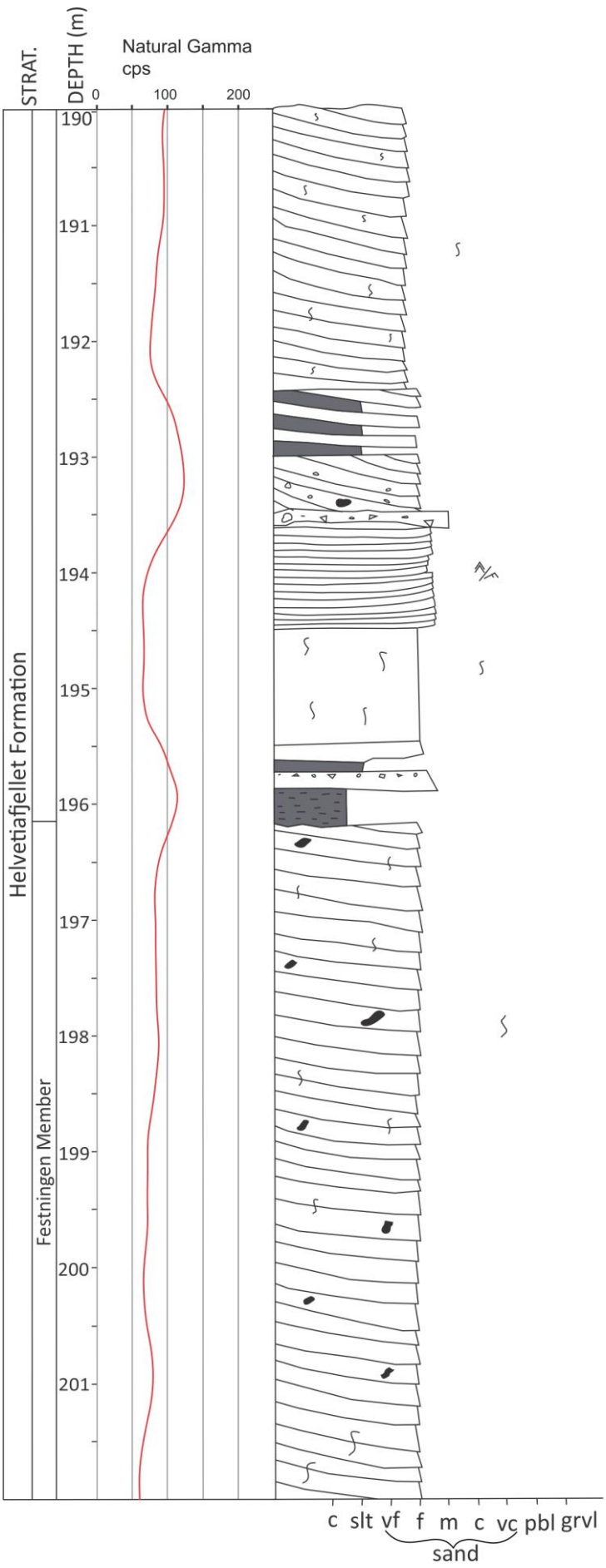
STRAT.
DEPTH (m)
Natural Gamma
cps
0
100
200
190
191
192
193
194
195
196
197
198
199
200
201
Helvetiafjellet Formation
Festningen Member
c slt vf f m c vc pbl grvl
sand

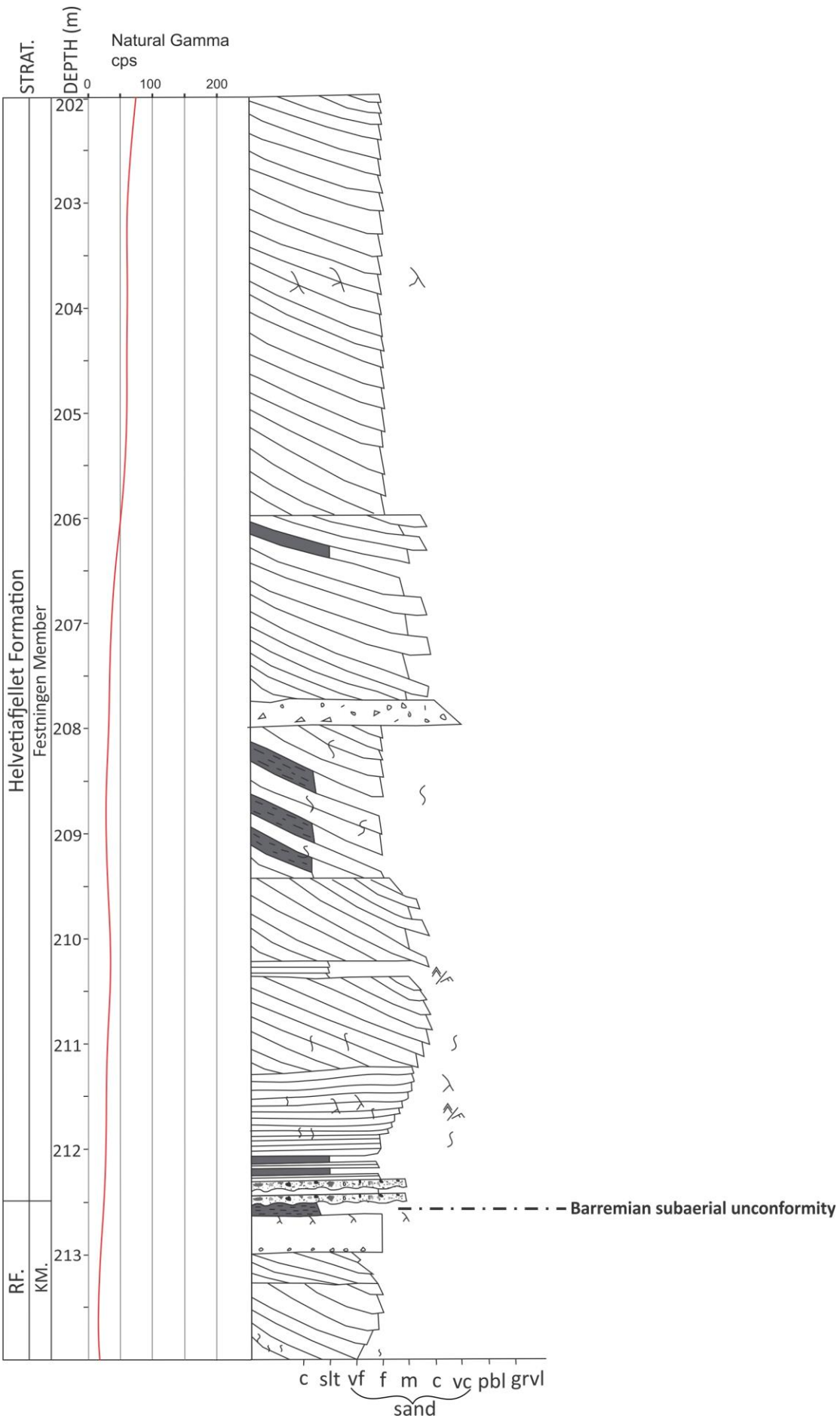
STRAT.
DEPTH (m)
Natural Gamma
cps
0
100
200
202
203
204
205
206
207
208
209
210
211
212
213
Helvetiafjellet Formation
Festningen Member
RF.
KM.
Barremian subaerial unconformity
c slt vf f m c vc pbl grvl
sand

Appendix B

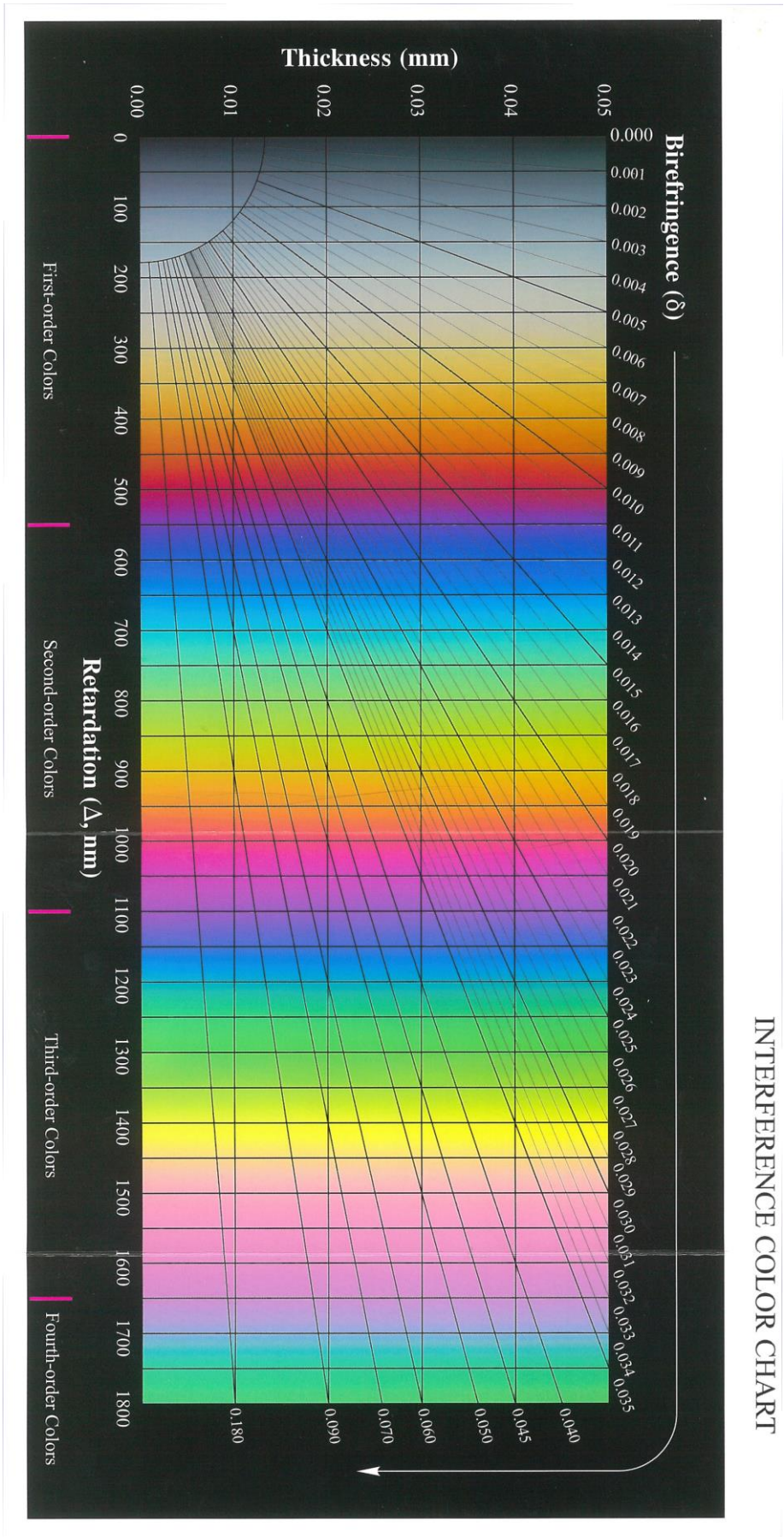
INTERFERENCE COLOR CHART
Thickness (mm)
0.00
0.01
0.02
0.03
0.04
0.05
Birefringence (δ)
0.000
0.001
0.002
0.003
0.004
0.005
0.006
0.007
0.008
0.009
0.010
0.011
0.012
0.013
0.014
0.015
0.016
0.017
0.018
0.019
0.020
0.021
0.022
0.023
0.024
0.025
0.026
0.027
0.028
0.029
0.030
0.031
0.032
0.033
0.034
0.035
0.040
0.045
0.050
0.060
0.070
0.090
0.180
Retardation (Δ, nm)
0
100
200
300
400
500
600
700
800
900
1000
1100
1200
1300
1400
1500
1600
1700
1800
First-order Colors
Second-order Colors
Third-order Colors
Fourth-order Colors

Appendix C

Category	*New term*	*Description*	*Old term*
Master horizons	O	Surface accumulation of organic matter (peat, lignite, coal) overlying clayey or sandy part of soil	O
	A	Accumulation of humified organic matter mixed with mineral fraction. Occurs at the surface or below an O horizon	A
	E	Underlies an O or A horizon and is characterized by less organic matter, less sesquioxides (Fe_2O_3 and Al_2O_3), or less clay than the underlying horizon. This horizon is usually light colored as a result of abundant quartz	A2
	B	Underlies an O, A or E horizon and shows discernible enrichment in clay, carbonate, sesquioxides (Fe_2O_3 and Al_2O_3) or organic matter	B
	K	Subsurface horizon so impregnated with carbonate that it forms a massive layer	K
	C	Subsurface horizon more weathered than bedrock but lacking degree of weathering of A, E, B and K horizons	C
	R	Consolidated and unweathered bedrock	R
Gradations between master horizons	AB	Horizon with some characteristics of A and of B, but with A characteristics dominant	A3
	BA	As above, but with B characteristics dominant	B1
	E/B	A horizon predominantly like B horizon but with tongues of E horizon	A&B
Subordinate	a	Highly decomposed organic matter	—
	b	Buried soil horizon (usually redundant for sequences of paleosols)	b
	c	Concretions or nodules	cn
	e	Organic matter intermediate in decomposition (between a and i)	—
	f	Frozen soil, with ice wedges or other evidence	f
	g	Evidence of strong gleying, such as pyrite	g
	h	Illuvial accumulation of organic matter	h
	i	Slightly decomposed organic matter	—
	k	Accumulation of carbonates less than for K	ca
	m	Evidence of cementation, such as root deflection	m
	n	Accumulation of sodium, halite, columnar peds	sa
	o	Residual accumulation of sesquioxides	—
	p	Plowing or other comparable human disturbance	p
	q	Accumulation of silica	si
	r	Weathered or soft bedrock	ox
	s	Illuvial accumulation of sesquioxides	ir
	t	Accumulation of clay	t
	v	Plinthite	—
	w	Colored or structural B	—
	x	Fragipan character (cemented with clay and silica and avoided by roots)	x
	y	Accumulation of gypsum or crystal casts	cs
	z	Accumulation of other salts or crystal casts	sa

Source: Adapted for paleosols from Soil Survey Staff (1975, 1998).